

SEPARATION AND RECOVERY OF SELECTED TRANSITION-METAL CATALYST SYSTEMS USING MEMBRANE PROCESSES

BONGANI MICHAEL XABA

B-Tech: Chemistry

Dissertation submitted in fulfilment of the requirements for the degree of Magister Technologiae: Chemistry in the Department of Chemistry, Faculty of Applied and Computer Sciences, Vaal University of Technology

Supervisor: S.J. Modise [BSc., BSc. Hons, PhD (Chemistry)]

Co-Supervisor: E.B. Naidoo [BSc., BSc. Hons, PhD (Chemistry)]

July, 2010

DECLARATION

I, _____ hereby declare that this work has not previously been accepted in substance for any degree and is not being concurrently submitted in candidature for any degree.

Signed.....

Date.....

ACKNOWLEDGEMENTS

I hereby wish to express my sincere gratitude to the following individuals who enabled this project to be successfully and timeously completed:

- Supervisor – Prof S.J. Modise. Thank you for the wisdom and knowledge you shared throughout this project. Your ideas and words of encouragement have guided me through unbearable times.
- Co-supervisor – Dr E.B. Naidoo. Thank you for the words of encouragement and support.
- Dr S.M. Nelana - In all our interactions, you were always firm and sometimes tough. I did not understand it at that time, but now I understand. I am grateful for the support and constructive criticism. You have equipped me survival skills.
- Lab partner – Mr T.J. Brooms. Through all the laughter and tears, we held on until the end. You have been a brother and friend through unbearable times. May GOD bless and prosper you.
- My wife – Lehlogonolo. Thank you for the emotional support and understanding. Through all the late nights in the lab and stressed times, you were always by my side. I love you.
- Dr S. Shrivastava – for AFM measurements.

If we knew what we were doing, it wouldn't be called research would it?

Albert Einstein (1879-1955) *German-Swiss-U.S. scientist*

ABSTRACT

Membrane separation processes offer a promising alternative to energy-intensive separation processes such as distillation and solvent extraction. NF and RO are among the most investigated membrane processes with a potential use in the chemical industry. Carbon-carbon coupling reactions feature in the top ten most used reactions in the chemical industry. These reactions often use homogeneous palladium, nickel and other precious catalysts which are often difficult to separate from reaction products. This leads to potential product contamination and loss of active catalysts. This not only poses a threat to the environment but is also costly to the chemical industry.

The purpose of this study was to investigate the efficiency of the recovery of the metal catalysts by selected membrane processes. Four commercial polymeric NF and RO membranes (NF90, NF270, BW30 and XLE) were selected for the study. Palladium catalysts commonly used in Heck and Suzuki coupling reactions were selected. These are $\text{Pd}(\text{OAc})_2$, $\text{Pd}(\text{OAc})_2(\text{PPh}_3)_2$, PdCl_2 and $\text{Pd}(\text{PPh}_3)_2\text{Cl}_2$. A range of organic solvents were also selected for the study. All the membranes were characterized for pure water permeability, pure solvent permeability, swelling, surface morphology and chemical structure.

The chemical and catalytic properties of the catalysts were determined. Catalytic activity was investigated by performing coupling reactions. These catalysts generally performed well in the Heck coupling reaction with sufficient yields realized. The catalysts showed poor activities in the Suzuki and Sonogashira coupling reactions. These coupling reaction systems were affected by rapid palladium black formation.

Catalyst retention studies showed the influence of membrane-solute interactions such as steric hindrance and size exclusion. The larger catalyst, Pd(OAc)₂(PPh₃)₂ was rejected better by all the membranes irrespective of the solvent used. The smaller catalyst, Pd(OAc)₂ was the most poorly rejected catalyst. This catalyst showed signs of instability in the selected solvents. An interesting finding from this study is that of higher rejections in water compared to other solvents for a particular catalyst. In this regard, the influence of solvent-solute effects was evident. Generally, higher rejections were observed in solvents with higher polarity. This has been explained by the concept of solvation. It has been shown that solvents with different polarity solvate solutes differently, therefore leading to a different effective solute diameter in each solvent.

Catalyst separation using NF90 membrane was attempted for the Heck coupling reaction system. The reaction-separation procedure was repeated for two filtration cycles with rapid activity decline evident. This was regarded as very poor showing of the catalyst separation efficiency of the membrane. Other authors in similar studies using SRNF membranes have reported reaction-separation processes of up to seven cycles. This observation shows the inferiority of polymeric membranes in organic solvent applications such as catalyst separation.

TABLE OF CONTENTS

CHAPTER 1- OVERVIEW	1
1.1 INTRODUCTION	2
1.2 MEMBRANE TECHNOLOGY	6
1.3 OBJECTIVE OF THE RESEARCH.....	12
1.4 SCOPE OF THE STUDY	12
REFERENCES.....	14
CHAPTER 2 – LITERATURE SURVEY	20
2.1 TRANSITION-METAL CHEMISTRY.....	23
2.2 HOMOGENEOUS CATALYSIS.....	29
2.3 MEMBRANE PROCESSES.....	38
2.4 MEMBRANE TECHNOLOGY IN HOMOGENEOUS CATALYSIS.....	44
REFERENCES.....	48
CHAPTER 3 – EXPERIMENTAL AND ANALYTICAL METHODS	65
3.1 MATERIALS	67
3.2 EXPERIMENTAL SETUP	69
3.3 ANALYTICAL INSTRUMENTATION	71
3.4 METHODOLOGY	73
3.5 CATALYST PREPARATION AND CHARACTERIZATION.....	78
3.6 CATALYST RETENTION MEASUREMENTS	80
3.7 CATALYST SEPARATION AND REUSE	81
REFERENCES.....	83
CHAPTER 4 – RESULTS AND DISCUSSIONS	86
4.1 MEMBRANE CHARACTERIZATION	88
4.2 CATALYST CHARACTERIZATION.....	116
4.3 CATALYST RETENTION MEASUREMENTS	122
4.4 CATALYST SEPARATION AND REUSE	131

REFERENCES.....	135
CHAPTER 5 – CONCLUSIONS AND RECOMMENDATIONS	143
5.1 SUMMARY	145
5.2 CONCLUDING REMARKS.....	146
5.3 RECOMMENDATIONS	147
REFERENCES.....	148

LIST OF FIGURES

Figure 1. 1:	Typical homogeneous catalysts.....	4
Figure 1. 2:	Schematic representation of the cross-flow module.....	7
Figure 1. 3:	Schematic representation of the dead-end module.....	7
Figure 1. 4:	Isotropic membranes	8
Figure 1. 5:	Anisotropic membranes.	8
Figure 1. 6:	Filtration spectrum showing membrane processes.	9
Figure 2. 1:	Ligands commonly used in homogeneous catalysis	24
Figure 2. 2:	Oxidative addition reaction.....	26
Figure 2. 3:	Reductive elimination reaction	27
Figure 2. 4:	Ligand-substitution reaction	27
Figure 2. 5:	Migratory insertion reaction.....	28
Figure 2. 6:	β -hydrogen elimination reaction.....	28
Figure 2. 7 :	Heck coupling reaction.....	29
Figure 2. 8:	Suzuki coupling reaction	30
Figure 2. 9:	Sonogashira coupling reaction.....	30
Figure 2. 10:	Negishi coupling reaction	31
Figure 2. 11 :	Stille coupling reaction	31
Figure 2. 12:	Sulfonated-phosphines	32
Figure 2. 13:	Cationic bipyridyl ligand	33
Figure 2. 14:	NHC-porphyrin ligand system	34
Figure 2. 15:	PEPPSI-based catalyst system	34
Figure 2. 16:	Commonly used palladium catalysts and precursors	35
Figure 2. 17:	General structure of PEG.....	36
Figure 3. 1:	Structures of the catalysts used in the study.....	68
Figure 3. 2:	Dead-end unit used for filtration.....	70
Figure 3. 4:	Graphic representation of a catalyst single-component solution	80
Figure 3. 5:	Graphic representation of a coupling reaction mixture.....	81

Figure 3. 6:	Schematic of catalyst separation and reuse procedure	82
Figure 4. 1:	Relationship of water flux and pressure (Kedem-Katchalsky approach).....	89
Figure 4. 2:	Relationship of water flux and pressure (Košutić approach)	92
Figure 4. 3:	Plots of methanol flux in NF90, NF270, BW30 and XLE	96
Figure 4. 4:	Plots of ethanol flux in NF90, NF270, BW30 and XLE	97
Figure 4. 5:	Plots of 2-propanol flux in NF90, NF270, BW30 and XLE.....	97
Figure 4. 6:	Plots of acetonitrile flux in NF90, NF270, BW30 and XLE	98
Figure 4. 7:	Relationship between solvent flux and viscosity at 25°C	99
Figure 4. 8:	Relationship between solvent flux and molecular weight	101
Figure 4. 9:	Relationship between membrane swelling and molecular weight	104
Figure 4. 10:	Relationship between membrane swelling and flux	105
Figure 4. 11:	Schematic representation of pore-reduction swelling in NF membranes.....	105
Figure 4. 12:	Uncharged solutes retention curves showing interpolated MWCO.....	107
Figure 4. 13:	SEM micrographs showing the top view of the membranes	108
Figure 4. 14:	SEM micrograph showing the cross-sectional view of XLE membrane.....	109
Figure 4. 15:	AFM image showing the surface detail of the membrane	111
Figure 4. 16:	Plots of RMS roughness and pure water permeability	113
Figure 4. 17:	FTIR spectra showing the chemical structure of the membranes	114
Figure 4. 18:	FTIR spectra showing the chemical structure of Pd(OAc) ₂	117
Figure 4. 19:	FTIR spectra showing the chemical structure of Pd(PPh ₃) ₂ Cl ₂	118
Figure 4. 20:	FTIR spectra showing the chemical structure of Pd(OAc) ₂ (PPh ₃) ₂	118
Figure 4. 21:	Catalyst retention results in acetonitrile at 10 bar	123

Figure 4. 22:	Catalyst retention results in acetonitrile at 20 bar	124
Figure 4. 23:	Catalyst retention results in 2-propanol at 10 bar	126
Figure 4. 24:	Catalyst retention results in 2-propanol at 20 bar	127
Figure 4. 25:	Catalyst retention results in water at 10 bar	129
Figure 4. 26:	Catalyst retention results in water at 20 bar	130
Figure 4. 27:	Pd(OAc) ₂ retention and recycle results in acetonitrile at 10 bar	133
Figure 4. 28:	Pd(PPh ₃) ₂ Cl ₂ retention and recycle results in acetonitrile at 10 bar.....	134

LIST OF TABLES

Table 1. 1:	Comparison of homogeneous and heterogeneous catalysis	5
Table 3. 1:	Chemicals and reagents used in the study	67
Table 3. 2:	Catalysts used in the study	68
Table 3. 3:	Membrane characteristics as specified by the supplier	69
Table 3. 4:	Instrument settings for GC analysis of the alcohol	76
Table 3. 5:	Instrument settings for GC analysis of coupling products	78
Table 4. 1:	Pure water permeability values (Kedem-Katchalsky approach) .	90
Table 4. 2:	Pure water permeability values (Košutić Approach).....	93
Table 4. 3:	Observations of membrane compatibility with organic solvents.	94
Table 4. 4:	Physical properties of selected solvents	95
Table 4. 5:	Results of swelling measurements.....	103
Table 4. 6:	Properties of uncharged solutes used for MWCO determination	107
Table 4. 7:	Results of AFM roughness measurements	112
Table 4. 8:	Results of Heck coupling reaction.....	120
Table 4. 9:	Results of Suzuki coupling reaction	121
Table 4. 10:	Results of Sonogashira coupling reaction.....	122
Table 4. 11:	Results of Heck catalyst reaction – recycle procedure.....	132

GLOSSARY OF TERMS

AFM	Atomic force microscopy
ATR	Attenuated total reflectance
CFM	Chemical force microscopy
CSIR	Council for Scientific and Industrial Research
Da	Dalton
DCM	Dichloromethane
DFT	Density functional theory
DME	Dimethoxyethane
DMF	N,N-dimethylformamide
EAN	Effective atomic number
ED	Electrodialysis
FEGSEM	Field emission gun scanning electron microscopy
FID	Flame ionization detector
FTIR	Fourier transform infra-red
GC	Gas chromatography
HKR	Hydrolytic kinetic resolution
IL	Ionic liquid
IPS	Institute for Polymer Science
IUPAC	International Union of Pure and Applied Chemistry
LFSE	Ligand field stabilization energy
LPRO	Low pressure reverse osmosis
MeCN	Acetonitrile
MF	Microfiltration
MW	Molecular weight
MWCO	Molecular weight cut-off
NF	Nanofiltration
NHC	N-heterocyclic carbene
OSN	Organic solvent nanofiltration
PA	Polyamide

PEG	Polyethylene glycol
PEPPSI	Pyridine enhanced precatalyst preparation, stabilization and initiation
PSD	Pore size distribution
RMS	Root mean squared
RO	Reverse osmosis
SE	Secondary electron
SEM	Scanning electron microscopy
SHP	Steric hindrance pore
SRNF	Solvent-resistant nanofiltration
TCD	Thermal conductivity detector
THF	Tetrahydrofuran
UF	Ultrafiltration
UV-VIS	Ultraviolet-visible
WRC	Water Research Commission
WWF	World Wildlife Fund
bipy	Bipyridyl
en	Ethylenediamine
OAc	Acetate
Ox	Oxalate
PPh ₃	Triphenylphosphine
Pd(OAc) ₂	Palladium(II) acetate
Pd(OAc) ₂ (PPh ₃) ₂	Diacetato(bistriphenylphosphine)palladium(II)
Pd(PPh ₃) ₂ Cl ₂	Dichlorobis(triphenylphosphine)palladium(II)
PdCl ₂	Palladium(II) chloride
Et ₃ N	Triethylamine

LIST OF SYMBOLS

A	Effective membrane area
μ_i	Chemical potential of component i
$a_{i,M}$	Activity of component i
A_K	Membrane porosity
A_w	Pure water permeability
B_0	Specific permeability of the membrane
c_f	Concentration of feed
c_p	Concentration of permeate
$D_{i,M}$	Diffusion coefficient of component i
f_1	Mass transfer coefficients
f_2	Mass transfer coefficients
H_F	Wall-correction parameter
J	Solvent flux
J_w	Pure water flux
L_i	Proportionality factor
M	Molecular weight
Q	Membrane swelling
R	Rejection
R	Gas constant
r_P	Effective pore radius
r_s	Stokes radius
S_D	Steric hindrance factors for permeation diffusion
S_F	Steric hindrance factors for permeation flow
t	Permeation time
V_i	Volume of component i
W_{dry}	Mass of dry membrane
W_{wet}	Mass of wet membrane
X_{sm}	Friction factor between the solvent molecules
z	Coordinate over the membrane
α	Measure of susceptibility of membrane active layer
ΔP	Feed pressure
Δx	Membrane thickness
$\Delta \gamma$	Surface energy difference between the membrane and solvent
$\Delta \pi$	Osmotic pressure

ε	Membrane porosity
η'	Ratio of solute radius r_s and pore radius r_p .
η	Viscosity of the mixture
ρ_s	Density of solvent
σ	Reflection coefficient
τ	Tortuosity factor
φ	Solvent parameter

CHAPTER 1- OVERVIEW

This chapter introduces the concept of catalysis. A brief description of different catalyst systems is given. Membrane technology is also introduced. A brief history of membrane development in South Africa is given. The objectives and scope of the study are outlined.

TABLE OF CONTENTS

1.1	INTRODUCTION	2
1.1.1	Catalysis.....	2
1.2	MEMBRANE TECHNOLOGY	6
1.2.1	Definition of a membrane	6
1.2.2	Characteristics of a membrane.....	7
1.2.3	Membrane Processes.....	9
1.2.4	Reverse Osmosis and Nanofiltration.	10
1.2.5	Membrane Technology in South Africa.....	10
1.3	OBJECTIVE OF RESEARCH	12
1.4	SCOPE OF THE STUDY	12
	REFERENCES.....	14

1.1 INTRODUCTION

Catalysis is one of the fundamental areas of research that has resulted in industrially applicable processes. Research in specialized fields like Fischer-Tropsch synthesis [1,2] and olefin metathesis [3] has resulted in technological advances and new business opportunities for the chemical industry. Sasol, Shell and Exxon Mobil are some of the companies that have benefited from the technology of catalysis [4]. Cornils & Herrmann estimated that in 2003, 85% of industrially performed chemical processes were performed using catalysts [5]. Armor [6] has recently stated that catalytic processes have increased to over 90%.

Interest in the control of chemical reactions began as early as in the 19th century [7]. In this era, the emergence of chemistry as a rational science was evident. A lot of research activity in the field of chemical reactions, led to observations that were not readily understood, such as of accelerated reactions as a result of one substance coming into contact with other reacting substances. This phenomenon was termed *catalysis*, as declared by Greek pioneer researcher Berzelius [8]. The substance causing this unknown phenomenon was termed *catalyst*.

1.1.1 Catalysis

1.1.1.1 Development of Catalysts

A definition of a catalyst from undergraduate chemistry textbooks has been a substance that speeds up the rate of a chemical reaction without being consumed in the process [9]. Atkins and de Paula elaborate that catalysts increase the rate by reducing the activation energy of the reaction [10].

Schrauzer [11] summarizes the principal functions of catalysts as:

- (1) increasing reaction rates by their ability to relax restrictions imposed by quantum mechanical selection rules of spin and angular momentum.
- (2) bringing reactants together in energetically and sterically favorable fashion (proximity effect)
- (3) introducing efficient alternative reaction pathways by virtue of specific interactions with the substrate.

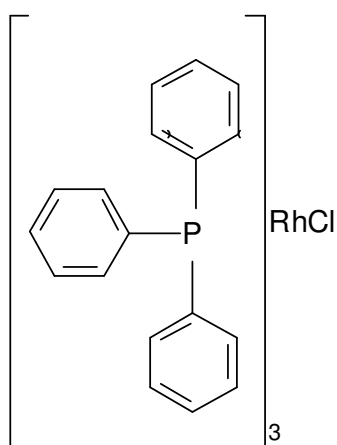
The definitions by all the authors [9,10,11] are generally accepted, and find common ground in the concept that catalysts decrease the activation energy of the reaction. Patterson and Pearce [8] have highlighted an important point that has been ignored or taken lightly. They state that the definitions may be sufficient; however observations in practice show that catalysts do undergo some kind of change during catalysis. Therefore it should be noted that in this case fundamental definitions differ significantly from practical observations.

1.1.1.2 Types of catalyst systems

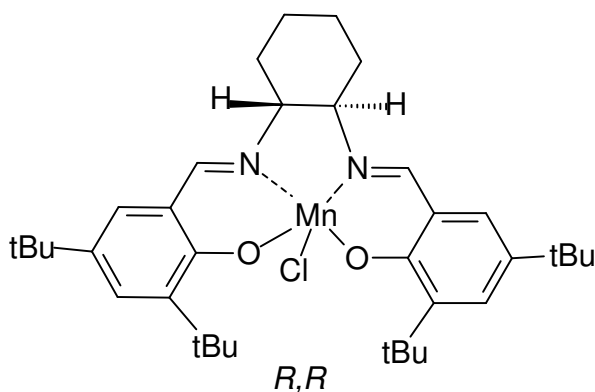
Catalysts are generally divided into two classes i.e. heterogeneous catalysts and homogeneous catalysts. Biological catalysts (enzymes) are now being added as a third class [12]. In heterogeneous catalysis, the catalyst is insoluble or is immobilized in the medium in which the reaction is taking place. Reactions of gaseous or liquid reagents occur at the surface of heterogeneous catalyst. In heterogeneous catalysts, which are usually made of a variety of elements deposited on a support, there is multitude of different active sites available for reaction. This sometimes poses a risk of lower conversions due to the active sites being [14].

In homogeneous catalysis, the catalyst is usually soluble in the reaction medium, and there is generally one type of active site [13,14]. Specialized homogeneous catalyst systems are continuously being developed. These catalyst systems consist of functionalized ligands which facilitate reactions under mild conditions [15]. Examples include the Wilkinson [16] and Jacobsen [17] catalyst systems shown below in Figure 1. 1.

The Wilkinson catalyst, chlorotris(triphenylphosphine)rhodium(I), is a rhodium complex used in the asymmetric hydrogenation of double bonds in the presence of chiral phosphine ligands [18]. The Jacobsen catalyst, (*R,R*)-*N,N'*-bis(3,5-di-*tert*-butylsalicylidene)-1,2-cyclohexane-diaminomanganese(III) chloride, is a manganese- and sometimes cobalt-salen complex used in the epoxidation of olefins [19].



Wilkinson catalyst



Jacobsen catalyst

Figure 1. 1: Typical homogeneous catalysts

From the industrial point of view, heterogeneous systems have great practical advantages over homogeneous systems, because they can be easily separated from the reaction mixture. Attempts have been made to obtain the same functionality of a heterogeneous catalyst in homogeneous catalysts by immobilizing the catalysts or by using large polymer-bound systems to aid ease of separation [20,21].

Separation in chemical industrial operations is mainly aimed at obtaining lower product contamination by catalysts, therefore ignoring the separation of the catalysts in their active form. Due to the expensive nature of the catalyst systems, operating costs escalate as a result of catalyst loss and recovery. Catalyst recovery processes require additional separation units such as distillation columns, extraction and adsorption systems [22].

Some of the principal differences between homogeneous and heterogeneous catalysts are listed in Table 1. 1. From the Table, it is clear that although the applicability of homogenous catalysts is limited, they are still preferred in certain operations owing to their high selectivity and activity.

Table 1. 1: Comparison of homogeneous and heterogeneous catalysis

	Homogeneous catalyst	Heterogeneous catalyst
Catalyst Properties		
Structure/ Stoichiometry	Defined	Undefined
Thermal stability	Low	High
Effectiveness		
Selectivity	High	Lower
Activity Loss	Irreversible reaction with products	Sintering of metal crystallites
Applicability	Limited	Wide
Catalyst separation		
Catalyst recycling	Possible	Easy
Cost of catalyst losses	High	Lower

1.2 MEMBRANE TECHNOLOGY

1.2.1 Definition of a membrane

A basic definition of a membrane has been given by Noble and Terry as a semi-permeable barrier between two phases [23]. This barrier can restrict the movement of molecules flowing across, in a specific manner. The barrier can be a solid, liquid or even a gas. Separation is achieved as a result of the semi-permeable nature of the membrane. A definition given by the IUPAC states that a membrane is a structure through which mass transfer takes place under a variety of driving forces [24]. A common ground between the two definitions mentioned above is that for separation to take place, some sort of selectivity is required.

The membrane has the ability to separate one component more readily than another component. This is because of differences in physical and/or chemical properties between the membrane and the permeating component. Transport through the membrane takes place as a result of a driving force acting on the feed. Driving forces can be gradients in pressure; concentration; electrical potential or temperature [25].

In a membrane separation process, a feed consisting of a mixture of two or more components is separated into a retentate - that part of the feed that does not pass through the membrane, i.e. is retained, and a permeate – that part of the permeate that does pass through the membrane [26]. Membrane separation processes can be run in a cross-flow and dead end modules as illustrated in Figure 1. 2 and Figure 1. 3.

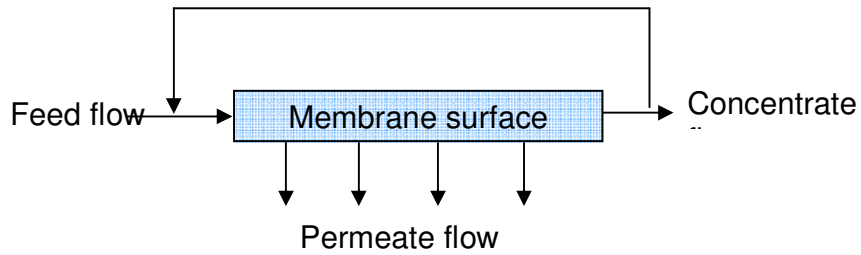


Figure 1. 2: Schematic representation of the cross-flow module

In the cross-flow module, the flow of the feed stream is parallel to the membrane, while the permeate flows through the membrane. The retentate may also be recycled back into the module in a continuous flow mode. In the dead end module however, the feed flows perpendicular to the membrane. The only outlet is through the membrane.

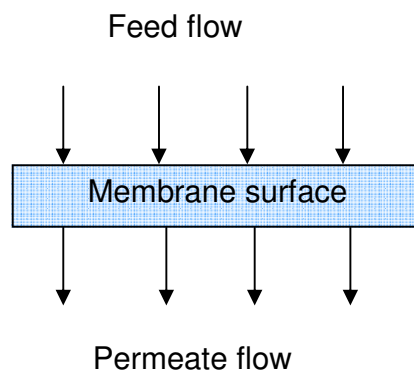


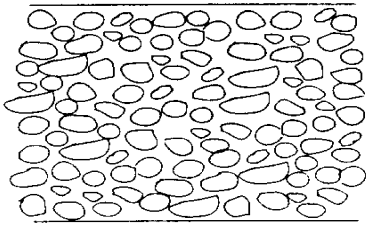
Figure 1. 3: Schematic representation of the dead-end module

1.2.2 Characteristics of a membrane

Different types of membranes have been prepared and distinguished by the type of material from which the membrane is prepared from. They can either be organic or inorganic. Organic membranes are manufactured from polymers such as polyamides, polyimides and polyacrylonitriles, while inorganic membranes are constructed from ceramics, porous carbon, glass, alumina and sintered metal [27,28].

Membranes can also be classified into isotropic and anisotropic types. Isotropic membranes are uniform in composition and physical nature across the cross-section of the membrane. These types of membranes are illustrated in Figure 1. 4. Isotropic membranes can be divided into various sub-categories, namely microporous and non-porous. [23].

Isotropic porous membrane



Dense non-porous membrane

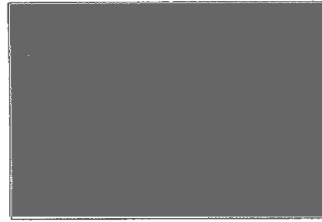
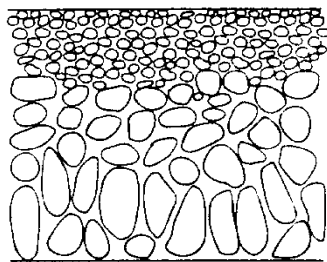


Figure 1. 4: Isotropic membranes

Anisotropic membranes are non-uniform across the membrane cross-section and they typically consist of layers [29]. Anisotropic porous membranes are also known as Loeb-Sourirajan membranes [30]. There are two types of anisotropic membranes; phase-separation and thin-film composite membranes as illustrated in Figure 1. 5. Phase-separation membranes are homogeneous in chemical composition but not in structure.

Anisotropic porous membrane



Thin-film composite membrane

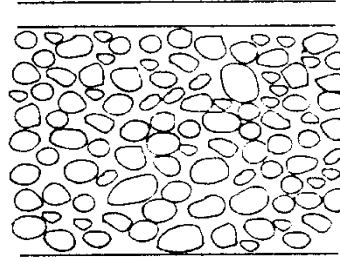


Figure 1. 5: Anisotropic membranes

On the other hand thin-film composite membranes are both chemically and structurally heterogeneous. These membranes often consist of a highly porous substrate coated with a dense film of a different polymer [30].

1.2.3 Membrane Processes

Membrane processes can be classified based on the pore size and range in which they separate. Microfiltration (MF), ultrafiltration (UF), nanofiltration (NF) and reverse osmosis (RO) have been progressively used for water treatment in order to remove suspended solids and reduce the content of organic and inorganic matters [31]. The pore size range of the different membrane processes are illustrated in Figure 1. 6. It can be seen from the figure that MF separates fine particles in the micron range. UF separates from the micron range down to macromolecular range. NF separates in the macromolecular range, while RO separates down to the ionic range.

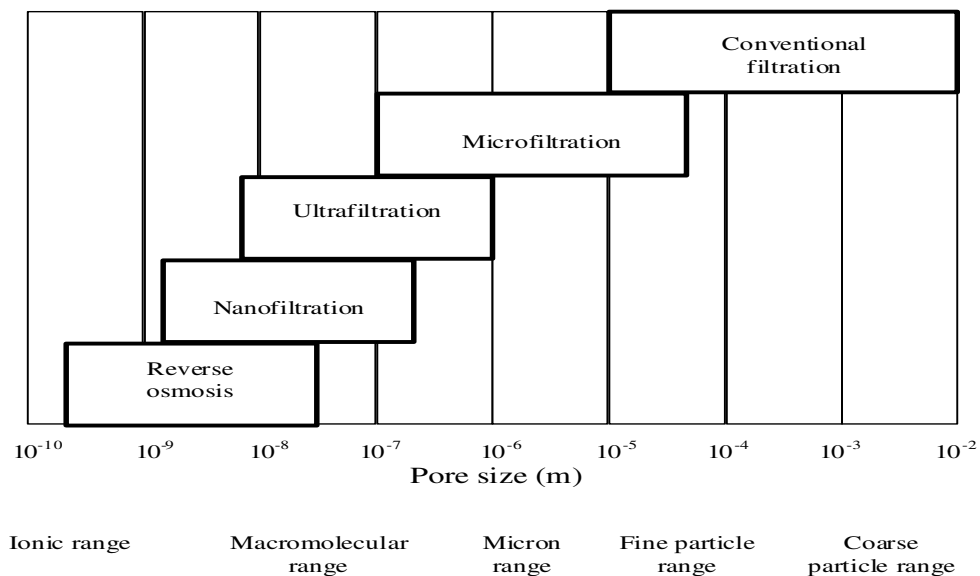


Figure 1. 6: Filtration spectrum showing membrane processes

1.2.4 Reverse Osmosis and Nanofiltration.

NF falls between UF and RO as illustrated above. Its separation characteristics are based on the sieve effect, but most commercial NF membranes are charged [32]. So ion rejection by NF membranes results from the combination of electrostatic and steric interactions associated with charge shielding, Donnan exclusion and the degree of hydration [33].

1.2.5 Membrane Technology in South Africa

The earliest interest in membrane technology in South Africa, according to Offringa [34], began in 1953 with the development of electrodyalisis (ED) systems and their membranes, at the Council for Scientific and Industrial Research (CSIR). This research laid the foundation for a better understanding of the thermodynamic and physical processes involved in ED. Initial research on polymeric membranes started in 1973 at the Institute for Polymer Science (IPS), in the University of Stellenbosch. This institution has become one of the strongest research hubs in membrane technology in South Africa.

In recognition of the future potential benefits of membrane and desalination technologies, the Water Research Commission (WRC) investment in this field of research has been relatively high. In the 2008/09 financial year, the WRC invested R88,7 million in projects that focused on water resources and water utilization [35]. WRC was successful in establishing viable research and development capabilities. These capabilities include multidisciplinary capacity building which resulted from multi-institutional co-operation during research execution. Institutions such as Stellenbosch University and Durban Institute of Technology are some of the institutes involved in such partnerships [36].

Jacobs *et al.* [37] published a paper in the field of polymer and membrane preparation. In their work funded by the WRC, they modified hydrophobic polysulphone membranes with poly(ethylene-oxide) to add some hydrophilic character to the membranes. The modified membranes showed smaller pore sizes and slightly higher rejection of PEG solutions. The study contributed to a broader knowledge and expertise in the area of membrane modification and preparation, where the stability of the membrane is important.

In a recent development, a South African company called VWS Envig (Pty) Ltd [38], was awarded contracts to supply water treatment plants for the production of potable water for the communities of Cannon Rocks and Boknes near Port Elizabeth. The company has also been awarded the contract to refurbish an existing RO plant in the Bushmans River Mouth near Port Elizabeth. The completed plant will produce 1800 m³ per day, and is said to be the largest desalination plant in South Africa [39].

However, the size of the desalination plants in South Africa are nowhere near the scale of desalination plants in operation, in planning or under construction in Europe, North America, Australia, China and India [40]. The World Wildlife Fund [41] has expressed concern over the application of desalination technology as a way to solve the world's water shortages. In a report published in 2007, WWF states that potential impacts of desalination include brine build-up, green house gas emissions and destruction of prized coastal areas [42].

The organization is not the first to cast a shadow of doubt over desalination technology. In 2006, a US-based organization, the Pacific Institute also published a report criticizing the indiscriminate construction of large desalination plants without proper investigations into the potential economic and environmental costs [40].

1.3 OBJECTIVE OF RESEARCH

Carbon-carbon coupling reactions feature in the top ten most used reactions in the chemical industry as stated by Pink *et al.* [43]. These types of reactions often use homogeneous palladium, nickel and other precious catalysts. These catalysts are often difficult to separate from reaction products, this leads to potential product contamination and loss of active catalysts. This not only poses a threat to the environment but is also costly to the chemical industry. The purpose of this study is to investigate the efficiency of the recovery of the metal catalysts by selected membrane processes.

The main objectives of the study are:

- Characterization of selected reverse osmosis (RO) and nanofiltration (NF) membranes.
- To study the rejection of selected transition-metal catalysts by RO and NF membranes.
- To perform coupling reactions using the selected transition-metal catalysts.
- To validate the concept of catalyst recovery by separating the catalyst from the reaction mixture.

1.4 SCOPE OF THE STUDY

Four commercial polymeric NF and RO membranes (NF90, NF270, BW30 and XLE) were selected for the study. These membranes are commonly used in wastewater treatment and other applications [44]. Known palladium catalysts used in Heck and Suzuki coupling reactions were selected. These are Pd(OAc)₂, Pd(OAc)₂(PPh₃)₂, PdCl₂ and Pd(PPh₃)₂Cl₂. A selection of solvents was also selected for the study. The rejection and separation of the catalysts by the polymeric membranes in the different solvents were studied.

The dissertation contains five chapters that address the research objectives. In this chapter, the concept of catalysis is introduced. A brief description of the different catalyst systems is given. This chapter also introduces membrane technology. A brief history of membrane development in South Africa is given.

A detailed literature review on transition-metal chemistry and their application as homogeneous catalysts is given in Chapter 2. A review is also given on theoretical concepts and models which govern transport in membrane separation.

The experimental and analytical part of the research is explained in Chapter 3. Methodology on characterization of the membranes by SEM, AFM, pure water permeability and neutral solutes rejection is discussed. Background and methodology on the selected homogenous catalysis reaction system is also given in this chapter.

Results obtained from experimental work are given in Chapter 4. This chapter discusses findings in detail. Discussions are aimed at addressing objectives set out in the problem statement. Chapter 5 gives concluding remarks and recommendations based on the conclusions drawn.

REFERENCES

1. STEYNBERG, A.P., ESPINOZA, R.L., JAGER, B. & VOSLOO, A.C. 1999. High temperature Fischer-Tropsch synthesis in commercial practice. *Applied Catalysis A: General*. **186** (1) 41 – 54.
2. DRY, M.E. 2002. The Fischer-Tropsch process: 1950 – 2000. *Catalysis Today*. **71** (1) 227 – 241.
3. MEYER, W.H., RADEBE, M.M.D., SERFONTEIN, W.D., RAMDHANI, U., DU TOIT, M. & NICOLAIDES, C.P. 2008. Homogeneous metathesis for the production of propene from butane. *Applied Catalysis A: General*. **340** 236 – 241.
4. BARTHOLOMEW, C.H. & FARRAUTO, R.J. 2006 Fundamentals of Industrial Catalytic Processes. 2nd ed. Hoboken, New Jersey: Wiley.
5. CORNILS, B. & HERRMANN, W.B. 2003. Concepts in homogeneous catalysis: the industrial view. *Journal of Catalysis*. **216** (1) 23 – 31.
6. ARMOR, J.N. 2010. A history of industrial catalysis. *Catalysis Today*. (*In Press*). Doi:10.1016/j.cattod.2009.11.019.
7. KAUFFMAN, G.B. 1994. Theories of coordination compounds. *In* Kauffman, G.B. eds. *Coordination Chemistry*. 1994. ACS Symposium. Washington DC: American Chemical Society.
8. PATTERSON, W.R. & PEARCE, R. 1981. Catalysis and chemical processes. Leonard Hill: Blackie & Son.

-
9. McMURRY, J. & FAY, R.C. 2004. Chemistry. 4th ed. New Jersey: Pearson – Prentice Hall.
 10. ATKINS, P. & DE PAULA, J. 2002. Physical Chemistry. 7th ed. New York: Oxford.
 11. SCHRAUZER, G.N. 1971. Transition metals in homogeneous catalysis. New York: Dekker.
 12. SCOUTEN, W.H. & PETERSEN, G. 1999. New biocatalysts: Essential tools for a sustainable 21st century chemical industry. American Chemical Society. http://www.chemicalvision2020.org/pdfs/chem_vision.pdf.
 13. COLE-HAMILTON, D.J. & TOOZE, R.P. 2006. Catalyst separation, recovery and recycling: chemistry and process design. *Catalysis by Metal Complexes*. **30**. Dordrecht: Springer.
 14. MASTERS, C. 1981. Homogeneous Transition-Metal Catalysis. A gentle art. London: Chapman & Hall.
 15. GUPTA, K.C. & SUTAR, A.K. 2008. Catalytic activities of Schiff base transition-metal complexes. *Coordination Chemistry Reviews*. **252** 1420 – 1450.
 16. MOTHERWELL, W.B. 2002. Curiosity and simplicity in the invention and discovery of new metal-mediated reactions for organic synthesis. *Pure and Applied Chemistry*. **74** (1) 135 – 142.

-
17. READY, J.M. & JACOBSEN, E.N. 2001. Highly active oligomeric (salen)Co catalysts for asymmetric epoxide ring-opening reactions. *Journal of American Chemical Society*. **123** (11) 2687 – 2688.
 18. BUTLER, I.S. & HARROD, J.F. 1989. Inorganic chemistry. Principles and applications. California: Benjamin/Cummings.
 19. WALSH, P.J., LURAIN, A.E. & BALSELLS, J. 2003. Use of achiral and meso ligands to convey asymmetry in enantioselective. *Chemical Reviews*. **103** 3297 – 3344.
 20. DATTA, A., EBERT, K. & PLENIO, H. 2003. Nanofiltration for homogeneous catalyst separation: Soluble polymer-supported palladium catalysts for Heck, Sonogashira and Suzuki coupling of aryl halides. *Organometallics*. **22** (1) 4685 – 4691.
 21. COTTON, F.A. & WILKINSON, G. 1980. Advanced Inorganic Chemistry. A Comprehensive Text. New York: Wiley.
 22. SCARPELLO, J.T., NAIR, D., FREITAS DOS SANTOS, L.N., WHITE, L.S. & LIVINGSTON, A.G. 2002. The Separation of Homogeneous Organometallic Catalysts using Solvent Resistant Nanofiltration. *Journal of Membrane Science*. **203** (11) 71 – 85.
 23. NOBLE, R.D. & TERRY, P.A. 2004. Principles of Chemical Separation with Environmental Applications. Cambridge University Press.
 24. KOROYOS, W.J., MA, Y.H. & SHIMIDZU, T. 1996. Terminology for membranes and membrane processes. IUPAC recommendations. *Pure and Applied Chemistry*. **68** (7) 1479 – 1489.

-
25. MULDER, M. 1998. Basic Principles of Membrane Technology. 2nd ed. Netherlands: Alinea.
 26. SEADER, J.D. & HENLEY, E.J. 1998. Separation Process Principles. New York: Wiley.
 27. MOITSHEKI, L.J. 2003. Nanofiltration: Fouling and Chemical Cleaning. MSc. Dissertation. Potchefstroom University for Christian Higher Education. Potchefstroom. South Africa.
 28. PINNAU, I. & FREEMAN, B.D. 1999. Formation and modification of polymeric membranes: overview. *In* Freeman *et al.* Membranes Formation and Modification. ACS Symposium Series. Washington DC. American Chemical Society.
 29. FREEMAN, B. & SAGLE, A. 2004. Fundamentals of Membranes for Water Treatment, *In* PARCHER, M. The Future of Desalination in Texas. Vol 2, Technical Papers, Case Studies and Desalination Technology Resources.
 30. BAKER, W.R. 2004. Membrane Technology and Applications. New York: Dekker.
 31. M'NIF, A., BOUGUECHA, S., HAMROUNI, B. & DHAHBI, M. 2007. Coupling of membrane processes for brackish water desalination. *Desalination*. **203** (1) 331 – 336.
 32. TEIXEIRA, M.R., ROSA, M.J. & NYSTRÖM, M. 2005. The role of membrane charge on nanofiltration performance. *Journal of Membrane Science*. **265** (1) 160 – 166.

-
33. GOZALVEZ-ZAFRILLA, J.M., SANTAFE-MOROS, A. & LORA-GARCIA, J. 2005. Performance of commercial nanofiltration membranes in the removal of nitrate ions. *Desalination*. **185** (1-3) 281 – 287.
 34. <http://www.scienceinafrica.co.za/2002/february/membrane.htm>. Accessed 04/01/2008.
 35. WRC Annual Report 2008/09. Report No: RP130/2009. Water Research Commission. South Africa.
 36. WRC. 2002. Membrane Technology. Water Research Commission. South Africa.
 37. ROUX, S.P., JACOBS, E.P., VAN REENEN, A.J., MORTEL, C. & MEINCKEN, M. 2006. Hydrophilisation of polysulphone ultrafiltration membranes by incorporation of branched PEO-block-PSU copolymers. *Journal of Membrane Science*. **276** (1) 8 – 15.
 38. <http://www.vwsenvig.co.za/en/press/PR2009/20090727,13405.htm> accessed on 26/03/2010.
 39. <http://www.vwsenvig.co.za/en/press/PR2010/20100224,15273.htm> accessed on 26/03/2010.
 40. WRC. 2007. The Water Wheel. Desalination No Holy Grail, says Nature Group. **6** (5) Water Research Commission. South Africa.
 41. WWF. 2007. Making Water: Desalination – Option or Distraction for a Thirsty World?

<http://assets.panda.org/downloads/desalinationreportjune2007.pdf>.

42. WRC. 2007. Municipal Sectors drive South African Desalination Plant markets. Water Research Commission. South Africa.
43. PINK, C.J., WONG, H., FERREIRA, F.C. & LIVINGSTON, A.G. 2008. Organic solvent nanofiltration and adsorbents; a hybrid approach to achieve ultra low palladium contamination of post coupling reaction products. *Organic Process Research and Development*. **12** (4) 589 – 595.
44. <http://www.dow.com/liquidseps/> accessed 25/05/2009.

CHAPTER 2 – LITERATURE SURVEY

This chapter gives a brief literature survey on transition-metal chemistry. The application of these metals as catalysts is explored in Section 2.2. In this case, design of catalysts and ligands is discussed. An introduction into carbon-carbon coupling reactions is given in this section. A review on theoretical concepts and models which govern transport in membrane processes is outlined in Section 2.3. The application of membrane processes in homogeneous catalysis is discussed in Section 2.4.

TABLE OF CONTENTS

2.1	TRANSITION-METAL CHEMISTRY	23
2.1.1	General Description.....	23
2.1.2	Organometallic Chemistry	23
2.1.2.1	<i>Types of Ligands</i>	24
2.1.2.2	<i>Effective Atomic Number – 18 Electron Rule</i>	25
2.1.2.3	<i>Stability of Organometallic Compounds</i>	25
2.1.3	Fundamental Reactions of Organometallic Complexes.....	26
2.1.3.1	<i>Oxidative Addition</i>	26
2.1.3.2	<i>Reductive Elimination</i>	27
2.1.3.3	<i>Ligand Substitution</i>	27
2.1.3.4	<i>Migratory Insertion Reaction</i>	28
2.1.3.5	<i>β-Elimination (β-Hydrogen elimination)</i>	28
2.2	HOMOGENEOUS CATALYSIS	29
2.2.1	Palladium and Nickel Catalyzed Reactions	29
2.2.2	Developments in Heck, Suzuki and Sonogashira Coupling Reactions	32
2.2.2.1	<i>Ligand Design</i>	32
2.2.2.2	<i>Catalyst Design</i>	35
2.2.2.3	<i>Solvent Selection</i>	35
2.3	MEMBRANE PROCESSES	38
2.3.1	Transport in Membranes	38
2.3.1.1	<i>Pore-Flow Model</i>	39
2.3.1.2	<i>Steric Hindrance Pore Model</i>	40
2.3.1.3	<i>Solution Diffusion Model</i>	41
2.3.1.4	<i>Solution diffusion with Imperfections Model</i>	41
2.3.2	Membrane Characterization	42
2.3.2.1	<i>Membrane Molecular Weight Cut Off (MWCO)</i>	42
2.3.2.2	<i>Porosity</i>	43
2.3.2.3	<i>Surface Morphology</i>	44

2.4	MEMBRANE TECHNOLOGY IN HOMOGENEOUS CATALYSIS	44
	REFERENCES.....	48

2.1 TRANSITION-METAL CHEMISTRY

2.1.1 General Description

Transition-metals are elements which occupy Groups 3 to 12 in the Periodic Table. Gerloch and Constable have explained that the term “transition” comes from the position of the elements in the periodic table. These are found in between metallic elements and non-metals [1]. The transition elements are also called transition-metals due to their typical metallic properties [2].

One of the most important characteristic of transition-metals is the electron placement in the *d* and *f* orbitals [3]. The elements occupy a place in the Periodic Table where the *d*-orbitals are being filled. Purcell and Kotz have attributed the use of these metals in coordination chemistry and organometallic chemistry to their partially filled shells.

2.1.2 Organometallic Chemistry

Most of the chemistry of transition-metals deals with the formation of organometallic compounds. According to Elschenboich and Salzer [4], an organometallic compound is defined as a compound with some degree of polar bonding $M^{\delta+} - C^{\delta-}$ between the metal-carbon atoms. They elaborate that the organometallic compounds of the *d*-block transition-metals can be classified according to the ligand type. These ligand types are discussed in detail in the following sections. In view of this definition, it is important to understand the structure and bonding of the transition-metal organometallic compounds [5]. Therefore some aspects of organometallic chemistry are briefly discussed in the sections below.

2.1.2.1 Types of Ligands

The importance of ligands has been highlighted in the definition of organometallic compounds. In this section, the various classifications of ligands will be highlighted. Hegedus [6] has conveniently classified ligands into (1) formal anions, (2) formal neutrals and (3) formal cations. Ligands can also be classified based on the number of atoms that bond to the metal [7]. Ligands which bond to the metal with one atom are called monodentate, those which bond to metal by two atoms are called bidentate and those which bond to the metal by three or more atoms are called polydentate [8].

The significance of this classification is shown in homogeneous catalysis where bidentate ligands such as bis-(diphenylphosphinoethane) catalyze enantioselective reactions more effectively than monodentate ligands such as triphenylphosphine [9]. Examples of bidentate ligands commonly used in homogeneous catalysis are illustrated in Figure 2. 1 below.

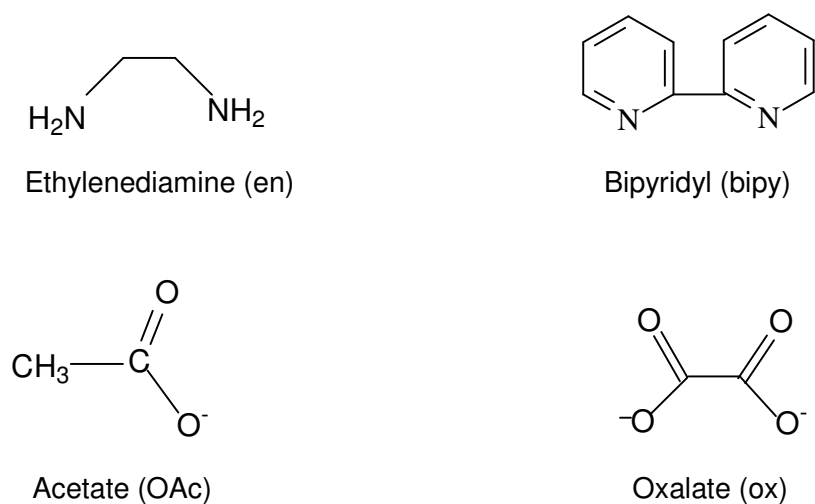


Figure 2. 1: Ligands commonly used in homogeneous catalysis

Another classification of ligands that is of importance in homogeneous catalysis is based on the nature of bonding interaction of the ligands with metals. In this classification, ligands can either be *hard* or *soft* based on their polarizability [10]. Hard ligands have low polarizability. These tend to form complexes with metals at high oxidation states such as Fe^{3+} , Ti^{4+} and Pt^{4+} . Examples are NH_3 , H_2O , N , O and F^- . Soft ligands have high polarizability. These tend to form complexes with metals at low oxidation states such as Fe^{2+} , Pd^0 and Pt^0 . Examples are PPh_3 , Br^- , I^- , Cl^- and CO .

2.1.2.2 Effective Atomic Number – 18 Electron Rule

To account for bonding, Sidgwick [11] developed a rule that summarizes structure and coordination properties of organometallic compounds. The rule, termed the effective atomic number (EAN) states that thermodynamically stable transition-metal organometallic compounds are formed when the sum of the metal *d*-electrons plus the electrons from the donor ligands equals 18 [12,13].

An exception to the EAN rule is encountered in metals with d^8 - and d^{10} - electron configurations. Shriver and Atkins [14] have cited steric and electronic effects as some of the reasons for the observed stability of the d^8 - and d^{10} complexes. These are said to cause insufficient crowding of ligands around the metal to obey the 18 electron rule. It is important to note that the EAN determines the maximum allowable number of ligands for any transition-metal in any oxidation state [15,16].

2.1.2.3 Stability of Organometallic Compounds

The stability of organometallic compounds is influenced by metal-ligand interactions and the type and number of ligands involved in bonding, among other factors [17]. Parameters such as the ligand field stabilization energy (LFSE) have been developed to explain stability in metal-ligand interactions [18].

Porterfield [19] describes the LFSE as the energy by which particular *d*-electronic transition is stabilized by the splitting of metal *d*-orbitals by a ligand [20]. Pontikis *et al.* [21] have studied the stability and electronic structure of octahedral complexes using density functional theory (DFT) calculations. Their results indicated that the distortion energetics of the octahedral complexes are dominated by electrostatic and steric interactions. This is in opposition to intrinsic covalent effects associated with the electronic structure of the metal. This is in agreement with the explanation by Lever *et al.* [17] regarding the stability of organometallic complexes.

2.1.3 Fundamental Reactions of Organometallic Complexes

There are few fundamental reactions of organometallic complexes which demonstrate how these complexes either promote or catalyze reactions. These reactions are usually expressed in a form of a catalytic cycle. In this section the individual reactions are discussed in some detail.

2.1.3.1 Oxidative Addition

Oxidative addition involves the reaction of a molecule such as H₂ with a low-valent coordinatively unsaturated metal complex. This occurs under bond cleavage forming two bonds [20]. The metal increases its formal oxidation state by two units. The coordination number of the metal centre also increases by two as illustrated in Figure 2. 2. Dedieu [22] has shown, using Pt and Pd systems that the oxidative addition product has some covalent character, when the metal moves from M⁰ to M²⁺ oxidation state.

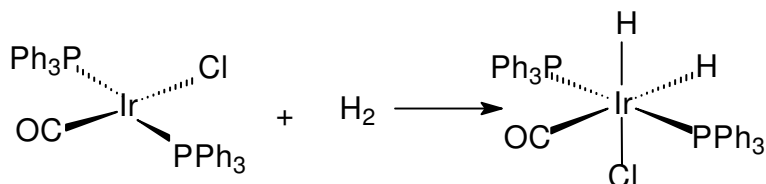


Figure 2. 2: Oxidative addition reaction

2.1.3.2 Reductive Elimination

Reductive elimination is a reaction where the coordination number of the central metal decreases at the same time as its formal oxidation state decreases [12]. Figure 2. 3 shows an example of reductive elimination of CH₃I group from an iridium complex. Furuya *et al.* [23] have recently studied the mechanism of a palladium-catalyzed fluorination. They showed that reductive elimination is the mechanism by which the C–F bond is removed from the palladium complex. The elimination occurs via the aryl-Pd(IV)-fluoride complex which is stabilized by pyridyl-sulfonamide ancillary ligands.

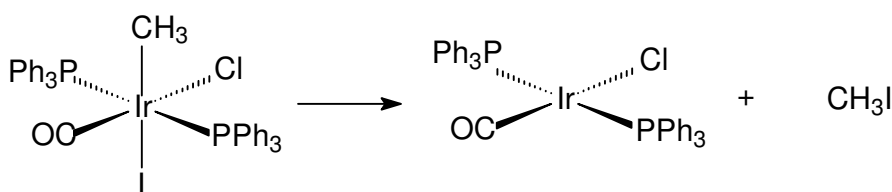


Figure 2. 3: Reductive Elimination reaction

2.1.3.3 Ligand Substitution

It is believed that substitution reactions of square planar complexes almost always proceed via an associative mechanism. This involves an intermediate which contains both the leaving ligand and entering ligand [24]. It is assumed that the entering ligand approaches the complex from the one side of the plane over the ligand to be displaced. The leaving ligand moves down as the entering ligand approaches. At this point the intermediate has a trigonal bipyramidal configuration as illustrated in Figure 2. 4 [25].

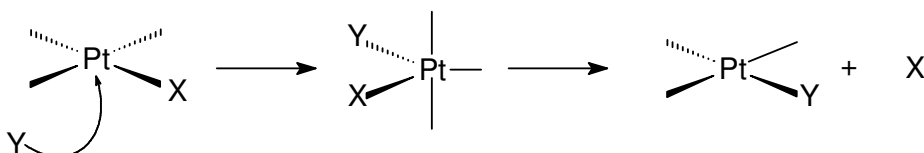


Figure 2. 4: Ligand-substitution reaction

2.1.3.4 Migratory Insertion Reaction

Insertion reactions are addition reactions in which the central metal does not change its oxidation state. These reactions involve breaking a metal-carbon bond and formation of a carbon-carbon bond. In addition, a bond is formed between the metal and the incoming ligand. The ligand is usually a Lewis base such as CO [26]. The mechanism is shown in Figure 2. 5. It has been shown that migratory insertion is the one of the mechanisms by which metal-alkyl bonds are formed in the copolymerization of CO and olefins catalyzed by transition-metal complexes [27].

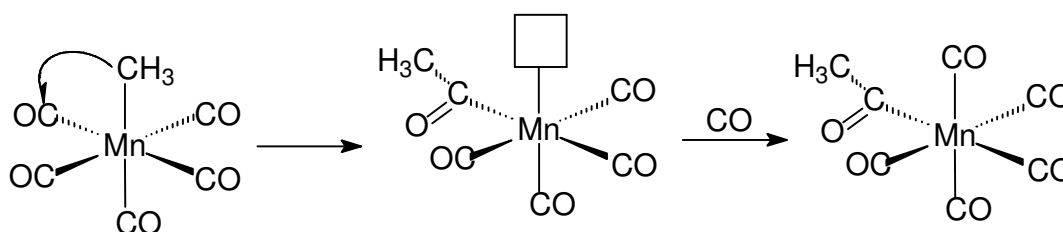


Figure 2. 5: Migratory insertion reaction

2.1.3.5 β -Elimination (β -Hydrogen elimination)

β -Hydrogen elimination is actually the reverse reaction of insertion. In this reaction a β -hydrogen of an alkyl group migrates to the metal atom [28]. β -elimination requires a coordinatively unsaturated metal complex since it results in an increase in the coordination number of central metal. Reductive elimination and β -elimination are competitive reactions [29]. The mechanism is illustrated in Figure 2. 6.

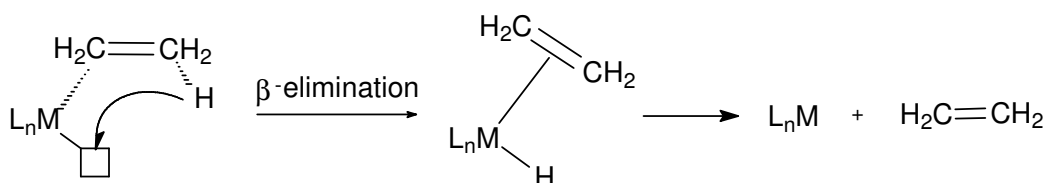


Figure 2. 6: β -hydrogen elimination reaction

2.2 HOMOGENEOUS CATALYSIS

2.2.1 Palladium and Nickel Catalyzed Reactions

Coupling reactions catalyzed by organometallic complexes are some of the most powerful tools for synthesis of aromatic and heteroaromatic compounds [30,31]. Some of the reactions are Heck, Suzuki-Miyaura, Sonogashira, Stille, Negishi, Kumada and Buchwald-Hartwig coupling [32]. The reactions are used extensively in synthesis due to the availability of starting materials and simplicity of operation [33]. Each reaction is discussed briefly in the following sections.

2.2.1.1 Heck Reaction

The Heck reaction involves coupling of an alkene with an aryl or alkyl halide to form a vinylarene or diene as illustrated in Figure 2. 7 [34]. In the Heck reaction, the catalyst can be added directly. The catalyst can also be produced in-situ by reduction of palladium salts in the presence of suitable ligands [35]. The Heck reaction is the most studied reaction among the coupling reactions [36].

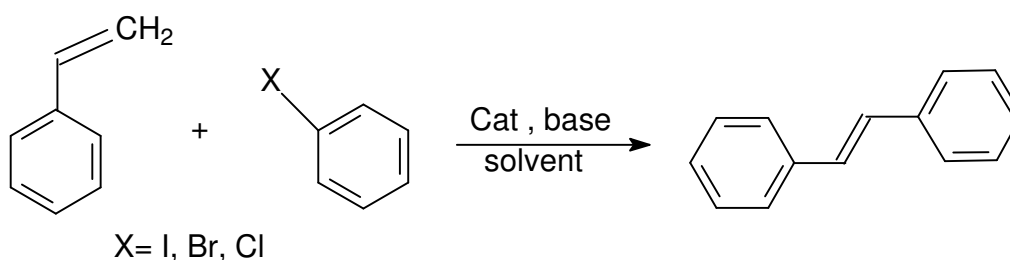


Figure 2. 7 : Heck Coupling Reaction

2.2.1.2 Suzuki-Miyaura Reaction

The Suzuki-Miyaura reaction involves coupling of aryl halides with aryl boronic acids to form biaryls [37]. Boronic compounds are usually stable and insensitive to air and water. These compounds can also be easily handled in a variety of solvents apart from those commonly used on cross-coupling reactions [38]. A representative Suzuki coupling reaction is illustrated in Figure 2. 8 below.

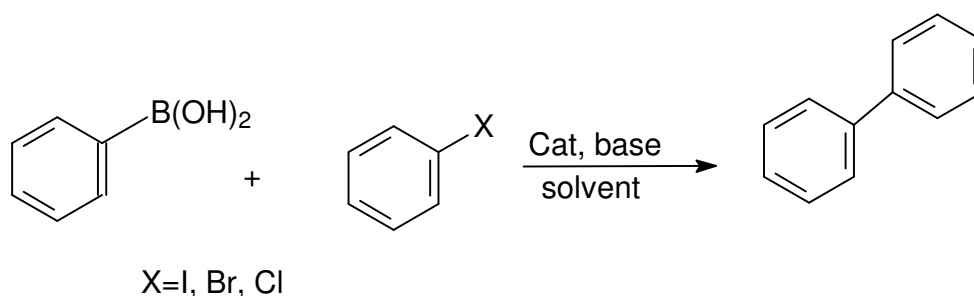


Figure 2. 8: Suzuki Coupling Reaction

2.2.1.3 Sonogashira Reaction

The Sonogashira reaction involves coupling of terminal alkynes with aryl and vinyl halides to yield alkynylarenes in the presence of a palladium catalyst and a copper co-catalyst [39]. The reaction was independently reported by Heck, Cassar and Sonogashira groups in 1975 [40]. The reaction is illustrated in Figure 2. 9.

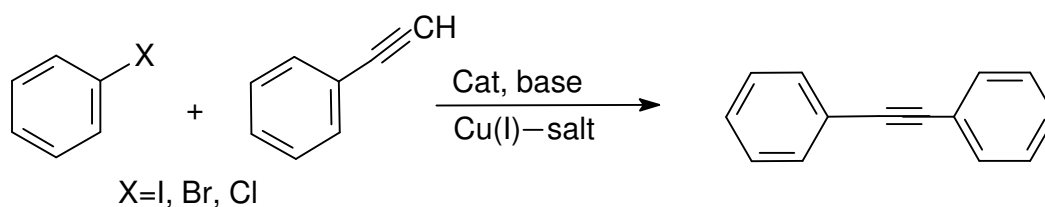


Figure 2. 9: Sonogashira Coupling Reaction

2.2.1.4 Negishi Reaction

The Negishi coupling reaction involves the coupling of aryl halides with arylzinc halides or benzylic zinc halides in the presence of a palladium or nickel catalyst, to form unsymmetrical biaryls and biaryl methanes as illustrated in Figure 2. 10 [41]. Negishi *et al.* [42] have emphasized the importance of the right selection of ligands, co-catalysts, solvents and other additives in the Negishi coupling reaction. In their paper, they illustrated a range of optimum conditions for the reaction.

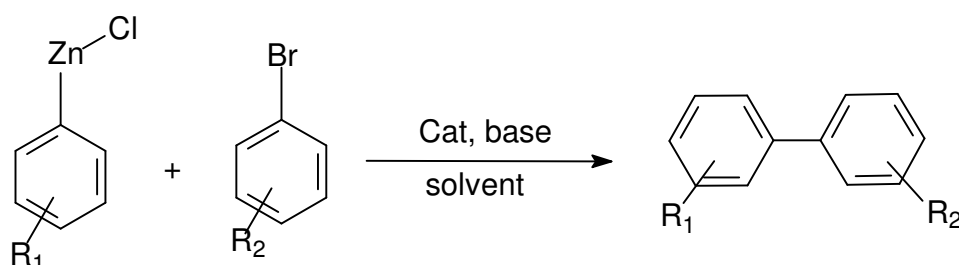


Figure 2. 10: Negishi Coupling Reaction

2.2.1.5 Stille Reaction

The Stille reaction is the palladium catalyzed coupling of organo-stannanes with vinyl or aryl halides to form 1,3-dienes as illustrated in Figure 2. 11 [43,44]. The reaction is tolerant to a large range of functional groups, and hence the reaction has been extensively used in the synthesis of natural products and in biological research [45,46]. There are concerns however, regarding the toxicity of tin compounds residues in the final product of Stille reactions [35].

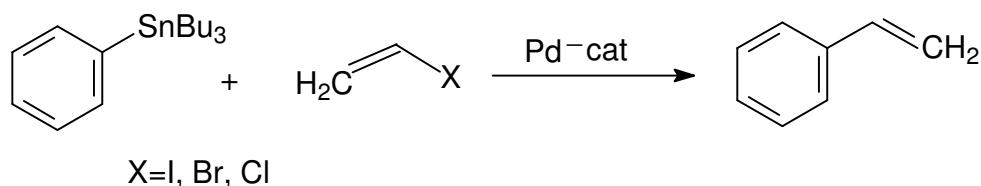


Figure 2. 11 : Stille Coupling Reaction

2.2.2 Developments in Heck, Suzuki and Sonogashira Coupling Reactions

2.2.2.1 Ligand Design

Phosphines are the most commonly used ligands [47]. The wide use of phosphines can be attributed to their properties. These ligands can be easily designed to carry functional groups or other substituents that can change the properties of the catalyst [48].

An example is given by Pinault and Bruce [49]. They highlight in their paper, the use of water-soluble ligands based on functionalized-phosphines. The phosphines contain polar groups such as sulfonates and carboxylates which aid catalysis in aqueous medium. Typical sulfonated phosphines used by Pinault and Bruce are illustrated in Figure 2. 12.

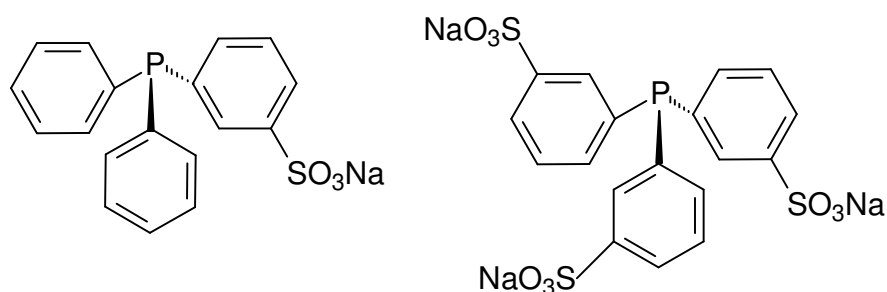


Figure 2. 12: Sulfonated-phosphines [adapted from Pinault and Bruce 49]

A disadvantage of polar functionalized-phosphines is that they are usually sensitive to air and are prone to oxidation. This limits their ability to stabilize the catalyst in reaction [50]. In view of this, research has been focused on the development of catalysts and ligands which can enable catalysis under mild conditions [51]. From the industrial point of view, cost control is important. Consequently a variety of ligandless palladium systems, air-stable ligands and phosphine-free ligands have been developed [52], examples are *N*-Heterocyclic and *P*-Heterocyclic. Nitrogen-based ligands are briefly discussed below.

Hsu *et al.* [53] have reported high yields in the bipyridine-modulated oxidative Heck reaction of arylboronic acids and olefins. In their work, they used 4,4'-dimethyl 2,2'-bipyridine and Pd(OAc)₂ as ligand and precursor respectively. Huang *et al.* [54] have used a water-soluble and air-stable palladium(II)cationic 2,2'-bipyridyl system in the Heck coupling of aryl iodides and alkenes. The catalyst system was prepared by combination of Pd(NH₃)₂Cl₂ and the cationic bipyridyl compound shown in Figure 2. 13.

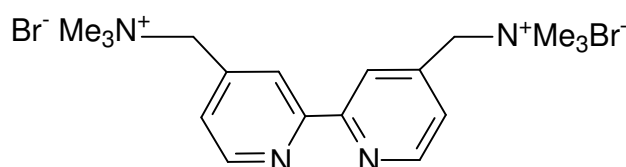


Figure 2. 13: Cationic bipyridyl ligand [adapted from Huang *et al.* 54]

Diebolt *et al.* [55] reported yields greater than 95% in the palladium-catalyzed Suzuki coupling of aryl chlorides and phenylboronic acids. They used a palladium complex of the type [PdCl₂(NHC){P(OR)₃}], with the *N*-heterocyclic carbene *N,N'*-bis(2,6-diisopropylphenyl)imidazol-2-ylidene. Wang *et al.* [56] used a similar rationale. In their Suzuki coupling study, they used a tetraimidazolium salt based on a porphyrin to prepare the *N*-heterocyclic carbene ligand illustrated in Figure 2. 14. Their results showed that the catalytic activity depends on the structure of the porphyrin core and the NHC.

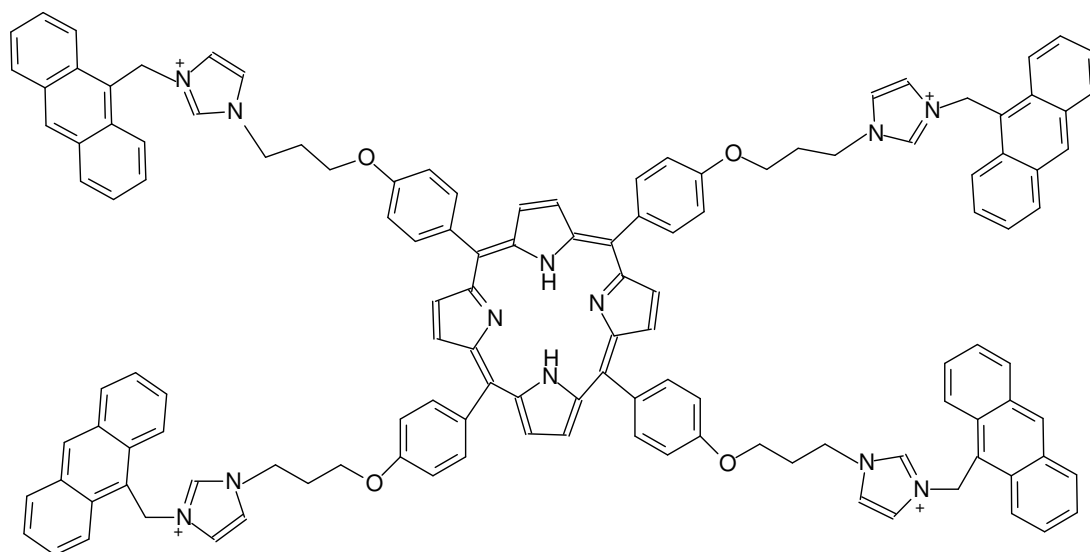


Figure 2. 14: NHC-porphyrin ligand system [adapted from Wang *et al.* 56]

The efficiency of NHC has also been shown in the Sonogashira reaction. Ray *et al.* [57] reported effective coupling of aryl iodides with substituted acetylenes in air and mixed solvent. They used two NHC-based catalysts, *trans*-[1-benzyl-3-(3,3-dimethyl-2-oxobutyl)imidazol-2-ylidene]₂PdBr₂ and *cis*-[1-benzyl-3-(N-tert-butylacetamido)imidazol-2-ylidene]₂PdCl₂. Ray *et al.* claim that their catalyst system showed superior activity than the PEPPSI (pyridine enhanced precatalyst preparation, stabilization and initiation) -based catalyst developed by Kantchev *et al.* [58] as illustrated in Figure 2. 15.

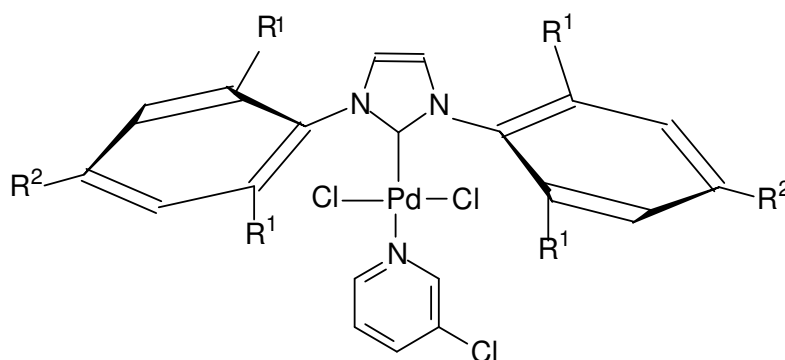


Figure 2. 15: PEPPSI-based catalyst system [developed by Kantchev *et al.* 58]

2.2.2.2 Catalyst Design

While much research has been focused on the development of ligands, efforts have also been made in the development of catalysts for Heck, Suzuki and Sonogashira reactions [59]. Palladium catalysts have been preferred over other metals such as nickel and iron. One reason for the preference stated by Slagt *et al.* [60], is the lower homocoupling observed with the use of palladium catalysts. It has been observed that under similar reaction conditions, nickel catalysts lead to more homocoupling than their palladium counterparts [41]. Palladium catalysts and precursors commonly used in coupling reactions are illustrated in Figure 2. 16 below. Palladium(II) chloride and palladium(II) acetate have been commonly used as both catalyst and precursor to other catalysts [61].

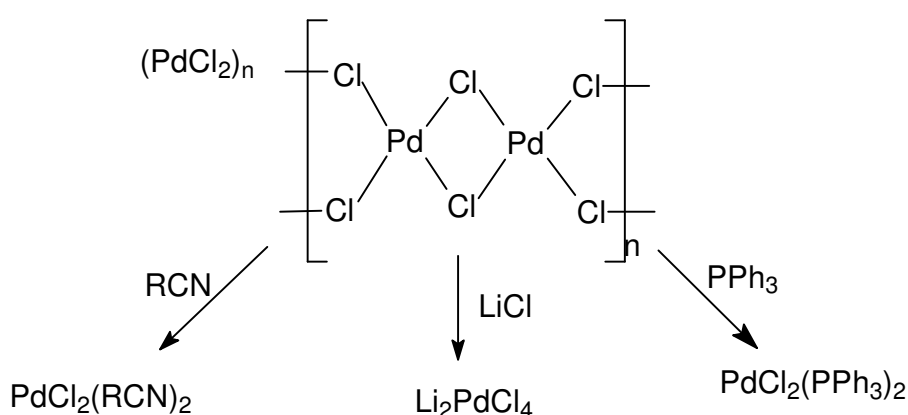


Figure 2. 16: Commonly used palladium catalysts and precursors

2.2.2.3 Solvent Selection

The correct selection of the solvent to be used in a C-C coupling reaction is essential. Gani *et al.* [62] have summarized the role of solvents in chemical reactions. Some of the roles include dissolution of solid reactants, heat transfer and phase transfer. Organic solvents such as tetrahydrofuran (THF), dichloromethane (DCM), chloroform, *N,N*-dimethylformamide (DMF), 1,2-dimethoxyethane (DME) and acetonitrile (MeCN) are the most frequently used in

C-C coupling reactions [63]. These solvents however, have been the center of attention lately due to their hazardous effects on to the environment [64,65,66]. In view of this, alternative solvents have been investigated for use in C-C coupling reactions [67].

PEG, which is a low molecular-weight polymer, has been of interest as a solvent for coupling reactions [68]. The polymer illustrated in Figure 2. 17, has advantages over conventional organic solvents, in that it can bring a heterogeneous character into the homogeneous reaction system [69]. PEG is also water-soluble, which further emphasizes the potential use in C-C coupling reactions. Corma *et al.* [70,71] used a PEG as a support and solvent in the Heck, Suzuki and Sonogashira reactions. The group reported yields greater than 95% in all reactions with PEG as solvent and scaffold. Although a significant amount homocoupling products were also observed. They concluded that PEG was a better solvent due to the observed yields and good stability.

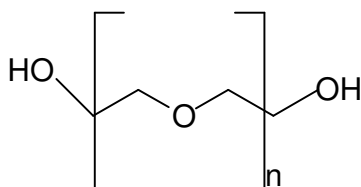


Figure 2. 17: General structure of PEG

Ionic liquids (ILs) are also some of alternative solvents currently investigated. Ionic liquids are actually poorly coordinated salts which are liquid at temperatures below 100°C [72]. Advantages of ILs over conventional solvents include non-flammability, non-volatility, high solvation and thermal stability. Singh *et al.* [73] have reported the application of functionalized ILs in the Heck coupling. The IL/catalyst system consisting of [bmim][OAc]/PdCl₂(CH₃CN)₂ showed significant efficiency without loss activity even after eleven-times of reuse.

Water is the greenest alternative solvent that is currently of interest [69]. This solvent is non-toxic, non-flammable and inexpensive [74]. Water also possesses other attractive properties. These include a large dielectric constant, high heat capacity and high boiling point [75]. The application of water in organic reactions however, is limited by the low solubility of organic molecules in water [76].

With the current drive towards “green chemistry”, research efforts show promising developments in aqueous organic reactions [77]. Studies of Heck, Suzuki and Sonogashira reactions in water are briefly discussed below. Said *et al.* [78] have compared Heck coupling in water and DMF. In their study, they obtained low yields of ~40 % when using water alone as compared to ~90% when using DMF. A combination of water-DMF showed no difference. The use of a phase-transfer reagent, Aliquat-336, resulted in yields of >95%.

These findings are in agreement with the review by Liu and Xiao in which they showed the need for phase-transfer reagents in aqueous Heck reaction [67]. It can be concluded that Heck coupling in water has limited applicability due to this need for auxiliary reagents. The Suzuki coupling reaction has been reported in aqueous medium, with the help of water-soluble ligands. Fleckenstein and Plenio [79] have reported efficient coupling of N-heterocyclic chlorides and N-heterocyclic boronic acids in aqueous medium. The duo reported yields >99% from using a sulfonated ligand in water.

Aqueous Sonogashira reaction is the most promising of the three reactions. Studies have reported excellent yields in water with or without copper as cocatalyst. Liang *et al.* [80] have reported yields >95% in the copper-free Sonogashira coupling in water under aerobic conditions. The studies also highlight the need for increased research efforts in aqueous organic reaction.

2.3 MEMBRANE PROCESSES

The use of membrane in non-aqueous media has drawn a lot of attention in recent years [81]. An emerging field particularly in pressure-driven processes is organic solvent nanofiltration (OSN) [82]. Lab-scale and commercial scale applications of OSN membranes have been reported [83,84]. In the development and application of membrane process, characterization of membranes and modelling are essential steps [85]. Modelling is important because it can lead to a better understanding of transport mechanism involved in membrane process [86].

2.3.1 Transport in Membranes

Transport mechanisms through NF membranes are not yet clarified. A lot of debate is ongoing as to which transport models should be used to describe certain membrane processes [87]. Current theoretical models for mass transfer through NF membranes are based on diffusion, adsorption, ion exchange, ion coupling and concentration polarization [88].

Gibbins *et al.* refer to two main theoretical models describing the membrane transport mechanism as (i) Pore-flow and (ii) solution-diffusion [89]. These will be discussed briefly. The derivation of these models is however beyond the scope of this work.

2.3.1.1 Pore-Flow Model

In the pore-flow model, it is assumed that transport occurs by pressure-driven convective flow through the membrane pores. Separation of the different components is achieved by size exclusion [90]. The pore-flow model is characterized by the relation of the reflection coefficient σ to the rejection R by a function η' as shown in Equation 2.1. η' is described as the ratio of solute radius r_s and pore radius r_p .

$$\sigma = 1 - \frac{c_p}{c_r} = 1 - \frac{2(1-R)}{2-R} = f(\eta') \quad \text{Equation 2.1}$$

where c_p – concentration of permeate

c_f – concentration of feed

$\eta' = r_s/r_p$ which is the ratio of solute and pore radii

The relationship between the reflection coefficient σ and the rejection R is derived from the Spiegler-Kedem equation and is expressed by Equation 2.2 [91].

$$R = 1 - \frac{c_p}{c_m} = \frac{\sigma(1-F)}{(1-\sigma F)} \quad \text{Equation 2.2}$$

Where

$$F = \exp\left(-\frac{1-\sigma}{P} J_v\right) \quad \text{Equation 2.3}$$

In the Spiegler-Kedem equation, the rejection R is given as a function of flux J and solute permeability P . σ and P can be determined experimentally, R as a function of J . Generally the convective solute transport takes place when σ is equal to 100%. This condition is applicable to dense membranes with no pores available for convective transport. Transport in RO membranes can be described using this model [88].

2.3.1.2 Steric Hindrance Pore Model

The pore-flow model was modified by Nakao and Kimura, by eliminating the wall correction factors, and successfully proposed the Steric Hindrance pore (SHP) model [92]. For uncharged solutes, where convective transport of a solute through the membrane is not influenced by electrostatic interaction, the separation is achieved through size effects. In light of this, the SHP model can be used to calculate the pore radius and the pore ratio of membrane porosity to thickness [93]. The SHP can be described by Equations 2.4 and Equation 2.5 below.

$$\sigma = 1 - H_F S_F \quad H_F = 1 + \frac{16}{9} \eta'^2 \quad \text{Equation 2.4}$$

$$P_S = H_D S_D D_S \left(\frac{A_K}{\Delta x} \right) \quad H_D = 1 \quad \text{Equation 2.5}$$

H_F is the wall-correction parameter that represents the effects of the pore wall. A_K is the membrane porosity, and Δx is the membrane thickness [81]. S_F and S_D are steric hindrance factors for permeation flow and diffusion respectively. These factors are expressed by Equations 2.6 and 2.7 respectively.

$$S_F = (1 - \eta')^2 [2 - (1 - \eta')^2] \quad \text{Equation 2.6}$$

$$S_D = (1 - \eta')^2 \quad \text{Equation 2.7}$$

During transport, dissolved components encounter certain steric hindrance and interactions with the pore wall. A molecule smaller than the diameter of the membrane pore is partially retained due to these effects. A solute with the same size as the diameter is completely retained [94].

2.3.1.3 Solution Diffusion Model

A transport model that is often used to describe transport in organophilic nanofiltration is the solution-diffusion model, as reviewed by Wiljmans and Baker [95]. In the model it is assumed that each permeation component dissolves in the membrane phase, followed by diffusion through the membrane as a result of concentration gradient [96]. The general form of the solution-diffusion model is expressed by Equation 2.8 below:

$$J_i = -L_{i,M} \frac{\delta\mu_i}{\delta z} = -L_{i,M} \left(RT \frac{\delta \ln a_{i,M}}{\delta z} + V_i \frac{\delta P_M}{\delta z} \right) \quad \text{Equation 2.8}$$

where L_i is the proportionality factor, μ_i the chemical potential of component i , $a_{i,M}$ the activity of component i , V_i the molar volume of component i , z is the coordinate over the membrane ($z = 0$ for the feed, permeate $z = \delta_M =$ thickness of the membrane in (m)) [97].

2.3.1.4 Solution diffusion with Imperfections Model

In organophilic NF, it has often been observed that transport through the swollen membrane cannot be described solely by diffusive flow [98]. Mason and Lonsdale [99] extended the solution-diffusion model by taking into account the viscous transport that also takes place through imperfections in the membrane. An extra term for the viscous flow was added to the solution-diffusion model as expressed by Equation 2.9.

$$J_i = \frac{c_{i,M} D_{i,M} V_i}{RT \delta_M} (\Delta P - \Delta \pi) + \frac{c_{i,M} B_0}{\eta \delta_M} \Delta P \quad \text{Equation 2.9}$$

In the equation η is the viscosity of the mixture permeating through the membrane in (Pa s) and B_0 is the specific permeability of the membrane in (m^2).

2.3.2 Membrane Characterization

A consistent and reliable method of measuring separation performance of membranes is essential and allows end users to make an informed selection [100]. Membrane characterization parameters may be described as either performance related or morphology related. Performance-related parameters describe membrane functionality such as flux and rejection. Morphological parameters which include physical and chemical parameters describe the structure of the membrane [101].

2.3.2.1 Membrane Molecular Weight Cut Off (MWCO)

Molecular weight cut-off is described as the molecular weight for which 90% rejection of the solute is achieved by the membrane [102]. The MWCO concept is based on the observation that molecules generally get larger as their masses increase. As molecules get larger, sieving effects due to steric hindrance increase and a larger molecule is rejected by the membrane more than the smaller molecule. MWCO may also be related to diffusion since larger molecules diffuse more slowly than smaller molecules [103].

Hilal *et al.* [104] have highlighted that MWCO determination depends on experimental conditions such as the nature of the feed solution and the type of membrane module. They showed this by using a mixture of polyethyleneglycols (PEG) with different molecular weights. Their results also showed that some membranes have larger and smaller pores respectively, than specified by the manufacturer.

2.3.2.2 Porosity

Porosity has been regarded as another useful parameter to describe separation in membranes. Porosity is usually expressed as pore density, PSD or effective number of pores in the membrane's upper active layer [105]. Bowen and Welfoot [106] have theoretically investigated the effects of log-normal pore size distribution on the rejection of uncharged solutes and NaCl. They showed that theoretical log-normal function is not suitable for NF membranes, due to the large pore size tail of the distribution dominating the rejection and flux. Their results also showed that interpretation based on uncharged solutes data alone cannot give useful quantitative information about the membrane pore size distributions. But when used in conjunction with other surface characterization techniques, show good agreement of pore size distribution.

Košutič *et al.* [107] investigated the porosity of NF and RO membranes by permeation of uncharged compact organic molecules. In order to ascertain the influence of the porous structure of the membrane skin on the retention mechanism of different solutes, the PSD's were determined at almost 690 kPa. Their results showed distinction between the PSD of NF and RO membranes. The RO membranes showed a wide PSD and bimodal distribution with maxima at 0.52 nm and 0.80 nm. The PSD of NF membranes showed maxima at larger pore sizes, the first one between 0.95 nm and 1.10 nm and the second maximum around 1.55 nm. This clearly shows the presence of larger surface pores.

2.3.2.3 Surface Morphology

Studies have shown that surface morphology and structure influence permeability, rejection and colloidal fouling behavior of NF and RO membranes [108]. Scanning Electron Microscopy (SEM) and Atomic Force Microscopy (AFM) have been used to provide direct characterization of the membrane pore size distribution [103]. AFM has been used more often than SEM, because AFM measurements can be performed at atmospheric pressure and no pre-treatment is required prior to analysis [109].

Boussu *et al.* [110] studied the surface roughness and hydrophobicity of NF membranes using different modes of AFM. Measurements were performed in both non-contact and tapping modes respectively. Although the roughness values are different for non-contact AFM and tapping mode AFM, Boussu *et al.* found no difference between the two modes in ranking the NF membranes with respect to their surface roughness.

2.4 MEMBRANE TECHNOLOGY IN HOMOGENEOUS CATALYSIS

The separation and recycling of homogeneous catalysts used in organic synthesis is often essential in order to perform economically and environmentally acceptable processes. In this area of homogeneous catalyst separation and recycling, much attention has been on catalyst immobilization, development of enlarged catalysts, interphase chemistry and phase tagging for biphasic catalysis or ionic liquids [111,112,113].

However these are less attractive due to the need for additional steps required to obtain these modified catalysts, which display properties that may be different from their homogeneous analogues [114]. A more promising approach is the use of pressure-driven membrane processes.

Interest in the application of membrane technology in homogeneous catalysis started as early as in 1976, at the Du Pont de Nemours Company. Grosser *et al.* [115], used polyimide RO membranes to separate soluble transition-metal complexes from reaction mixtures. They reported 60-99% rejection of $\text{RhCl}(\text{PPh}_3)_3$ from adiponitrile solutions, obtained by hydrogenation of 1,4-dicyanobutene. They also observed separation of RuCl_3 catalyst used in the hydrodimerization of acrylonitrile.

The potential of RO was further studied by Ilinich *et al.* in 1993 at the Boreskov Institute of Catalysis. They applied RO in separation of soluble iron-containing phosphotungstenate catalyst used in the detoxication of NO and H_2S . They found the retention of NO_3^- product decreased with the concentration of the heteropoly tungsten catalyst reaching negative values, whereas the retention of catalyst was 99% [116].

Following the development of suitable membranes for non-aqueous applications, the use of ultra- and nanofiltration techniques became the center of attention in the late 2001. Nair *et al.* [117,118] used a semi-continuous NF-coupled Heck system as a way to improve productivity of a homogeneous catalyst. The tested Heck-catalyst was $\text{Pd}(\text{OAc})_2(\text{PPh}_3)_2$ with $\text{P}(\text{o-tolyl})_3$ as a stabilizing agent, in the reaction of styrene and iodobenzene to form trans-stilbene. The study utilized composite solvent-resistant NF (SRNF) membranes, MPF-50 and MPF-60 produced by Koch. Their results showed up to 97% rejection of palladium catalyst in different solvents, and allowed subsequent catalyst recycle and reuse.

The prospective of SRNF was evident in 2002, with a number of papers published in the area of homogeneous catalyst-separation [111, 112, 117, 119]. Most of these studies used SRNF membranes that include the commonly used MPF range from KOCH, STARMEM range from W.R. Grace and the Desal-5 from Osmonics.

Scarpello *et al.* [112] used the membranes to separate three commonly used homogeneous catalysts (the Jacobsen catalyst, Wilkinson catalyst and Pd-BINAP) and obtained up to 95% rejection with good solvent fluxes in the majority of systems tested. Datta *et al.* [113] used a dense PDMS-PAN SRNF membrane to separate a phosphinated-polymer supported palladium catalyst from Suzuki and Heck coupling reaction products. The polymer enlarged catalyst was prepared from (1-Ad)₂P- substituted poly(methylstyrene), a suitable palladium source such as Pd(PhCN)₂Cl₂, Pd(OAc)₂ or Pd(dba)₂, and a base. The membrane showed quantitative retention of the catalyst of up to 99%. Furthermore the catalyst was reused up to nine times and showed constant yields of coupling products and constant turnover frequencies.

Other types of membranes have also been investigated for the separation of homogeneous catalysts. Gallego *et al.* [119] have used a zeolite membrane, synthesized from commercial γ -Al₂O₃ tubular ceramic membrane supports, to separate the palladium catalyst [Pd(μ -Cl)(Ph₂P-(CH₂)₄-PPh₂)](CF₃SO₃)₂ from reaction products. Their target system was the Diels-Alder reaction of acroleine and cyclopentadiene to yield 5-norbornene-2-carboxylaldehyde. The zeolite membrane showed close to 100% retention of the palladium catalysts.

Chowdhury *et al.* [114] reported a recovery of a polyoxometallate oxidation catalyst from an aqueous and organic media by using a mesoporous γ -Al₂O₃ membrane. The group recycled a water-soluble Na₁₂[WZn₃(ZnW₉O₃₄)₂] catalyst and obtained up to 97% retention. A toluene-soluble catalyst [MeN(n-C₈H₁₇)₃]₁₂[WZn₃(ZnW₉O₃₄)₂], was also recovered with quantitative retentions of up to 99.9%. XPS depth-profiling measurements on the alumina membranes showed the catalyst does not enter the pores of the membrane substantially even after repeated nanofiltration measurements.

Aerts *et al.* [120] applied SRNF in the recycling of cobalt Jacobsen catalyst used in the hydrolytic kinetic resolution (HKR) of epoxides. This research group used the commercially available SRNF membranes such as the MPF range and the Desal range. They also used a ceramic membrane supplied by VITO. Their target system was the Co-Jacobsen catalyzed HKR of 1,2-epoxyhexane and styrene oxide. The filtration experiments were carried out in diethyl ether, isopropyl alcohol and under solvent-free conditions. Average retentions of up to 93% were obtained with the commercial membranes.

Ferreira *et al.* [121] used the STARMEM 120 SRNF membrane in the separation of an osmium catalyst from the Sharpless asymmetric dihydroxylation reaction. The catalyst system consisted of the $K_2OsO_2(OH)_4$ salt and the chiral ligand $(DHQD)_2PHAL$. Their results highlighted the efficiency of the nanofiltration membrane in separating the catalyst system. They observed 30% loss of the osmium catalyst through the permeate stream, which subsequently points out product contamination. They concluded that the loss may be attributed to the existence of free osmium species in the mixture which lead to lower rejections of the osmium complex.

In recent developments, van der Gryp *et al.* [122] from the North-West University have used STARMEM series of OSN membranes in the separation of five Grubbs-type catalysts from a metathesis reaction system. They used the metathesis reaction of 1-octene to 7-tetradecene and ethane as a model reaction. They reported that STARMEM 228 was the best membrane giving catalysts rejections of up to 99% therefore confirming catalyst separation from the mixture.

REFERENCES

1. MIESSLER, G.L. & TARR, D.A. 1991. Inorganic chemistry. Englewood Cliffs: Prentice-Hall.
2. GERLOCH, M. & CONSTABLE, E.C. 1994. Transition-metal chemistry. New York. VCH-Weinheim.
3. MASTERS, C. 1981. Homogeneous transition-metal catalysis, a gentle art. London. Chapman & Hall.
4. ELSCHENBROICH, C. & SALZER, A. 2001. Organometallics. A concise introduction. 2nd revised ed. Wienheim: VCH.
5. NICHOLLS, D. 1983. Complexes of the first-row transition-metal elements. Hong Kong. MacMillan Press.
6. HEGEDUS, L.S. 1999. Transition metals in the synthesis of organic molecules. 2nd ed. California: University Science Books.
7. SPESSARD, G.O. & MIESSLER, G.L. 1997. Organometallic chemistry. New Jersey: Prentice-Hall.
8. BRADY, J.E. & HOLUM, J.R. 1988. Fundamentals of chemistry. 3rd ed. New York: Wiley.
9. PRETORIUS, M. 2004. Bi- and tridentate ligands and their use in catalysis. PhD Thesis. Rand Afrikaans University.

-
10. CRABTREE, R.H. 2001. Organometallic chemistry of the transition metals. 3rd ed. New York: Wiley-Interscience.
 11. SIDGWICK, N.V. 1927. The electronic theory of valency. New York: Cornell University Press.
 12. HUHEEY, J.E, KEITER, A.E. & KEITER, R.L. 1993. Inorganic chemistry. Principles of structure and reactivity. 4th Ed. HarperCollins College Publishers.
 13. LAING, M. 1994. Effective atomic number and VSEPR 60 years later. *In* Kauffman, G.B. eds. *Coordination chemistry*. 1994. ACS Symposium. Washington DC: American Chemical Society.
 14. SHRIVER, D.F. & ATKINS, P.W. 1999. Inorganic chemistry. 3rd ed. Oxford: University Press.
 15. OWEN, S.M. & BROOKER, A.T. 1991. A guide to modern inorganic chemistry. Singapore: Longman.
 16. JEAN, Y. 2005. Molecular orbitals of transition-metal complexes. New York. Oxford University Press.
 17. LEVER, A.B.P. & SOLOMON, E.I. 1999. Ligand field theory and the properties of transition-metal complexes. *In* Inorganic electronic structure and spectroscopy, Volume 1: Methodology. Eds. Solomon, E.I & Lever, A.B.P. New Jersey: John Wiley & Sons Publishers.
 18. MURRELL, J.N., KETTLE, S.F.A. & TEDDER, J.M. 1965. Valence theory. London: John Wiley & Sons Publishers.

-
19. PORTERFIELD, W.W. 1993. Inorganic chemistry. A unified approach. 2nd ed. California: Academic Press Inc.
 20. MOODY, B. 1991. Comparative inorganic chemistry. 3rd ed. London: Edward Arnold Publishers.
 21. PONTIKIS, G., BORDEN, J., MARTÍNEK, V. & FLORIÁN, J. 2009. Linear energy relationships for the octahedral preference of Mg, Ca and transition-metal ions. *Journal of Physical Chemistry*. **113** (15) 3588 – 3593.
 22. DEDIEU, A. 2000. Theoretical studies in palladium and platinum molecular systems. *Chemical Reviews*. **100** (2) 503 – 600.
 23. FURUYA, T., BENITEZ, D., TKATCHO UK, E., STROM, A.E., TANG, P., GODDARD, W.A. & RITTER, T. 2010. Mechanism of C –F reductive elimination from Pd(IV) fluorides. *Journal of American Chemical Society*. **132** (11) 3793 – 3807.
 24. BASOLO, F. 1965. Substitution reactions of square planar complexes. *In* Mechanisms of inorganic reactions. Kleinberg, J. *et al* eds. *Advances in Chemistry*. 1965. Washington D.C: American Chemical Society.
 25. JOLLY, W.L. 1976. The principles of inorganic chemistry. Kogakusa. McGraw-Hill.
 26. RIX, F.C. & BROOKHART, M. 1995. Energetics of migratory insertion reactions in Pd(II) acyl ethylene, alkyl ethylene, and alkyl carbonyl complexes. *Journal of American Chemical Society*. **117** (3) 1137 – 1138.

-
27. CURLEY, J.J., KITIAHVILI, K.D., WATERMAN, R. & HILLHOUSE, G.L. 2009. Sequential insertion reactions of carbon monoxide and ethylene into the Ni-C bond of a cationic nickel(II) alkyl complex. *Organometallics*. **28** (8) 2568 – 2571.
28. ALEXANIAN, E.J. & HARTWIG, J.F. 2008. Mechanistic study of β -hydrogen elimination from organoplatinum(II) enolate complexes. *Journal of American Chemical Society*. **130** (1) 15627 – 15635.
29. BLUM, O. & MILSTEIN, D. 1995. Mechanism of a directly observed β -hydride elimination process of iridium alkoxo complexes. *Journal of American Chemical Society*. **117** (16) 4582 – 4594.
30. BLASER, H.U., PUGIN, B. & SPINDLER, F. 2005. Progress in enantioselective catalysis assessed from an industrial point of view. *Journal of Molecular Catalysis A: Chemical*. **231** (1-2) 1 – 20.
31. GURAM, A.S., KING, A.O., ALLEN, J.G., WANG, X., SCHENKEL, L.B., CHAN, J., BUNEL, E.E., FAUL, M.M., LARSEN, R.D., MARTINELLI, M.J. & REIDER, P.J. 2006. New air-stable catalysts for general and efficient Suzuki-Miyaura cross-coupling reactions of heteroaryl chlorides. *Organic Letters*. **8** (9) 1787 – 1789.
32. PINK, C.J., WONG, H., FERREIRA, F.C. & LIVINGSTON, A.G. 2008. Organic solvent nanofiltration and adsorbents; a hybrid approach to achieve ultra low palladium contamination of post coupling reaction products. *Organic Process Research and Development*. **12** (4) 589 – 595.

-
33. ZAPF, A. & BELLER, M. 2005. The development of efficient catalysts for palladium-catalyzed coupling reactions of aryl halides. *Chemical Communications*. 431 – 440.
34. HECK, R.F. & NOLLEY, J.P. 1972. Palladium-catalyzed vinylic hydrogen substitution reactions with aryl, benzyl and styryl halides. *Journal of Organic Chemistry*. **37** (14) 2320 – 2327.
35. BARNARD, C. 2008. Palladium-catalysed C-C coupling: Then and now. *Platinum Metals Revision*. **52** (1) 38 – 45.
36. YOO, K.S., YOON, C.H. & JUNG, K.W. 2006. Oxidative palladium(II) catalysis: A highly efficient and chemoselective cross-coupling method for carbon-carbon bond formation under base-free conditions. *Journal of American Chemical Society*. **128** (50) 16384 – 16393.
37. SUZUKI, A. 2002. Cross-coupling reactions via organoboranes. *Journal of Organometallic Chemistry*. **653** (1) 83 – 90.
38. LIU, S. & XIAO, J. 2007. Towards green catalytic synthesis – Transition-metal catalyzed reactions in non-conventional media. *Journal of Molecular Catalysis A: Chemical*. **270** (1-2) 1 – 43.
39. SONOGASHIRA, K. 2002. Development of Pd-Cu catalyzed cross-coupling of terminal acetylenes with sp²-carbon halides. *Journal of Organometallic Chemistry*. **653** (1-2) 46 – 49.
40. CHINCHILLA, R. & NAJERA, C. 2007. The Sonogashira reaction: A booming methodology in synthetic organic chemistry. *Chemical Review*. **107** (3) 874 – 922.

-
41. NEGISHI, E. & QIAN, M. 2005. Palladium-catalyzed cross-coupling reaction of alkynylzinc with benzylic electrophiles. *Tetrahedron Letters*. **46** (16) 2927 – 2930.
 42. NEGISHI, E., HU, Q., HUANG, Z., QIAN, M. & WANG, G. 2005. Palladium-catalyzed alkenylation by the Negishi coupling. *Aldrichimica Acta*. **38** (3) 78 – 88.
 43. SCOTT, W.J., CRISP, G.T. & STILLE, J.K. 1984. Palladium-catalyzed coupling of vinyl triflates with organostannanes. A short synthesis of Pleraplysillin-1. *Journal of American Chemical Society*. **106** (16) 4630 – 4632.
 44. STILLE, J.K., TUETING, D.R. & ECHAVARREN, A.M. 1989. Palladium-catalyzed coupling of organostannanes with vinyl epoxides. *Tetrahedron*. **45** (4) 979 – 992.
 45. AGUILAR-AGUILA, A. & PEÑA-CABRERA, E. 2007. Selective cross-couplings. Sequential Stille-Liebeskind/Srogl reactions of 3-chloro-4-arylthiocyclobutene-1,2-dione. *Organic Letters*. **9** (21) 4163 – 4166.
 46. PATERSON, I., RAZZAK, M. & ANDERSON, E.A. 2008. Total synthesis of (-)-saliniketals A and B. *Organic Letters*. **10** (15) 3295 – 3298.
 47. BARDER, T.E., WALKER, S.D., MARTINELLI, J.R. & BUCHWALD, S.L. 2004. Catalyst for Suzuki-Miyaura coupling processes: Scope and studies of the effect of ligand structure. *Journal of American Chemical Society*. **127** (13) 4685 – 4696.

-
48. KÜHL, O. 2007. The chemistry of functionalised N-heterocyclic carbenes. *Chemical Society Reviews*. **36** (1) 592 – 607.
49. PINAULT, N. & BRUCE, D.W. 2003. Homogeneous catalysts based on water-soluble phosphines. *Coordination Chemistry Reviews*. **241** (1-2) 1 – 225.
50. JAGTAP, S.V. & DESHPANDE, R.M. 2008. PdCl₂(bipy) complex- An efficient catalyst for Heck reaction in glycol-organic biphasic medium. *Catalysis Today*. **131** (1-2) 353 – 359.
51. SMITH, R.C., BODNER, C.R., EARL, M.J., SEARS, N.C., HILL, N.E., BISHOP, L.M., SIZEMORE, N., HEHEMANN, D.T., BOHN, J.J. & PROTASIEWICZ, J.D. 2005. Suzuki and Heck coupling reactions mediated by palladium complexes bearing trans-spanning diphosphines. *Journal of Organometallic Chemistry*. **690** (1) 477 – 481.
52. NELANA, S.M., CLOETE, J., LISENSKY, G.C., NORDLANDER, E., GUZEI, I.A., MAPOLIE, S.F. & DARKWA, J. 2008. Unconjugated diimine palladium complexes as Heck coupling catalysts. *Journal of Molecular Catalysis A: Chemical*. **285** (1) 72 – 78.
53. HSU, C.M., LI, C.B. & SUN, C.H. 2009. Bipyridine-modulated palladium-catalyzed oxidative Heck-type reactions of arylboronic acids and olefins. *Journal of Chinese Chemical Society*. **56** (5) 873 – 880.
54. HUANG, S.H., CHEN, J.R. & TSAI, F.Y. 2010. Palladium(II)/cationic 2,2'-bipyridyl system as a highly efficient and reusable catalyst for the Mizoroki-Heck reaction in water. *Molecules*. **15** (1) 315 – 330.

-
55. DIEBOLT, O., JURČÍK, V., DA COSTA, R.C., BRAUNSTEIN, P., CAVALLO, L., NOLAN, S.P., SLAWIN, A.M.Z. & CAZIN, C.S.J. 2010. Mixed phosphite/H-heterocyclic carbene complexes: Synthesis, characterization and catalytic studies. *Organometallics*. **29** (6) 1443 – 1450.
56. WANG, J.W., MENG, F.H. & ZHANG, L.F. 2009. Suzuki coupling reaction of aryl halides catalyzed by an N-heterocyclic carbene-PdCl₂ species based on a porphyrin at room temperature. *Organometallics*. **28** (7) 2334 – 2337.
57. RAY, L., BARMAN, S., SHAIK, M.M. & GHOSH, P. 2008. Highly convenient amine-free Sonogashira coupling in air in a polar mixed aqueous medium by *trans*- and *cis*-[(NHC)₂PdX₂] (X=Cl, Br) complexes of N/O-functionalized N-heterocyclic carbenes. *Chemistry- A European Journal*. **14** (22) 6646 – 6655.
58. KANTCHEV, E.A.B., O'BRIEN, C.J. & ORGAN, M.G. 2006. Pd-N-Heterocyclic carbene (NHC) catalysts for cross-coupling reactions. *Aldrichimica Acta*. **39** (4) 93 – 111.
59. BRAYTON, D.F., LARKIN, T.M., VICIC, D.A. & NAVARRO, O. 2009. Synthesis of a bis(phenoxyketimine) palladium(II) complex and its activity in the Suzuki-Miyaura reaction. *Journal of Organic Chemistry*. **694** (1-2) 3008 – 3011.
60. SLAGT, V.F., DE VRIES, A.M.H., DE VRIES, J.G. & KELLOGG, R.M. 2010. Practical aspects of carbon-carbon cross-coupling reactions using heteroarenes. *Organic Process Research & Development*. **14** (1) 30 – 47.

-
61. KLEIST, W., PRÖCKL, S.S. & KÖHLER, K. 2008. Heck reactions of aryl chlorides catalyzed by ligand free palladium salts. *Catalysis Letters*. **125** (1-2) 197 – 200.
 62. GANI, R., JIMÉNEZ-GONZÁLEZ, C. & CONSTABLE, D.J.C. 2005. Method for the selection of solvents for promotion of organic reactions. *Computers and Chemical Engineering*. **29** (1-2) 1661 – 1676.
 63. NICOLAU, K.C., BULGER, P.G., SARLAH, D. 2005. Palladium-catalyzed cross-coupling reactions in total synthesis. *Angewandte Chemie International Edition*. **44** 2768 – 2813.
 64. FRANZÉN, R. & XU, Y. 2005. Review on green chemistry – Suzuki cross-coupling in aqueous media. *Canadian Journal of Chemistry*. **83** 266 – 272.
 65. LIPSHUTZ, B.H. & GHORAI, S. 2008. Transition-metal catalyzed cross-couplings going green: in water at room temperature. *Aldrichimica Acta*. **41** (3) 59 – 72.
 66. CLARK, J.H. & TAVENER, S.J. 2007. Alternative solvents: shades of green. *Organic Process Research and Development*. **11** (1) 149 – 155.
 67. LIU, S. & XIAO, J. 2007. Toward green catalytic synthesis – transition metal-catalyzed reactions in non-conventional media. *Journal of Molecular Catalysis A: Chemical*. **270** (1) 1 – 43.
 68. HELDEBRANT, D.J. & JESSOP, P.G. 2003. Liquid poly(ethylene glycol) and supercritical carbon dioxide: a benign biphasic solvent system for use and recycling of homogeneous catalysts. *Journal of American Chemical Society*. **125** 5600 – 5601.

-
69. KERTON, F.M. 2009. Alternative solvents for green chemistry. RSC Green Chemistry Books Series. Royal Society of Chemistry.
70. CORMA, A., GARCÍA, H. LEYVA, A. 2005. Comparison between polyethyleneglycol and imidazolium ionic liquids as solvents for developing a homogeneous and reusable palladium catalytic system for the Suzuki and Sonogashira coupling. *Tetrahedron*. **61** 9848 – 9854.
71. CORMA, A., GARCÍA, H. LEYVA, A. 2006. Polyethyleneglycol as scaffold and solvent for reusable C-C coupling homogeneous Pd catalysts. *Journal of Catalysis*. **240** (1-2) 87 – 99.
72. GUJAR, A.C & WHITE, M.G. 2009. Ionic liquids as catalysts, solvents and conversion agents. *Catalysis. Royal Society of Chemistry*. **21** 154 – 190.
73. SINGH, R., SHARMA, M., MAMGAIN, R. & RAWAT, D.S. 2008. Ionic liquids: a versatile medium for palladium-catalyzed reactions. *Journal of Brazilian Chemical Society*. **19** (3) 357 – 379.
74. ANDERSON, K.W. & BUCHWALD, S.L. 2005. General catalysts for the Suzuki-Miyaura and Sonogashira coupling reactions of aryl chlorides and for the coupling of challenging substrate combinations in water. *Angewandte Chemie International Edition*. **44** 6173 – 6177.
75. CHANDA, A. & FOKIN, V.V. 2009. Organic synthesis “on water”. *Chemical Reviews*. **109** (2) 725 – 748.
76. MINAKATA, S. & KOMATSU, M. 2009. Organic reactions on silica in water. *Chemical Reviews*. **109** (2) 711 – 724.

-
77. ANASTAS, P.J., KIRCHOFF, M.M. & WILLIAMSON, T.C. 2001. Catalysis as a foundation pillar of Green chemistry. *Green Chemistry*. **221** (1-2) 3 – 13.
78. SAÏD, K., MOUSSAOUI, Y. & BEN SALEM, R. 2009. Heck coupling styrene with aryl halides catalyzed by palladium complexes in biphasic media. *Journal de la Société Chimique de Tunisie*. **11** 59 – 67.
79. FLECKENSTEIN, C.A. & PLENIO, H. 2007. Aqueous cross-coupling: highly efficient Suzuki-Miyaura coupling of N-heteroaryl halides and N-heteroaryboronic acids. *Green Chemistry*. **9** 1287 – 1291.
80. LIANG, B., DAI, M., CHEN, J. & YANG, Z. 2005. Copper-free Sonogashira coupling reaction with PdCl in water under aerobic conditions. *Journal of Organic Chemistry*. **70** (1) 391 – 393.
81. GEENS, J., BOUSSU, K., VANDERCASTEELE, C. & VAN DER BRUGGEN. 2006. Modelling of solute transport in non-aqueous nanofiltration. *Journal of Membrane Science*. **281** (1-2) 139 – 149.
82. BOAM, A. & NOZARI, A. 2006. Fine chemical: OSN – a lower energy alternative. *Filtration + Separation*. April.
83. SILVA, P., HAN, S. & LIVINGSTON, A.G. 2005. Solvent transport in organic solvent nanofiltration membranes. *Journal of Membrane Science*. **262** (1-2) 49 – 59.
84. PINK, C.J., WONG, H., FERREIRA, F.C. & LIVINGSTON, A.G. 2008. Organic solvent nanofiltration and adsorbents; a hybrid approach to achieve

ultra low palladium contamination of post coupling reaction products. *Organic Process Research and Development*. **12** (4) 589 – 595.

85. BARGEMAN, G., VOLLENBROEK, J.M., STRAATSMA, J., SCHROËN, C. G. P. H. & BOOM, R.M. 2005. Nanofiltration of multi-component feeds. Interactions between neutral and charged components and their effect on retention. *Journal of Membrane Science*. **247** (1-2) 11 – 20.
86. STRAATSMA, J., BARGEMAN, G., VAN DER HORST, H.C. & WESSELINGH, J.A. 2002. Can nanofiltration be predicted by a model? *Journal of Membrane Science*. **198** (1) 273 – 284.
87. SILVA, P. & LIVINGSTON, A.G. 2006. Effect of solute concentration and mass transfer limitations on transport in organic solvent nanofiltration – partially rejected solute. *Journal of Membrane Science*. **280** (1-2) 889 – 898.
88. HASSAN, A.R., ALI, N., ABDULL, N. & ISMAIL, A.F. 2007. A theoretical approach on membrane characterization: the deduction of fine structural details of asymmetric nanofiltration membranes. *Desalination*. **206** (1-3) 107 – 126.
89. GIBBINS, E., D'ANTONIO, M., NAIR, D., WHITE, L.S., DOS SANTOS, L. M., VANKELECOM, I. F.J. & LIVINGSTON, A.G. 2002. Observations on solvent flux and solute rejection across solvent resistant nanofiltration membranes. *Desalination*. **147** (1-3) 307 – 313.
90. PATTERSON, D.A., HAVILL, A., COSTELLO, S., SEE-TOH, Y.H., LIVINGSTON, A.G. & TURNER, A. 2009. Membrane characterization by SEM, TEM and ESEM: The implications of dry and wetted microstructure on

mass transfer through integrally skinned polyimide nanofiltration membranes. *Separation and Purification Technology*. **66** (1-2) 90 – 97.

91. WANG, X., SHANG, W., WANG, D., WU, L. & TU, C. 2009. Characterization and applications of nanofiltration membranes: State of the art. *Desalination*. **236** (1-3) 316 – 326.
92. NAKAO, S.S. & KIMURA, S. 1982. Models of membrane transport phenomena and their application for ultrafiltration data. *Journal of Chemical Engineering, Japan*. **15** (3) 200 – 205.
93. WANG, K.Y. & CHUNG, T.S. 2005. The characterization of flat composite nanofiltration membranes and their applications in the separation of Cephalexin. *Journal of Membrane Science*. **247** (1-2) 37 – 50.
94. VAN DER BRUGGEN, B. & VANDERCASTEELE, C. 2002. Modelling the retention of uncharged molecules with nanofiltration. *Water Research*. **36** (1-2) 1360 – 1368.
95. WIJMANS, J.G. & BAKER, R.W. 1995. The solution-diffusion model: a review. *Journal of Membrane Science*. **107** (1-2) 1 – 21.
96. LONSDALE, H., MERTEN, U. & RILEY, R. 1965. Transport properties of cellulose acetate osmotic membranes. *Journal of Applied Polymer Science*. **9** (1) 1341 – 1345.
97. DIJKSTRA, M.F.J. BACH, S. & EBERT, K. 2006. A transport model for organophilic nanofiltration. *Journal of Membrane Science*. **286** (1-2) 60 – 68.

-
98. ROBINSOM, J.P., TARLETON, E.S., MILLINGTON, C.R. & NIJMEIJER, A. 2004. Solvent flux through dense polymeric nanofiltration membranes. *Journal of Membrane Science*. **230** (1) 29 – 37.
99. MASON, E. & LONSDALE, H. 1990. Statistical-mechanical theory of membrane transport. *Journal of Membrane Science*. **51** (1) 43 – 45.
100. BOWEN, W.R. & MUKHTAR, H. 1996. Characterisation and prediction of separation performance of nanofiltration membranes. *Journal of Membrane Science*. **112** (1-2) 263 – 274.
101. SEE TOH, Y.H., LOH, X.X., BISMARCK, A., LI, K. & LIVINGSTON, A.G. 2007. In search of a standard method for the characterization of organic solvent nanofiltration membranes. *Journal of Membrane Science*. **291** (1-2) 120 – 125.
102. PATTERSON, D.A., LAU, L.A., ROENGPITHYA, C., GIBBINS, E.J. & LIVINGSTON, A.G. 2008. Membrane selectivity in the organic solvent nanofiltration of trialkylamine bases. *Desalination*. **218** (1-3) 248 – 256.
103. BELLONA, C., DREWES, J.E., XU, P. & AMY, G. 2004. Factors affecting the rejection of organic solutes during NF/RO treatment – a literature review. *Water Research*. **38** (12) 2795 – 2809.
104. HILAL, N., AL-ABRI, M., AL-HINAI, H. & ABU-ARABI, M. 2008. Characterization and retention of NF membranes using PEG, HS and polyelectrolytes. *Desalination*. **221** (1-2) 284 – 293.
105. MULDER, M. 1998. Basic Principles of Membrane Technology. 2nd ed. Netherlands: Alinea.

-
106. BOWEN, W.R. & WELFOOT, J.S. 2002. Modelling of membrane nanofiltration – pore size distribution effects. *Chemical Engineering Science*. **57** (1-2) 1393 – 1407.
107. KOŠUTIĆ, K., FURAČ, L., SIPOS, L. & KUNST, B. 2005. Removal of arsenic and pesticides from drinking water by nanofiltration membranes. *Separation and Purification Technology*. **42** (2) 137 – 144.
108. LEE, S. & LEE, C-H. 2007. Effect of membrane properties and pre-treatment on flux and NOM rejection in surface water nanofiltration. *Separation and Purification Technology*. **56** (1) 1 – 8.
109. HILAL, N., AL-ZOUBI, H., DARWISH, N.A. & MOHAMMAD, A.W. 2005. Characterisation of nanofiltration membranes using atomic force microscopy. *Desalination*. **177** (1-2) 187 – 199.
110. BOUSSU, K., VAN DER BRUGGEN, B., VOLODIN, A., VAN HAESSENDONCK, C. & VANDECASTEELE, C. 2005. Roughness and hydrophobicity studies of nanofiltration membranes using different modes of AFM. *Journal of Colloid and Interface Science*. **286** (1) 632 – 638.
111. LUTHRA, S.S., YANG, X., FREITAS DOS SANTOS, L.M., WHITE, L.S. & LIVINGSTON, A.G. 2002. Homogeneous phase transfer catalyst recovery and re-use using solvent resistant membranes. *Journal of Membrane Science*. **201** (1-3) 301 – 306.
112. SCARPELLO, J.T., NAIR, D., FREITAS DOS SANTOS, L.M., WHITE, L.S. & LIVINGSTON, A.G. 2002. The separation of homogeneous

-
- organometallic catalyst using solvent resistant nanofiltration. *Journal of Membrane Science*. **203** (1-2) 71 – 85.
113. DATTA, A., EBERT, K. & PLENIO, H. 2003. Nanofiltration for homogeneous catalyst separation: Soluble polymer-supported palladium catalysts for Heck, Sonogashira and Suzuki coupling of aryl halides. *Organometallics*. **22** (1) 4685 – 4691.
114. CHOWDHURY, S.R., WITTE, P.T., BLANK, D.H.A., ALSTERS, P.L. & TEN ELSHOF, J.E. 2006. Recovery of homogeneous polyoxometallate catalysts from aqueous and organic media by a mesoporous ceramic membrane without a loss catalytic activity. *Chemistry:-A European Journal*. **12** (1) 3061 – 3066.
115. GOSSER, L.W., KNOTH, W.H. & PARSHALL, G.W. 1977. Reverse osmosis in homogeneous catalysis. *Journal of Molecular Catalysis*. **2** (4) 253 – 263.
116. ILLINICH, O.M., SEMIN, G.L., VETCHINOVA, Y.S. & ZAMARAEV, K.I. 1994. Reverse osmosis for the separation of reaction solutions in homogeneous catalysis. *Journal of Membrane Science*. **86** (1-2) 37 – 45.
117. NAIR, D., SCARPELLO, J.T., WHITE, L.S., FREITAS DOS SANTOS, L.M., VANKELECOM, I.F.J. & LIVINGSTON, A.G. 2001. Semi-continuous nanofiltration-coupled Heck reactions as a new approach to improve productivity of homogeneous catalysts. *Tetrahedron Letters*. **42** (46) 8219 – 8222.
118. NAIR, D., LUTHRA, S.S., SCARPELLO, J.T., VANKELECOM, I.F.J., FREITAS DOS SANTOS, L.M., WHITE, L.S., KLOETZING, R.J., WELTON,

-
- T & LIVINGSTON, A.G. 2002. Increased catalytic productivity for nanofiltration-coupled reactions using highly stable catalyst systems. *Green Chemistry*. **4** (1) 319 – 324.
119. GÁLLEGO, I., MALLADA, R., URRIOLABEITIA, E.P., NAVARRO, R., MENÉNDEZ, M. & SANTAMARÍA, J. 2004. Selective separation of homogeneous catalysts using silicate membranes. *Inorganica Chimica Acta*. **357** (15) 4577 – 4581.
120. AERTS, S., BUEKENHOUDT, A., WEYTEN, H., GEVERS, L.E.M., VANKELECOM, I.F.J. & JACOBS, P.A. 2006. The use of solvent resistant nanofiltration in the recycling of the Co-Jacobsen catalyst in the hydrolytic kinetic resolution (HKR) of epoxides. *Journal of Membrane Science*. **280** (1-2) 245 – 252.
121. FERREIRA, F.C., BRANCO, L.C., VERMA, K.K., CRESPO, J.G. & AFONSO, C.A.M. 2007. Application of nanofiltration to re-use the sharpless asymmetric dihydroxylation catalytic system. *Tetrahedron: Asymmetry*. **18** (1-2) 1637 – 1641.
122. VAN DER GRYP, P., BARNARD, A., CRONJE, J-P., DE VLIETGER, D., MARX, S. & VOSLOO, H.C.M. 2010. Separation of different metathesis Grubbs-type catalysts using organic solvent nanofiltration. *Journal of Membrane Science*. **353** (1-2) 70 – 77.

CHAPTER 3 – EXPERIMENTAL AND ANALYTICAL PROCEDURE

In this chapter experimental and analytical methodology is discussed in detail. In Section 3.1, the membranes used in the study are identified. The chemicals and reagents used in membrane characterization are listed. The membrane unit used for filtration is described in Section 3.2. Analytical instrumentation used is outlined in the Section 3.3. Membrane characterization experiments and techniques are described in Section 3.4. Coupling reactions are dealt with in Section 3.5. Catalyst retention and reuse experiments are described in Section 3.6.

TABLE OF CONTENTS

3.1	MATERIALS.....	67
3.1.1	Chemicals and Reagents	67
3.1.2	Catalysts.....	68
3.1.3	Membranes	69
3.2	EXPERIMENTAL SETUP.....	69
3.3	ANALYTICAL INSTRUMENTATION	71
3.3.1	Gas Chromatography (GC)	71
3.3.2	Ultraviolet-Visible Spectrometry (UV-VIS)	71
3.3.3	Scanning Electron Microscopy (SEM)	72
3.3.4	Atomic Force Microscopy (AFM)	72
3.3.5	Fourier-Transform Infrared Spectroscopy (FTIR)	72
3.4	METHODOLOGY	73
3.4.1	Pure-Water Permeability	73
3.4.2	Membrane-Solvent Compatibility.....	74
3.4.3	Pure Solvent Permeability	74
3.4.4	Swelling Experiments	75
3.4.5	Uncharged Solutes Rejection	75
3.4.6	Scanning Electron Microscopy (SEM)	77
3.4.7	Atomic Force Microscopy (AFM)	77
3.4.8	Fourier Transform Infrared (FTIR)	77
3.5	CATALYST PREPARATION AND CHARACTERIZATION.....	78
3.5.1	Preparation and Characterization by FTIR	78
3.5.2	Carbon-carbon coupling reactions.....	78
3.5.2.1	<i>Heck Coupling Reaction</i>	79
3.5.2.2	<i>Suzuki Coupling Reaction</i>	79
3.5.2.3	<i>Sonogashira Coupling Reaction</i>	79
3.6	CATALYST RETENTION MEASUREMENTS	80
3.7	CATALYST SEPARATION AND REUSE	81
	REFERENCES.....	83

3.1 MATERIALS

3.1.1 Chemicals and Reagents

Chemicals and reagents used in the study were obtained commercially. These were of highest purity. All solvents were used as received. The chemicals are listed in Table 3. 1.

Table 3. 1: Chemicals and reagents used in the study

Chemical	Supplier	Formula	Grade
D-Glucose	Sigma-Aldrich	C ₆ H ₁₂ O ₆	AR 98%
Sucrose	Sigma-Aldrich	C ₁₂ H ₂₂ O ₁₁	AR 98%
Methanol	Sigma-Aldrich	CH ₄ O	Chromasolv 99,9%
Ethanol	Merck	C ₂ H ₆ O	LiChrosolv 99,8%
2-Propanol	Merck	C ₃ H ₈ O	LiChrosolv 99,8%
Acetonitrile	Sigma-Aldrich	C ₂ H ₃ N	Chromasolv 99,9%
Ethyl acetate	Merck	C ₄ H ₈ O ₂	LiChrosolv 99,8%
Dichloromethane	Merck	CH ₂ Cl ₂	LiChrosolv 99,9%
Tetrahydrofuran	Merck	C ₄ H ₈ O	LiChrosolv 99,7%
Toluene	Merck	C ₇ H ₁₀	LiChrosolv 99,9%
n-Hexane	Merck	C ₆ H ₁₄	LiChrosolv 99,9%
Iodobenzene	Sigma-Aldrich	C ₆ H ₅ I	Reagent Plus 98%
Bromobenzene	Sigma-Aldrich	C ₆ H ₅ Br	Reagent Plus 98%
Sodium carbonate	Sigma-Aldrich	Na ₂ CO ₃	AR 98%
Triethylamine	Sigma-Aldrich	C ₆ H ₁₅ N	Reagent Plus 99,5%
Pyrrolidine	Sigma-Aldrich	C ₄ H ₇ NO	Reagent Plus 98%
Phenylboronic acid	Sigma-Aldrich	C ₆ H ₅ B(OH) ₂	Reagent Plus 95%
Phenylacetylene	Sigma-Aldrich	C ₈ H ₆	Reagent Plus 98%
Styrene	Sigma-Aldrich	C ₈ H ₈	Reagent Plus >99%
2,2'-Bipyridyl	Merck	C ₁₀ H ₈ N ₂	Reagent Plus >99%
Triphenylphosphine	Sigma-Aldrich	C ₁₈ H ₁₅ P	AR >=95%
Trans-stilbene	Sigma-Aldrich	C ₁₄ H ₁₂	Reagent Plus 99,5%

3.1.2 Catalysts

Transition-metal catalysts [$\text{Pd}(\text{OAc})_2$, $\text{Pd}(\text{PPh}_3)_2\text{Cl}_2$ and PdCl_2] were obtained commercially from Sigma-Aldrich. $\text{Pd}(\text{OAc})_2(\text{PPh}_3)_2$ was prepared using the method described by Seayad *et al.* [1]. The molecular weight and structure of the catalysts are two parameters that are important in this study. The catalysts and their molecular weights are listed in Table 3. 2 below. The chemical configurations of the catalysts are illustrated in Figure 3. 1.

Table 3. 2: Catalysts used in the study

Catalyst	MW	Formula
Palladium(II)chloride	177.1 g.mol ⁻¹	PdCl_2
Palladium(II) acetate	224.5 g.mol ⁻¹	$\text{Pd}(\text{OAc})_2$
Dichlorobis(triphenylphosphine)palladium(II)	701.9 g.mol ⁻¹	$\text{Pd}(\text{PPh}_3)_2\text{Cl}_2$
Diacetatobis(triphenylphosphine)palladium(II)	749.0 g.mol ⁻¹	$\text{Pd}(\text{OAc})_2(\text{PPh}_3)_2$

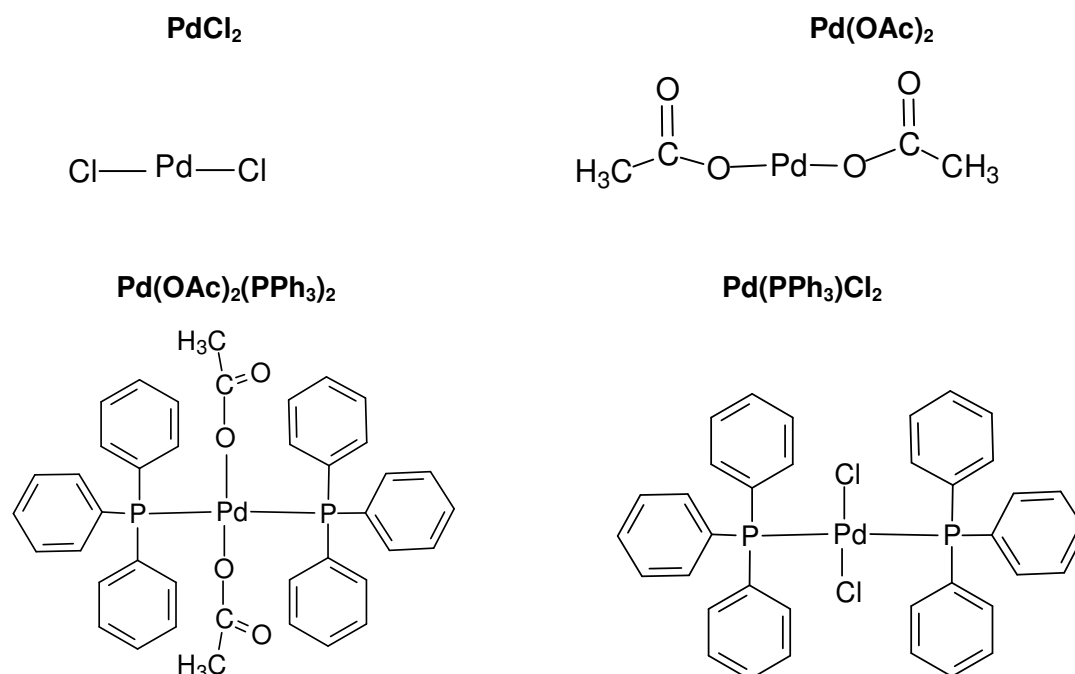


Figure 3. 1: Structures of the catalysts used in the study

3.1.3 Membranes

Four commercially available NF/RO membranes were used for this study (NF90, NF270, BW30 and XLE). The membranes were all supplied by Dow/FilmTec (Minneapolis, MN, USA) and are all thin-film composite membranes [2]. NF270 is made from polypiperazine and benzenetricarbonyl trichloride. NF90, BW30 and XLE are also made from benzenetricarbonyl trichloride as a starting material, but 1,3-phenylene amide is used instead of polypiperazine to complete interfacial polymerization [3]. The specifications of the membranes obtained from the supplier are given in Table 3. 3 below.

Table 3. 3: Membrane characteristics as specified by the supplier [2]

Membrane	NF90	NF270	BW30	XLE
Membrane Type	Aromatic PA	Aliphatic/ Aromatic PA	Aromatic PA	Aromatic PA
Molecular weight cut-off (Da)	150	200	N/A	N/A
Permeate flow at std conditions (l.h ⁻¹)	83-1620	134-2300	120-1660	52-2040
Maximum operating pressure (bar)	41	41	41	41
pH range	3-10	3-10	2-11	2-11

3.2 EXPERIMENTAL SETUP

A bench scale stainless steel dead-end module with a capacity of 1.2 litres was used. The unit is illustrated in Figure 3. 2. It was operated at pressures of up to 25 bar using nitrogen as a driving force. The unit was fitted with a Teflon-coated magnetic stirrer supported on the upper lid by a steel rod. Stirring was required to homogenize the sample and to minimize the effects of concentration polarization [4]. Disc samples of the different membranes with a diameter of 9 cm and an effective area of 0.0064 m² were cut and placed on a porous support disc.

The hold-up volume underneath the porous support disc was ~1 ml. Permeate was collected from a Teflon tube into a measuring cylinder. Filtration measurements were performed by loading feed solutions with a volume ranging from 250 ml to 600 ml at room temperature. The first 20 ml of permeate collected was discarded. Thereafter a certain volume of permeate was collected at a specified time.

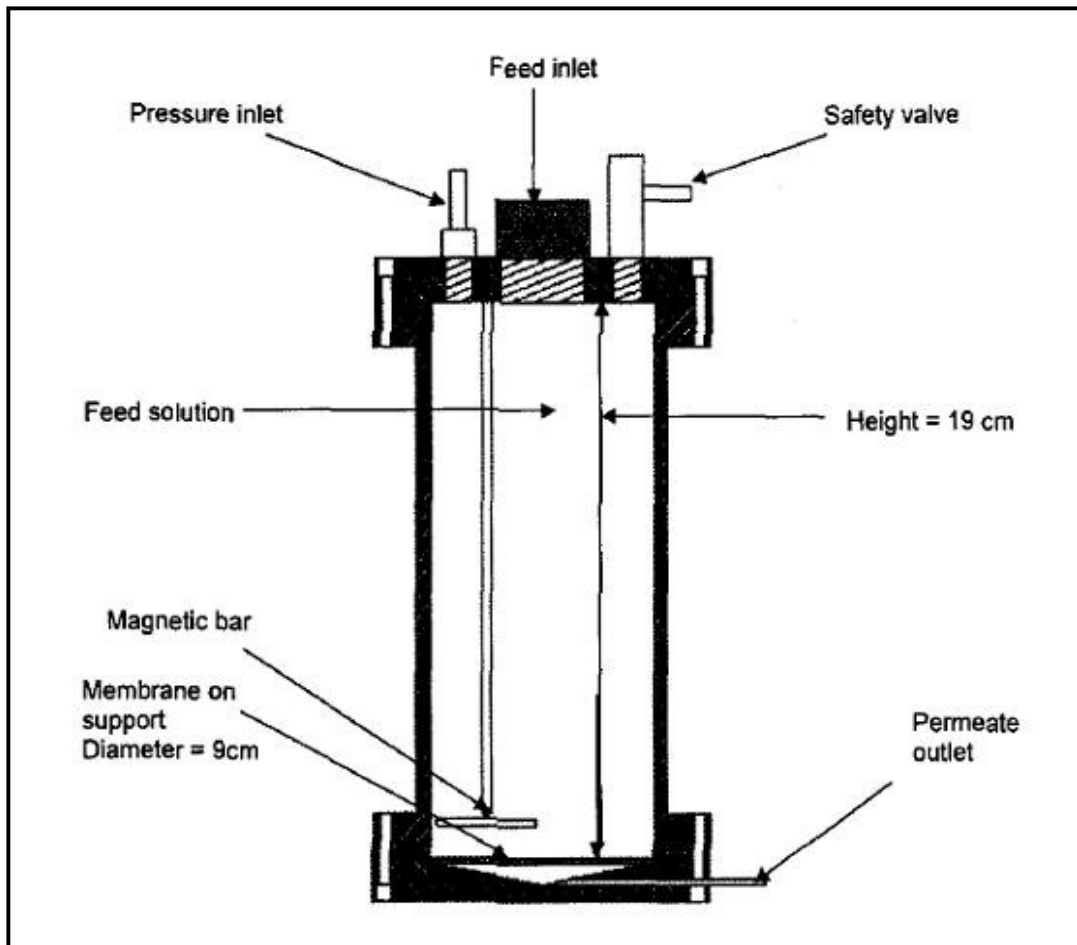


Figure 3. 2: Dead-end unit used for filtration

3.3 ANALYTICAL INSTRUMENTATION

All analytical instruments used in the study are discussed in this section. Most of the instruments were used in-house, and a few were outsourced externally.

3.3.1 Gas Chromatography (GC)

The concentration of 2-propanol in the feed and permeate obtained during membrane characterization were determined by gas chromatography (GC). GC was also used to determine conversions in C-C coupling reactions. A Perkin-Elmer Clarus 500 GC was used. The instrument is fitted with the Elite-5 packed column (5% Diphenyl/95% Dimethyl Polysiloxane) with 30 m x 0.32 mm x 0.25 dimensions. The instrument is also fitted with an FID and a TCD detector. Nitrogen was used as carrier gas. Air and hydrogen were used as auxiliary gases. 1 μ l samples were injected as they were, with no pre-treatment performed.

3.3.2 Ultraviolet-Visible Spectrometry (UV-VIS)

A Perkin-Elmer Lambda 25 UV-VIS Spectrophotometer was used to determine the concentrations of D-glucose, sucrose, Pd(OAc), PdCl₂, Pd(PPh₃)₂Cl₂ and Pd(OAc)₂(PPh₃)₂ in the feed and permeate. The instrument is equipped with two radiation sources, a deuterium lamp and a tungsten halogen lamp. These two sources are essential in order to cover the whole range of wavelengths in the UV and visible regions. The instrument also has a monochromator which is a concave grating with 1053 lines/mm in the center. The monochromator serves to produce a narrow beam of radiation, therefore improving resolution of spectra.

3.3.3 Scanning Electron Microscopy (SEM)

A Carl Zeiss ULTRA 55 FEGSEM was outsourced from Sasol Technology R&D for characterization of the morphology of the polymeric membranes. The state-of-the-art instrument has a field emission electron source which enables high resolution imaging. The instrument is fitted with an array of detectors which include an in-lens secondary electron (SE) detector and an Everhardt-Thornley SE. Imaging of the surface and cross-section was performed at acceleration voltages of 3 and 5 kV using the Everhardt-Thornley SE detector. The sample was set at working distance of 8 mm.

3.3.4 Atomic Force Microscopy (AFM)

A Park Scientific AFM instrument was outsourced from Witwatersrand University for surface roughness determination and imaging. Roughness has been observed to influence the flux and rejection behaviour of nanofiltration membranes [5]. Imaging was performed using contact mode in air at room temperature. Roughness measurements were performed over an area of 50 μm x 50 μm . Roughness was expressed as root mean square (RMS) roughness, which is defined as the square root of the mean value of the squares of the distance of the points from the image mean value [6].

3.3.5 Fourier-Transform Infrared Spectroscopy (FTIR)

Characterization of the chemical structure of the polymer was done using Fourier-transform Infrared spectroscopy (FTIR). FTIR gives information on the specific chemistry and orientation of the structure of the functional groups present in the membrane active layer [7]. A Perkin-Elmer Spectrum 400 Spectrophotometer fitted with a universal ATR sampler was used. The instrument is fitted with a universal sampler crystal that allows direct analysis of samples without pre-treatment.

3.4 METHODOLOGY

In this study, the membranes were characterized for pure water permeability, pure solvent permeability, swelling tendency and surface morphology by means of SEM and AFM. Uncharged solute rejection measurements and chemical structure determination were also performed. The catalysts were characterized by FTIR.

3.4.1 Pure-Water Permeability

Pure water permeability reflects the porous nature of a membrane. By measuring the membrane's dependence on pressure, it is possible to characterize the porosity of the membrane's active layer [8]. Membrane samples were immersed in ultra pure deionized water for 24 hour as a preconditioning procedure. Pure water permeability measurements were then performed at pressures of 5, 10, 15 and 20 bar respectively, while keeping the time constant. Pure water permeability was calculated using the Kedem-Katchalsky equation, described in Equation 3.1 [9]:

$$J_w = A_w \cdot (\Delta P - \sigma \Delta \pi) \quad \text{Equation 3.1}$$

J_w is the pure water flux, A_w is the pure water permeability, ΔP is the pressure difference, σ is the reflection coefficient and $\Delta \pi$ is the osmotic pressure difference. In the case where the feed and retentate both contain pure water, the osmotic pressure difference across the membrane becomes zero, therefore Equation 3.1 reduces to Equation 3.2:

$$J_w = A_w \cdot \Delta P \quad \text{Equation 3.2}$$

3.4.2 Membrane-Solvent Compatibility

Membrane appearance after soaking in organic solvents for a period of time can give a preliminary insight into the membrane stability in the solvents [10]. Flat sheet membrane samples were cut into discs with a diameter of 9 cm. Each membrane was immersed in methanol, ethanol, 1-propanol, 2-propanol, acetonitrile, ethylacetate, dichloromethane, tetrahydrofuran and toluene for 24 hours to check for stability. Stability was determined by visual inspection of the membrane surface and general appearance after contact with solvent. Suitable solvents were selected based on their compatibility with the membranes. These solvents were used in pure-solvent permeability studies and coupling reactions

3.4.3 Pure Solvent Permeability

Membrane samples were cut into discs with a diameter of 9 cm and immersed in ultra pure water for 24 hours. The preconditioned samples were then immersed for 2 hours in the solvent prior to filtration measurements. The volume of the feed solution ranged from 500 to 800 ml. During solvent permeation, the measuring cylinder used for permeate collection was covered to minimize solvent loss due to evaporation. Solvent flux was calculated by Equation 3.3:

$$J = \frac{V}{At} \quad \text{Equation 3.3}$$

where J is the solvent flux, V is the volume of solvent permeated, A is the effective membrane area and t is the permeation time.

3.4.4 Swelling Experiments

The interaction of the solvents with the membrane physical structure was further investigated by measuring the swelling tendency of the membranes. Membranes were cut and dried at room temperature in an open dish. Each dried membrane was weighed and immersed in the selected solvents. After equilibrium time of approximately 30 minutes, the membrane was removed from the solvent and quickly dried with a soft tissue to remove the solvent from the external surface before weighing. Swelling of the membrane was calculated by Equation 3.4 [11]:

$$Q = \frac{1}{\rho_s} \frac{W_{wet} - W_{dry}}{W_{dry}} \quad \text{Equation 3. 4}$$

In the equation, Q is the swelling, W_{wet} is the mass of wet membrane, W_{dry} is the mass of dry membrane and ρ_s the density of the solvent.

3.4.5 Uncharged Solutes Rejection

Uncharged solutes were used to determine the molecular weight cut-off (MWCO) of the membranes. 2-Propanol, D-glucose and sucrose were chosen for this investigation. Feed solutions of 0.1 vol% for the alcohols and 0.1 wt% for the sugars were prepared. 800 ml of each feed solution was charged into the dead-end unit for filtration at 10 and 20 bar pressure. A summary of instrument settings for alcohol analysis is given in.

Table 3. 4: Instrument settings for GC analysis of the alcohol

Injector temperature	305°C
Oven initial temperature	60°C (hold for 5 min)
Heating rate	10°C/min to 220°C
Carrier gas	Nitrogen
Detector	FID
Detector temperature	300°C

The concentrations of the sugars in the feed and permeate were determined by the Anthrone method [12], at a wavelength $\lambda = 630$ nm. Rejection of the solutes was calculated using Equation 3.5:

$$R = \left(1 - \frac{C_{permeate}}{C_{feed}} \right) \times 100\% \quad \text{Equation 3.5}$$

$C_{permeate}$ is the concentration of the permeate and C_{feed} is the concentration of the feed. The Stokes radius r_s (nm) of the solutes were calculated by the following expression [13]:

$$\log r_s = -1.485 + 0.461(\log M_w) \quad \text{Equation 3.6}$$

M_w is the molecular weight. The Stokes radius can be used to relate rejection to the membrane porosity. A plot of rejection vs stokes radius gives an indication of molecular weight-cut off.

3.4.6 Scanning Electron Microscopy (SEM)

Membrane samples were placed in liquid nitrogen for few hours, and cut to dimensions of ~5 mm x 5 mm. The samples were dried in an oven set at 40°C for 4 hours. The dried samples were mounted on aluminium stubs covered with double-sided carbon tape. The samples were coated with a thin layer of palladium-gold using a sputter coater. The coating prevents specimen-charging inside the microscope. Coating also protects samples from beam-damage. After coating, the membranes were loaded into the microscope for analysis.

3.4.7 Atomic Force Microscopy (AFM)

Membranes were cut into pieces with dimensions of ~8 mm x 8 mm. The samples were mounted on a stainless steel disc covered with double-sided carbon tape. No other preparative procedure was performed on the membranes. AFM allows analysis of samples at room temperature and pressure. Samples can be analysed directly either dry or in liquid [5].

3.4.8 Fourier Transform Infrared (FTIR)

The membranes were dried prior to analysis. The dried samples were pressed tightly against the crystal plate. 256 scans were obtained from 650 to 4000 cm^{-1} at 2 cm^{-1} resolution for each membrane sample. For wet samples such as reaction mixtures, a drop was placed on the crystal using a micropipette. The crystal was then pressed tightly until a spectrum was observed.

3.5 CATALYST PREPARATION AND CHARACTERIZATION

3.5.1 Preparation and Characterization by FTIR

$\text{Pd}(\text{OAc})_2(\text{PPh}_3)_2$ was prepared by mixing (0.2604 g, 1.16 mmol) $\text{Pd}(\text{OAc})_2$ and (0.6164 g, 2.35 mmol) PPh_3 in toluene with vigorous shaking. *n*-Hexane was added and the precipitate was filtered, and washed with *n*-hexane. The precipitate was dried under vacuum filtration. $\text{Pd}(\text{OAc})_2(\text{PPh}_3)_2$, $\text{Pd}(\text{OAc})_2$, $\text{Pd}(\text{PPh}_3)\text{Cl}_2$ and PdCl_2 were characterized by FTIR. 256 scans were obtained from 650 to 4000 cm^{-1} at 2 cm^{-1} resolution for each catalyst sample.

3.5.2 Carbon-carbon coupling reactions

C-C coupling reactions were performed to evaluate the catalysts performance. Catalytic reactions that were considered are Heck, Suzuki-Miyaura and Sonogashira coupling reactions. A summary of instrument settings for GC analysis of coupling products is given in Table 3. 5.

Table 3. 5: Instrument settings for GC analysis of coupling products

Injector temperature	305°C
Oven initial temperature	120°C (hold for 5 min)
Heating rate	10°C/min to 220°C (hold for 5 min)
Carrier gas	Nitrogen
Detector	FID
Detector temperature	300°C

3.5.2.1 Heck Coupling Reaction

A 100 ml two-necked round-bottom flask fitted with a reflux condenser, stirrer and thermometer was charged with the aryl halide (24.0 mmol), styrene (20.20 mmol), base (20.80 mmol) and water (5.5%). To the resultant mixture, the catalyst (0.0004 eq) and ligand (0.0016 eq) were added. The solution was made up to 27 ml with the solvent. The mixture was heated in an oil bath set at 80°C for 6-8 hours. Initial and final samples were taken for GC analysis using a needle and 1 ml syringe.

3.5.2.2 Suzuki Coupling Reaction

A 100 ml two-necked round bottom flask fitted with a reflux condenser, stirrer and thermometer was charged with the aryl halide (20.0 mmol), the aryl boronic acid (23 mmol) and *n*-propanol (25 ml). The mixture was gently stirred for 15 to 20 minutes. To the resultant solution, the catalyst (0.005 eq), ligand (0.016 eq), base (10 ml) and water (5 ml) were added. The solution was heated under reflux in an oil bath set at 80°C until the no further change in conversions was observed (~ 2 hours). Initial and final samples were taken for GC analysis using a needle and 1 ml syringe.

3.5.2.3 Sonogashira Coupling Reaction

A 100 ml two-necked round bottom flask fitted with a reflux condenser, stirrer and thermometer was charged with the aryl halide (20 mmol), phenylacetylene (25 mmol), base (40 mmol), palladium catalyst (0.005 eq) and ligand (0.016 eq) in water (20ml). The flask was heated in an oil bath at 70°C for 6-8 hours. After vigorous stirring, the reaction mixture darkened in colour. Initial and final samples were taken for GC analysis using a needle and 1 ml syringe.

3.6 CATALYST RETENTION MEASUREMENTS

In this phase of study, solvent-solute and membrane-solute interactions were of importance. The interaction and influence of the solvents on catalyst rejection was investigated. The catalyst rejection behaviour was initially determined in a single-component solution, where only the catalyst was present in solution as illustrated in Figure 3. 3. In this way, only the effect of the solvent on rejection can be determined.

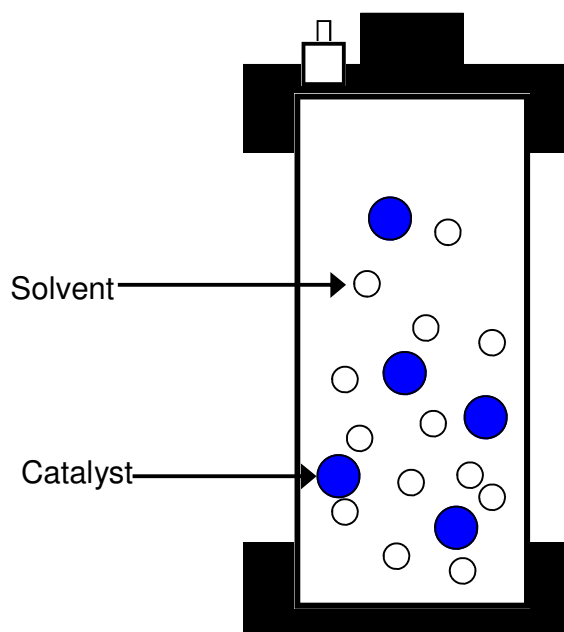


Figure 3. 3: Graphic representation of a catalyst single-component solution

Solutions of each palladium catalyst were prepared with concentration of 0.5 mmol. The feed solution was then charged into the dead-end unit for filtration at 10 and 20 bar. After 20 – 25 ml of permeate was collected, filtration was stopped. The retentate was sampled for UV-VIS analysis. The rejection of the palladium catalysts were calculated using Equation 3.4.

3.7 CATALYST SEPARATION AND REUSE

In the last phase of the study, the rejection of the catalysts in a real reaction mixture was investigated. The hypothesis was that sufficient catalyst rejection will enable separation of the catalyst from the mixture. Solute-solute interactions come into play once again. The influence of other reaction components such as the ligand and reactants on catalyst rejection was of importance. In this multi-component solution illustrated in Figure 3. 4, the catalyst rejection behaviour was expected to be different from that of the single- and binary-component solutions.

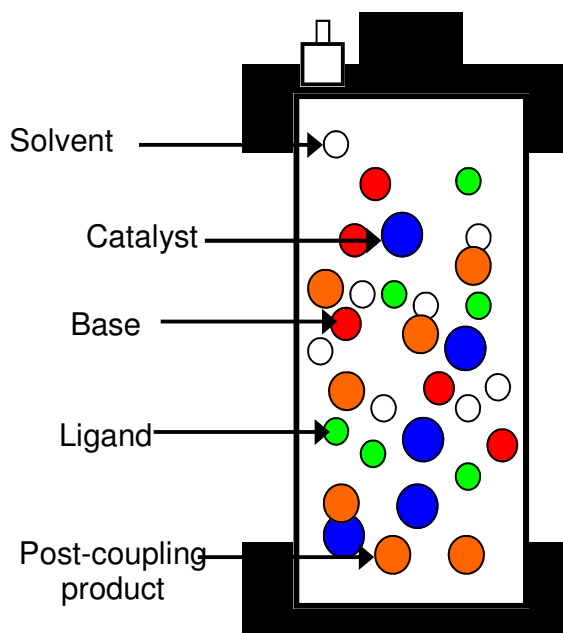


Figure 3. 4: Graphic representation of a coupling reaction mixture

The Heck coupling reaction was selected for attempted catalyst separation. The rationale followed by Nair *et al.* [14] was used. The reaction was performed as described in Section 3.5.2 and was allowed to proceed for 4 to 6 hours. At this point the reaction was stopped and cooled to room temperature. The cooled solution was immediately charged into the dead-end unit for filtration.

A feed sample was taken for UV-VIS analysis prior to filtration. After which filtration was performed at 10 bar until ~70% of the volume had permeated. The retentate was also sampled for UV-VIS analysis. The rejection of the catalyst by the membrane was then calculated using Equation 3.4. This concentrated retentate solution was then transferred back to the reaction flask. Fresh reactants and solvent were topped up. A second reaction was initiated and followed for 4 hours.

The same filtration protocol was performed and the retentate was used to initiate a third reaction. The third reaction was followed until no further change in conversions could be observed. This procedure was repeated two times per membrane in order to get an overall concept of the efficiency of catalyst separation. A summarized flow scheme for the catalyst separation and reuse procedure is illustrated in Figure 3. 5.

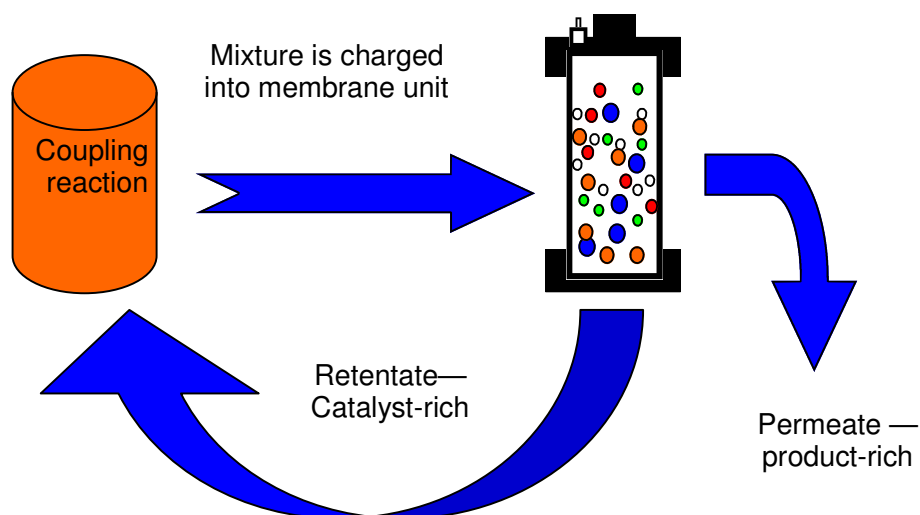


Figure 3. 5: Schematic of catalyst separation and reuse procedure

REFERENCES

1. SEAYAD, A., KELKAR, A.A., TONIOLO, L. & CHAUDHARI, R.V. 2000. Hydroesterification of styrene using an in situ formed Pd(OTs)₂(PPh₃)₂ complex catalyst. *Journal of Molecular Catalysis A: Chemical*. **151** (1) 47 – 59.
2. <http://www.dow.com/liquidseps/> accessed 25/05/2009.
3. BOUSSU, K., ZHANG, Y., COCQUYT, J., VAN DER MEEREN, P., VOLODIN, A., VAN HAESDONCK, C., MARTENS, J.A. & VAN DER BRUGGEN, B. 2006. Characterization of polymeric nanofiltration membranes for systematic analysis of membrane performance. *Journal of Membrane Science*. **278** (1-2) 418 – 427.
4. KRIEG, H.M., MODISE, S.J., KEIZER, K. & NEOMAGUS, H.W.J.P. 2004. Salt rejection in nanofiltration for single and binary salt mixtures in view of sulphate removal. *Journal of Membrane Science*. **175** (1-2) 205 – 215.
5. HILAL, N., AL-ZOUBI, H., DARWISH, N.A. & MOHAMMAD, A.W. 2005. Characterisation of nanofiltration membranes using atomic force microscopy. *Journal of Membrane Science*. **177** (1-2) 187 – 199.
6. FREGER, V. 2004. Swelling and morphology of the skin layer of polyamide composite membranes: An atomic force microscopy study. *Environmental Science and Technology*. **38** (11) 3168 – 3175.
7. XU, P. & DREWES, J.E. 2006. Viability of nanofiltration and ultra-low pressure reverse osmosis membranes for multi-beneficial use of methane produced water. *Separation and Purification Technology*. **52** (1) 67 – 76.

-
8. KOŠUTIĆ, K., DOLAR, D. & KUNST, B. 2006. On the experimental parameters characterizing the reverse osmosis and nanofiltration membranes' active layer. *Journal of Membrane Science*. **282** (1-2) 109 – 114.
 9. VAN DER BRUGGEN, B. & VANDECASTEELE, C. 2001. Flux decline during nanofiltration of organic components in aqueous solution. *Environmental Science & Technology*. **35** (17) 3535 – 3540.
 10. SCARPELLO, J.T., NAIR, D., FREITAS DOS SANTOS, L.M., WHITE, L.S. & LIVINGSTON, A.G. 2002. The separation of homogeneous organometallic catalyst using solvent resistant nanofiltration. *Journal of Membrane Science*. **203** (1-2) 71 – 85.
 11. GEENS, J., VAN DER BRUGGEN, B. & VANDECASTEELE, C. 2004. Characterization of the solvent stability of polymeric nanofiltration membranes by measurement of contact angles and swelling. *Chemical Engineering Science*. **59** (1-2) 1161 – 1164.
 12. DE BRUYN, J.W., VAN KEULEN, H.A. & FERGUSON, J.H.A. 1968. Rapid method for the simultaneous determination of glucose and fructose using anthrone reagent. *Journal of the Science of Food and Agriculture*. **19** (10) 597 – 601.
 13. WANG, K.Y. & CHUNG, T.S. 2005. The characterization of flat composite nanofiltration membranes and their applications in the separation of Cephalexin. *Journal of Membrane Science*. **247** (1-2) 37 – 50.
 14. NAIR, D., LUTHRA, S.S., SCARPELLO, J.T., WHITE, L.S., FREITAS DOS SANTOS, L.M. & LIVINGSTON, A.G. 2002. Homogeneous catalyst

separation and re-use through nanofiltration of organic solvents.
Desalination. **147** (1-2) 301 – 306.

CHAPTER 4 – RESULTS AND DISCUSSION

This chapter deals with results obtained in membrane characterization, catalyst characterization and rejection measurements. The results are discussed, with the aim of highlighting observations on membrane-solvent, solute-solvent and membrane-solute interactions respectively. These interactions are important as they influence the rejection and flux properties of the polymeric membranes. The rejection behaviour of the transition-metal catalysts is also discussed in detail. At this point, the applicability of membranes in separating the catalyst from a real reaction mixture is probed, with the aim of reusing the catalyst.

TABLE OF CONTENTS

4.1	MEMBRANE CHARACTERIZATION.....	88
4.1.1	Pure Water Permeability.....	88
4.1.2	Membrane-Solvent Compatibility.....	93
4.1.3	Pure Solvent Permeability	95
4.1.4	Swelling Experiments	102
4.1.5	Uncharged Solute Rejection Measurements	106
4.1.6	Morphological Investigation by Scanning Electron Microscopy (SEM)	108
4.1.7	Topography and Surface Roughness Investigation by Atomic Force Microscopy (AFM)	110
4.1.8	Membrane Chemical Structure Investigation by Fourier Transform – Infra Red Spectroscopy (FTIR).....	113
4.2	CATALYST CHARACTERIZATION.....	116
4.2.1	Catalyst chemical structure investigation by Fourier Transform – Infra Red Spectroscopy (FTIR).....	116
4.2.2	Carbon-carbon Coupling Reactions.....	119
4.3	CATALYST RETENTION MEASUREMENTS	122
4.3.1	Retention Measurements in Acetonitrile.....	122
4.3.2	Retention Measurements in 2-Propanol	125
4.3.3	Retention Measurements in Water	128
4.4	CATALYST SEPARATION AND REUSE	131
	REFERENCES.....	135

4.1 MEMBRANE CHARACTERIZATION

Results obtained from membrane characterization techniques are unpacked in this section. The results showcase the most suitable membranes for later application in catalyst rejection and reuse.

4.1.1 Pure Water Permeability

Pure water permeability was investigated using two methods. These are Kedem-Katchalsky model for irreversible thermodynamics [1] and the Košutić method [2]. The rationale for the approach is to show the robustness of the pure water permeability method. The Kedem-Katchalsky model is expressed in Equation 4.1:

$$J_w = A_w (\Delta P - \sigma \Delta \pi) \quad \text{Equation 4.1}$$

where J_w is the water flux, A_w is the membrane permeability, ΔP is the pressure difference, σ is the reflection coefficient and $\Delta \pi$ is the osmotic pressure difference. In the case where only pure water is present, the osmotic pressure difference becomes zero, therefore Equation 4.1 reduces to Equation 4.2:

$$J_w = A_w \cdot \Delta P \quad \text{Equation 4.2}$$

Pure water permeability A_w is obtained from a slope of J_w vs. ΔP shown in Figure 4. 1. Values of A_w , obtained from the Kedem-Katchalsky model, are listed in Table 4. 1.

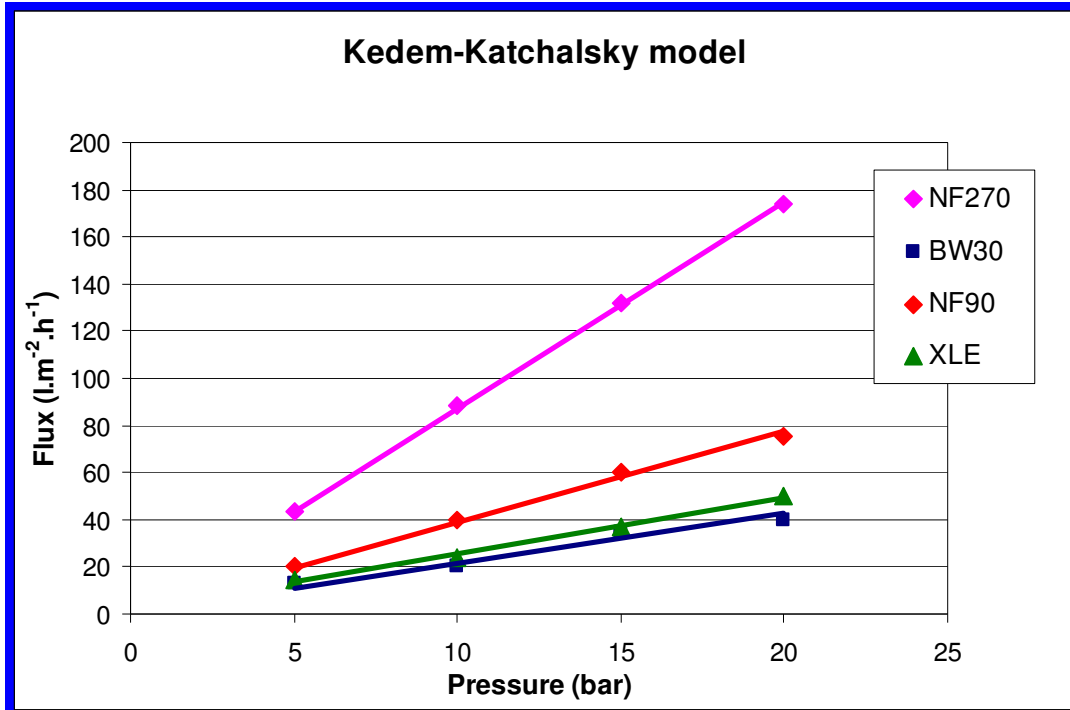


Figure 4. 1: Relationship of water flux and pressure (Kedem-Katchalsky approach)

The approach by Košutić *et al.* [2] expresses pure water permeability by Equation 4.3:

$$\frac{J_w}{\Delta P} = A_w \cdot e^{-\alpha \Delta P} \quad \text{Equation 4.3}$$

This equation can be expressed in logarithmic form as shown in Equation 4.4:

$$\ln\left(\frac{J_w}{\Delta P}\right) = \ln A_w - \alpha \Delta P \quad \text{Equation 4.4}$$

where A_w is the pure water permeability that depends on the membrane pore radius, membrane tortuosity, water viscosity and the active layer thickness, and α represents the measure of the susceptibility of the membrane active layer

structure under pressure. Porosity of the membranes can be related to the water permeability by Darcy's law as described in Equation 4.5 [3]:

$$A_w = \frac{r_p^2}{8 \eta \Delta x} \quad \text{Equation 4.5}$$

where r_p is the effective membrane pore radius, η is the viscosity and Δx is the effective membrane thickness. Therefore, values of A_w can be used to estimate membrane porosity [4].

Table 4. 1: Pure water permeability values (Kedem-Katchalsky approach)

Membrane	A_w (l.m ⁻² .h ⁻¹ .bar ⁻¹)
NF90	3.8
NF270	8.9
BW30	2.1
XLE	2.4

Results from the Kedem-Katchalsky approach show a linear relationship between water flux and applied pressure. The water flux through all the membranes shows an increase with increasing pressure. NF270 has the highest fluxes. The fluxes can be expressed in a decreasing order as NF270 > NF90 > XLE > BW30. Values of A_w , obtained from the slope of the Kedem-Katchalsky approach, show that NF270 has the largest pure water permeability followed by NF90, XLE and BW30 in the same order as mentioned previously.

It is interesting to note that the pure water permeability value of NF270 is twice that of NF90, and more than four-times that of XLE and BW30. It is consequently, expected that the pore sizes will follow the same trend. According to Equation 4.3, the effective membrane pore radius will increase proportionally with pure water permeability. This is in line with observations in literature where NF90 is classified as a “tight” membrane while NF270 is classified as “loose” in terms of pores [5, 6].

It can also be noted from the results that BW30 and XLE are similar in terms of pore sizes. Nghiem and Coleman [7] have proposed that BW30 has no pores at all. It can be presumed that XLE has the same non-porous structure owing to the similar pure water permeability as BW30. This is in line with the membranes classification by the supplier. These are classified as low pressure RO membranes (LPRO) [8]. NF90 has pure water permeability which lies between that of NF270 and the RO membranes.

The results from the linear regression method by Košutić *et al.* are given in Figure 4. 2. The results give emphasis to the relationship between the membrane active layer and pressure as indicated by α . The value of α for NF90 shows that the membrane has pore sizes in between those of RO and NF. NF90 has α value of 34×10^{-4} and NF270 of 8×10^{-4} . These values point to differences in the membrane active layer structure, and subsequent separation performance. The values of α for BW30 and XLE indicate that these membranes have the narrowest pores with α value above 100×10^{-4} . The large values of α are in agreement with the non-porous nature proposed by Nghiem and Coleman [7].

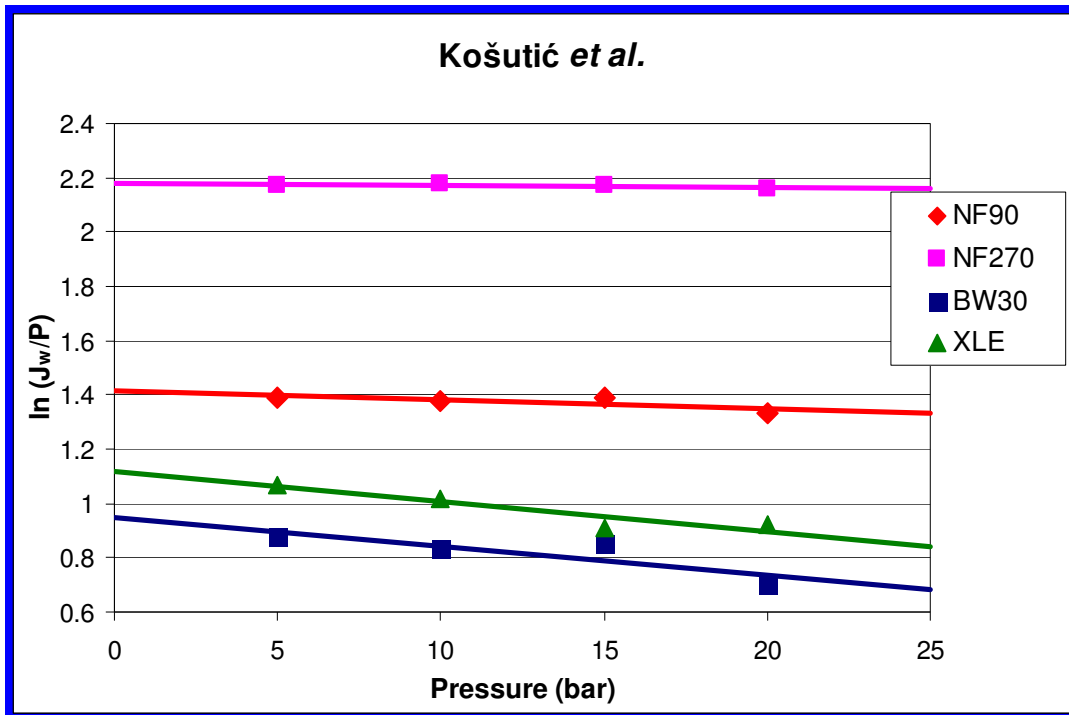


Figure 4. 2: Relationship of water flux and pressure (Košutić approach)

The steep slope of the graphs relates to the structure of the pores of the membranes [2]. The steeper slope corresponds to a less porous membrane structure. The values of A_w from this method agree well with those from the Kedem-Katchalsky method. The Košutić method however, shows extra sensitivity to changes in membrane active layer structure. This is evident in the values for BW30 and XLE. The difference in the pore sizes is much more pronounced. From the Košutić approach, the membranes can be placed in the following order concerning their pore sizes: NF270 > NF90 > XLE > BW30. Pure water permeability coefficients (A_w) of the membranes obtained from the Košutić method confirm the observed trend of porosity.

Table 4. 2: Pure water permeability values (Košutić Approach)

Membrane	$\ln A_w$	α 10^{-4}	A_w ($\text{l.m}^{-2}.\text{h}^{-1}.\text{bar}^{-1}$)
NF90	1.42	34	4.14
NF270	2.18	8	8.85
BW30	1.12	112	3.06
XLE	0.99	105	2.59

The linear dependence of the pure water flux J_w on pressure points to an unchangeable membrane porosity, and therefore an unchangeable membrane active layer. If the pure water permeability of a membrane is not constant, it indicates changes in the membrane's porous structure.

4.1.2 Membrane-Solvent Compatibility

The interaction of polymeric membranes with organic solvents has been observed to be significantly different from that with aqueous media [9]. For this reason it was necessary to initially determine the effect of the solvents on the physical integrity of the membranes. Certain solvents are known to cause changes in polymer morphology at a molecular level [10]. These solvents influence the structure and therefore lead to changes in physical polymer appearance. The visual observations on the membranes exposed to selected solvents are given below in Table 4. 3.

Table 4. 3: Observations of membrane compatibility with organic solvents.

Solvent	NF90	NF270	BW30	XLE
Methanol	Remained flat	Remained flat	Remained flat	Remained flat
Ethanol	Remained flat	Remained flat	Remained flat	Remained flat
1-Propanol	Remained flat	Remained flat	Remained flat	Remained flat
2-Propanol	Remained flat	Remained flat	Remained flat	Remained flat
Acetonitrile	Minor swelling	Minor swelling	Excessive swelling	Minor swelling
Ethyl acetate	Curled immediately	Curled immediately	Curled immediately	Curled immediately
Dichloromethane	Curled, translucent	Curled, translucent	Curled, translucent	Curled, translucent
Tetrahydrofuran	Curled, translucent	Curled, translucent	Curled, translucent	Curled, translucent
Toluene	Curled, translucent	Curled, translucent	Curled, translucent	Curled, translucent

The membranes showed stability in most of the solvents tested. Alcohols gave the best results with all the membranes remaining stable and retaining their structure and appearance. Acetonitrile caused some swelling and blistering of the top layer of most membranes, with significant swelling and blistering observed in BW30. However, the overall structures of the membranes were not altered significantly. Ethylacetate also caused some curling in all the membranes. Although the overall structure of each membrane remained intact. All the membranes showed signs of chemical attack, in dichloromethane, tetrahydrofuran and toluene. The membranes immediately curled and became translucent on contact with the solvents.

After 24 hours separate entities, which are thought to be the active layer and the support, were observed floating on the solvent. The solvent had clearly damaged and completely changed the membrane structures. This was the case with all the membranes. The results show that non-polar aprotic and polar aprotic solvents are generally non-compatible with polymeric membranes [11].

Our results agree with Yang *at al.* [12] observations. They observed that membranes designed for aqueous systems lose their structural integrity when exposed to harsh organic solvents. It was therefore decided that compatible solvents should be used. Therefore methanol, ethanol, 1-propanol, 2-propanol and acetonitrile were used in subsequent phases of the study. The physical properties of the solvents are given in Table 4. 4. Water is included in the table as it was also used as a solvent in catalytic reactions.

Table 4. 4: Physical properties of selected solvents

Solvent	MW (g.mol ⁻¹)	Viscosity @ 25°C (cP)	Hansen parameter ^[13] (MPa ^{1/2})	Polarity parameter ^[14] E_T^N
Methanol	32.04	0.54	29.60	0.76
Ethanol	46.07	1.10	26.50	0.65
2-Propanol	60.10	2.04	23.60	0.54
Acetonitrile	41.05	0.37	24.40	0.46
Water	18.02	1.00	47.80	1.00

4.1.3 Pure Solvent Permeability

Steady state fluxes were determined to evaluate the relationship of solvent flux, pressure, molecular weight and viscosity of the solvent. Solvent flux can be described by the Hagen-Poiseuille equation for viscous flow illustrated in Equation 4.6 [15]:

$$J_s = \left(\frac{\epsilon r^2}{8 \Delta x \tau} \right) \left(\frac{\Delta P}{\eta} \right) \quad \text{Equation 4.6}$$

where, J_s is the solvent flux, ϵ is the porosity, r is the average pore radius, ΔP is the pressure difference, η is the viscosity, Δx is the effective membrane thickness and τ is the tortuosity factor. The Hagen-Poiseuille equation shows the relationship between flux, pressure and viscosity. According to the equation an increase in pressure will result in a corresponding increase in flux. The solvent fluxes were therefore plotted against pressure to confirm this relationship. The plots are given in Figure 4. 3 to Figure 4. 6

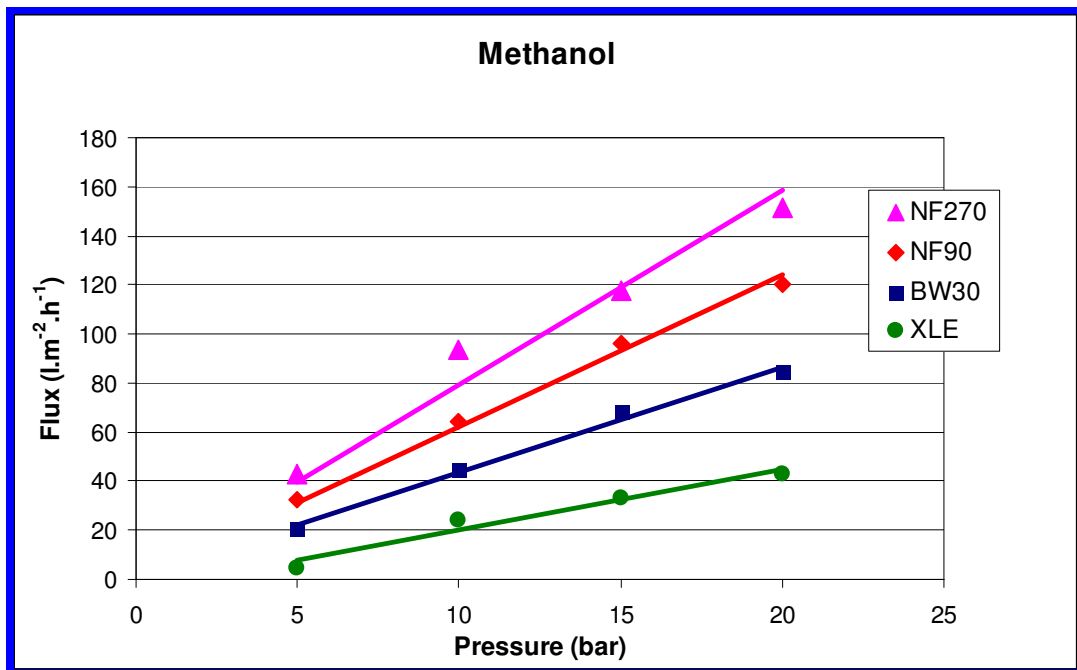


Figure 4. 3: Plots of methanol flux in NF90, NF270, BW30 and XLE

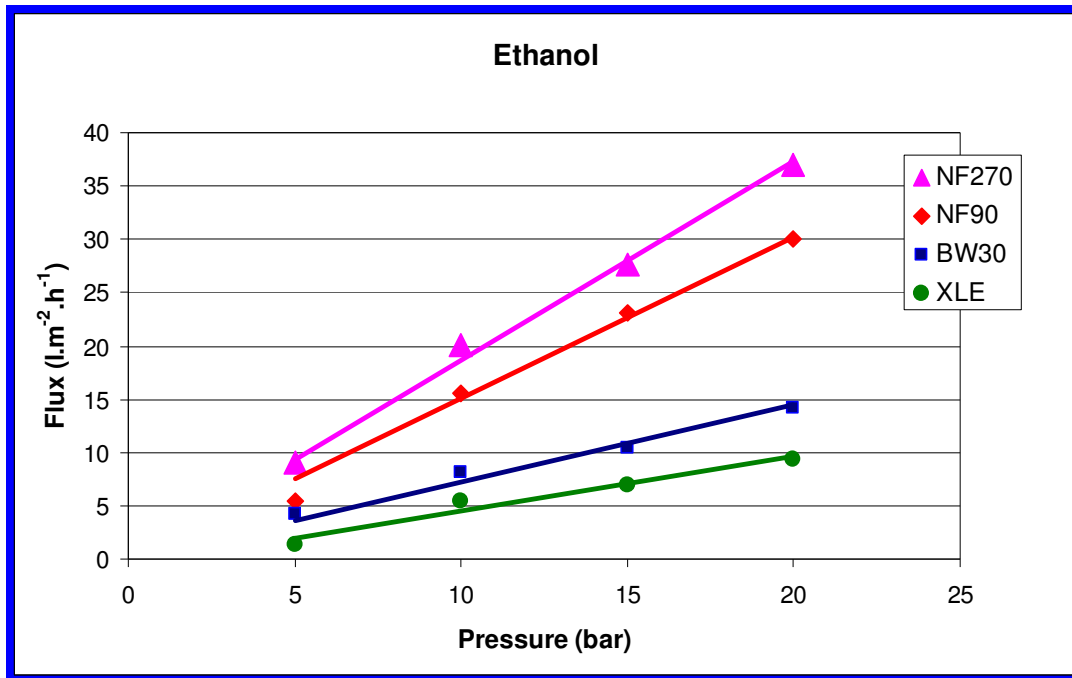


Figure 4. 4: Plots of ethanol flux in NF90, NF270, BW30 and XLE

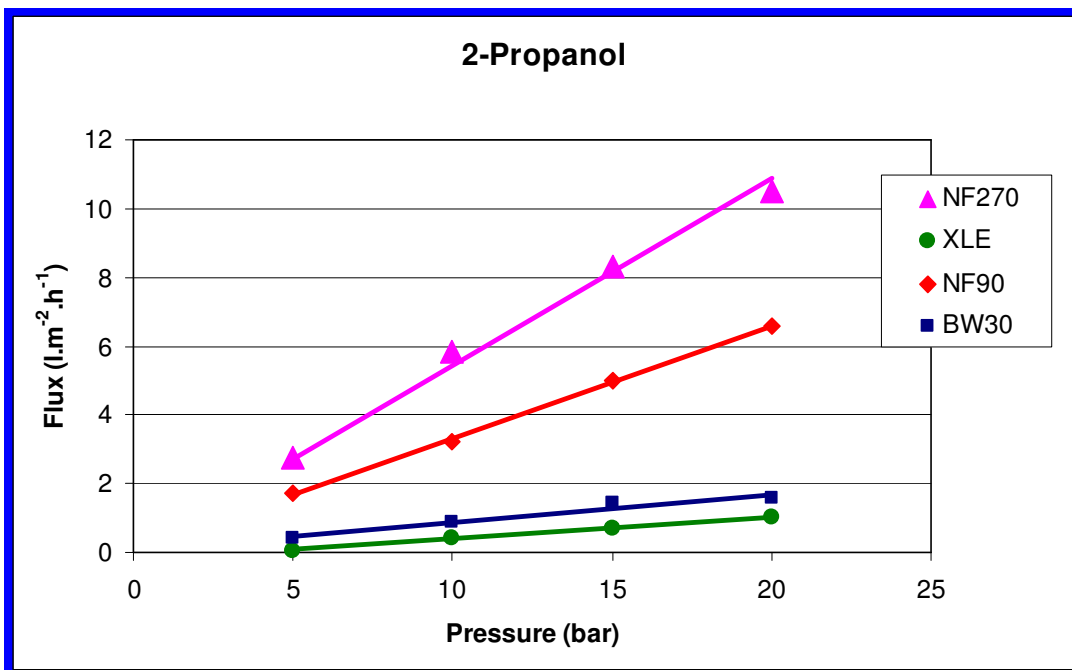


Figure 4. 5: Plots of 2-propanol flux in NF90, NF270, BW30 and XLE

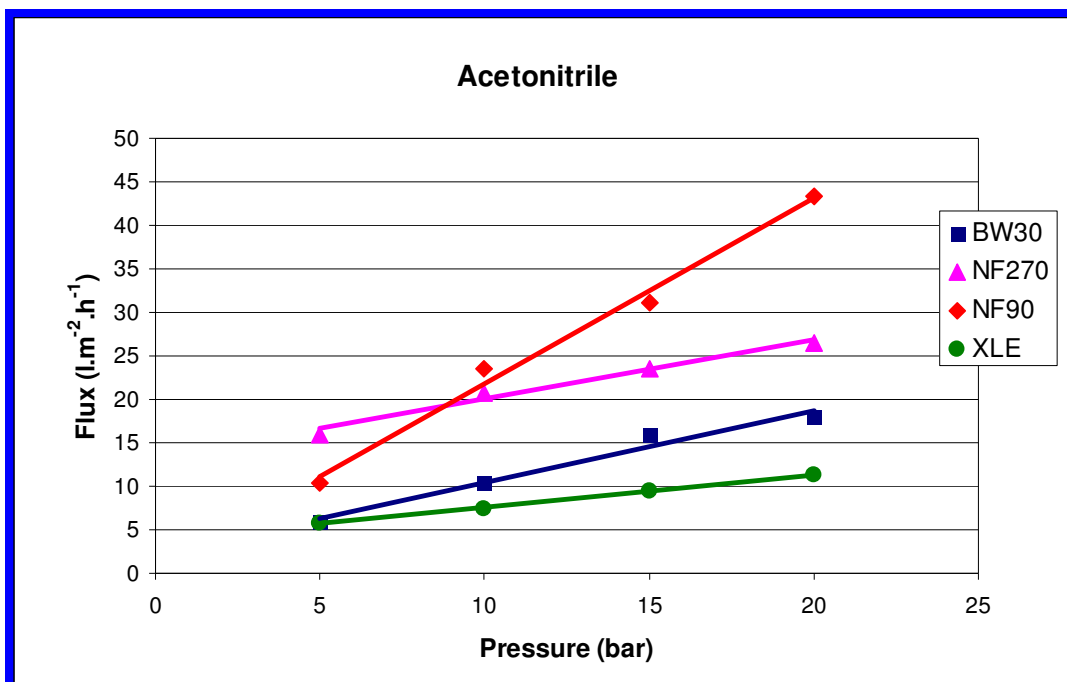


Figure 4. 6: Plots of acetonitrile flux in NF90, NF270, BW30 and XLE

The results show a good correlation with Equation 4.6. All the solvents showed steady constant fluxes which increase with increasing pressure. Looking closer at the membrane behaviour in each solvent, it can be seen that NF270 generally shows higher fluxes followed by NF90, BW30 and XLE respectively.

The trend is readily constant in the homologous series of alcohols. A strange behaviour is observed in acetonitrile, where NF90 shows significantly higher fluxes than NF270, BW30 and XLE respectively. The high acetonitrile fluxes in NF90 may result from minor swelling of the active layer observed during filtration. Minor swelling may also have led to the smaller fluxes in NF270. The effect of swelling is on flux discussed in detail in Section 4.1.4.

For the homologous series of alcohols, methanol shows the highest fluxes in all the membranes. Methanol is followed by ethanol and lastly 2-propanol. Methanol fluxes range from 20 to 100 $\text{l.m}^{-2}.\text{h}^{-1}$ at 10 bar. The fluxes range from 40 to 150 $\text{l.m}^{-2}.\text{h}^{-1}$ at 20 bar. Ethanol fluxes range from 5 to 20 $\text{l.m}^{-2}.\text{h}^{-1}$ at 10 bar and 10 to 35 $\text{l.m}^{-2}.\text{h}^{-1}$ at 20 bar. 2-Propanol fluxes are the lowest ranging from 0.5 to 6 $\text{l.m}^{-2}.\text{h}^{-1}$ and 1 to 10 $\text{l.m}^{-2}.\text{h}^{-1}$ at 10 and 20 bar respectively.

From these observations, it can be seen that there are some properties of the solvents that influence their permeability. Equation 4.6 highlights that solvent transport in nanofiltration membranes is influenced by viscous flow. This is evident from the plot of solvent flux against viscosity illustrated in Figure 4. 7.

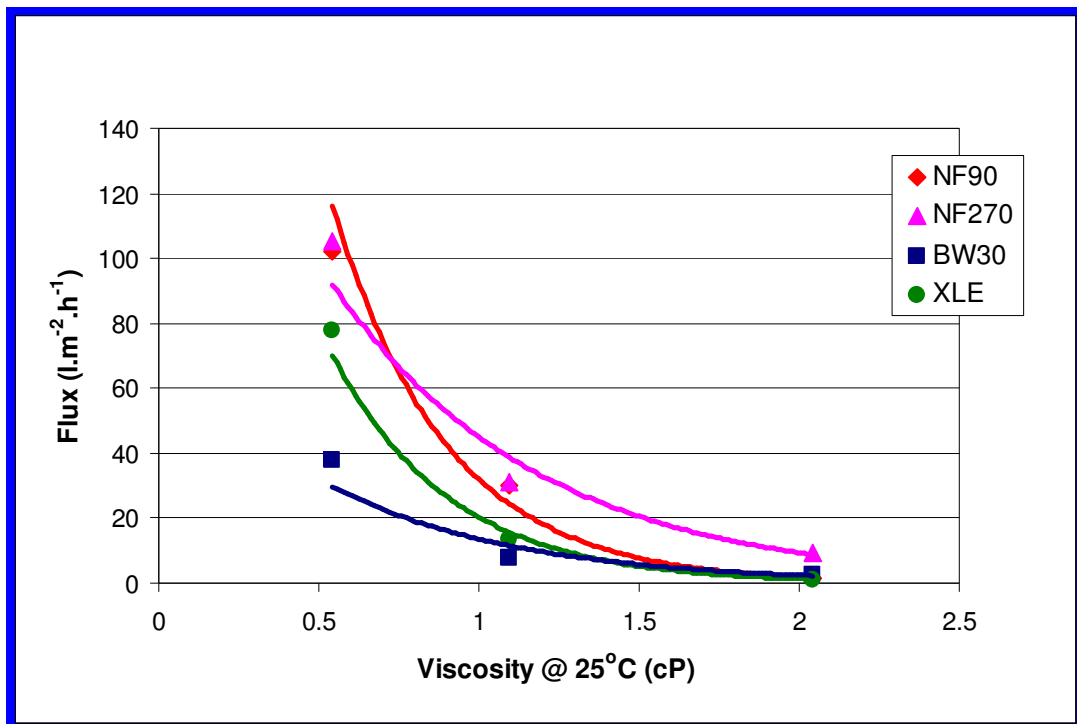


Figure 4. 7: Relationship between solvent flux and viscosity at 25°C

The results show an increase in solvent flux with decreasing viscosity of solvents. All the membranes show similar behaviour which correlate with the Hagen-Poiseuille model. The results show that solvent with low viscosity will flow through the membrane with ease more than that with high viscosity. The resistance to flow will therefore lead to lower fluxes in the membranes.

Jonsson and Boesen added additional parameters to the Hagen-Poiseuille model [16]. These parameters describe the frictional component of transport of solutes through nanofiltration membranes. In the model, described by Equation 4.7, the molecular weight M is included as an additional parameter describing frictional component of transport, X_{sm} is the friction factor between the solvent molecules and the membrane pore wall and C is the concentration.

$$J = \frac{\epsilon r^2}{8\eta} \left[\frac{I}{1 + \frac{r^2 X_{sm} C}{8\eta M}} \right] \frac{\Delta P}{\tau \Delta x} \quad \text{Equation 4.7}$$

However it is the resistance-in-series model developed by Machado *et al.* that best describes our observations [17]. The model is described by Equation 4.8.

$$J = \frac{\Delta P}{\phi' [\Delta\gamma + f_1 \mu] + f_2 \mu} \quad \text{Equation 4.8}$$

The model describes permeation of the solvent through composite polymeric membranes. In Equation 4.8, f_1 and f_2 are constants characterizing the individual mass transfer coefficients and pore radii. ϕ is the solvent parameter, $\Delta\gamma$ is the surface energy difference between the membrane and solvent. It has been reported that permeation through the membrane pores will only occur when the applied pressure overcomes the surface energy difference [15].

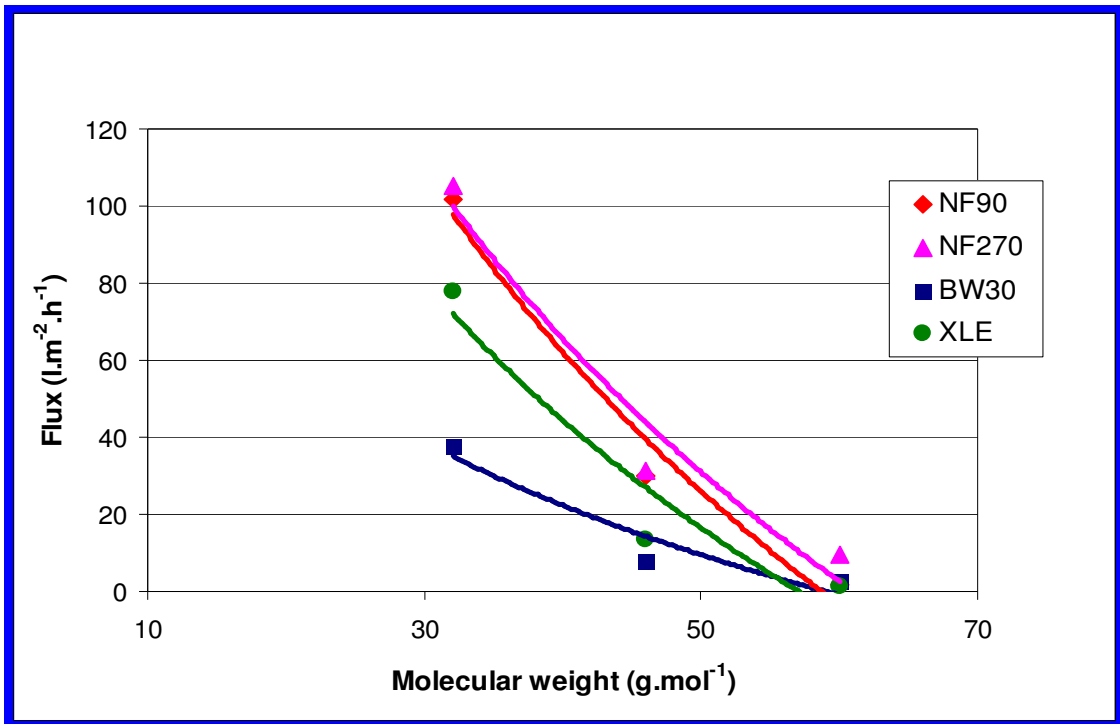


Figure 4. 8: Relationship between solvent flux and molecular weight

Noordman and Wesselingh [18] have explained that viscous flow of a component through narrow pores is a function of the relative size of the component. Therefore from Equation 4.8, it can be expected that the surface energy difference $\Delta\gamma$ will be large for a component with a larger molecular weight than for a component with smaller molecular weight. Consequently, the flux will decrease with increasing surface energy difference. The plots illustrated in Figure 4. 8 agree well with the above proposition. For the homologous series of alcohols, the flux of 2-propanol in all the membranes is the lowest. This is in line with its larger molecular weight and size.

The membranes show a similar trend to that observed in pure water permeability studies. NF270 shows a sharp decrease in solvent flux with increasing molecular weight and viscosity. This membrane is followed by NF90, XLE and BW30. The behaviour of XLE and BW30 is not clear in terms of solvent fluxes. XLE was shown to be more porous than BW30 in pure water permeability studies. BW30 shows higher fluxes than XLE for pure organic solvents. This discrepancy in solvent fluxes may be explained by swelling behaviour of the membranes when in contact with organic solvents.

4.1.4 Swelling Experiments

Section 4.1.2 and 4.1.3 have highlighted the influence of membrane-solvent interactions. These interactions are especially important in nanofiltration of organic solvents [19]. Solvent effects may include swelling of the polymeric material upon contact with the solvent. Swelling has been observed to have a negative effect on the separation performance and lifetime of the polymeric membrane material [20].

Tarleton *et al.* [21] observed that the degree of swelling has a more prominent effect on flux than viscosity of the mixture. Silva *et al.* [22] ruled out swelling as an explanation for higher flux of ethyl acetate compared to toluene in STARMEM 122 and MPF50 membranes. This was due to the equivalent swelling behaviour observed in both solvents.

The authors however acknowledged that solvent effects may lead to pore-structure changes such as swelling of the polymer matrix. In our study, the swelling behaviour of the membranes in acetonitrile, 2-propanol and water was investigated. These three solvents are the main solvents used in coupling reactions and catalyst retention studies. Swelling which is defined as the volume of liquid absorbed by the membranes, was calculated using Equation 3.4, described in Section 3.4.4.

$$Q = \frac{1}{\rho_s} \frac{W_{wet} - W_{dry}}{W_{dry}} \quad \text{Equation 3. 4}$$

In the equation, Q is the swelling, W_{wet} is the mass of wet membrane, W_{dry} is the mass of dry membrane and ρ_s the density of the solvent. The swelling results are listed in Table 4. 5. The results show that the selected membranes swell more in the organic solvent than in water. Swelling is more pronounced in 2-propanol, followed by acetonitrile and lastly water. The trend is similar in all the membranes. The results are in accord with observations by Zhao and Yuan [23]. They also observed higher degree of swelling in water compared to ethanol and methanol. The results however show disagreement to observations by Geens *et al.* [24]. The authors observed higher swelling in water, compared to organic solvents.

Table 4. 5: Results of swelling measurements

Solvent	Swelling (cm ³ .g)			
	NF90	NF270	BW30	XLE
Water	0.23	0.41	0.38	0.31
Acetonitrile	0.43	0.60	0.58	0.51
2-Propanol	0.50	0.72	0.68	0.63

It was important to rationalize our observations of higher swelling in organic solvents compared to water. To begin with, the relationship between swelling and molecular weight of the solvent was investigated. The plots are illustrated in Figure 4. 9.

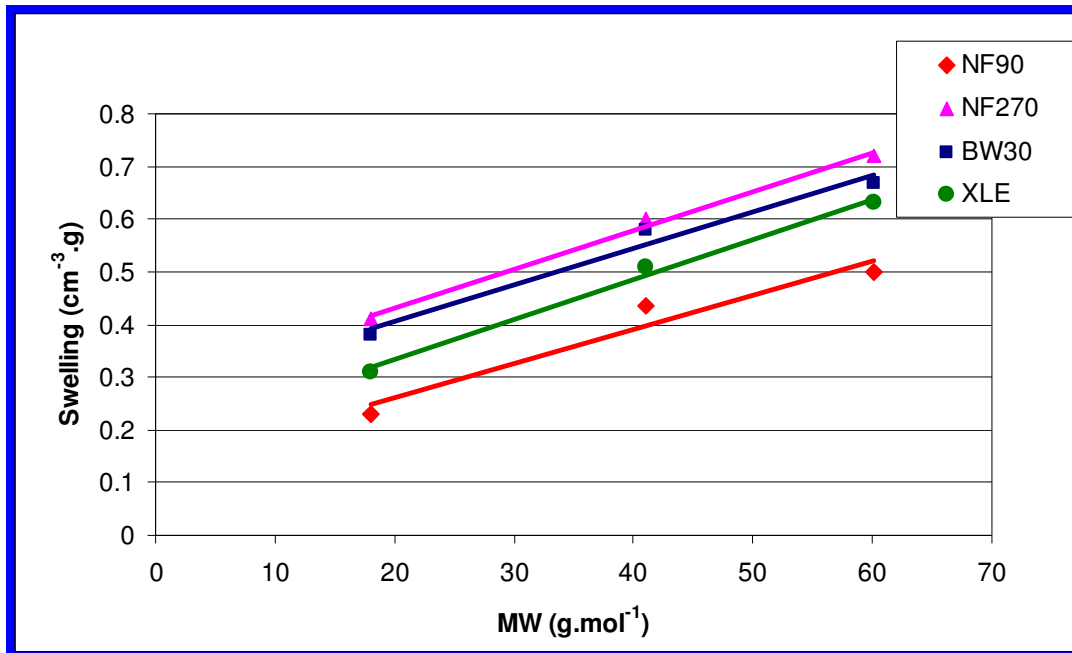


Figure 4. 9: Relationship between membrane swelling and molecular weight

The results show that for the selected solvents, membrane swelling increases linearly with increasing molecular weight. The results show that swelling is more pronounced in 2-propanol, which is the solvent with a larger molecular weight. Looking at the membranes, it can be seen that NF270 shows higher swelling in all the solvents. NF270 is followed by BW30, XLE and lastly NF90.

In light of the observations above, the influence of swelling on solvent flux was investigated. The results illustrated in Figure 4. 10 show flux decline with increasing swelling degree. NF270 shows the steepest flux decline. A strange observation from the results is that of NF90. The membrane also shows a rather steep flux decline despite low swelling degree when compared to NF270, BW30 and XLE. A steady flux decline with increasing swelling was observed for BW30 and XLE .

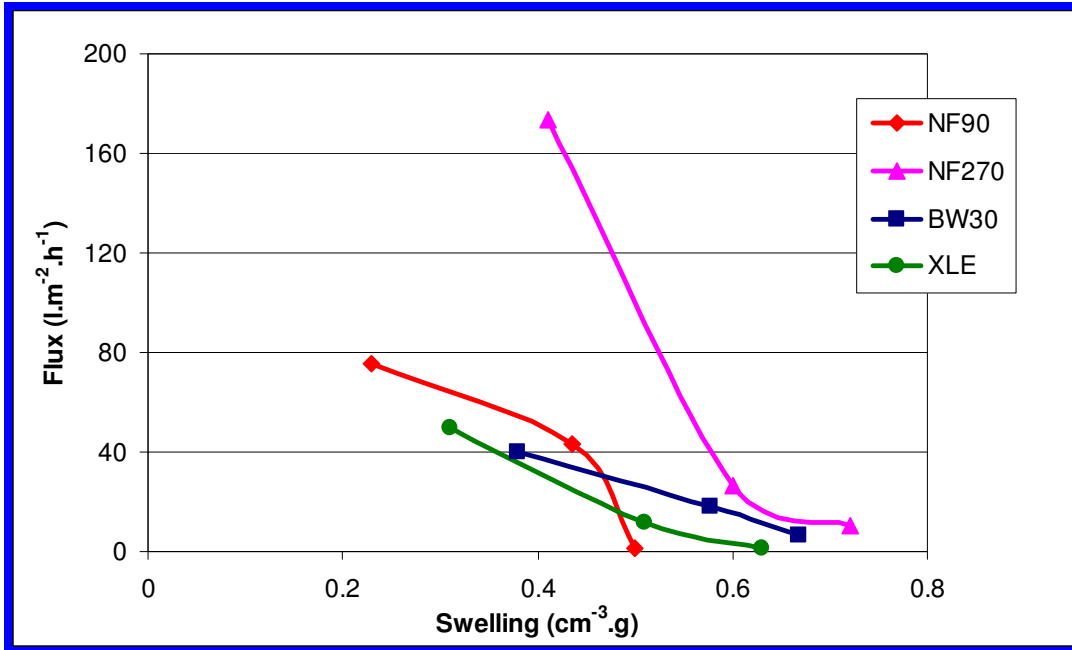


Figure 4. 10: Relationship between membrane swelling and flux

It is clear from the results that swelling has a negative effect on the flux behaviour of the membranes. The effect can be attributed to changes in the polymer matrix, as already mentioned by other authors [22,23,24]. Freger *et al.* [25] explained that swelling leads to disruption of cross-linking and formation of new hydrophobic and hydrophilic functional groups in the membrane structure. This change in cross-linking has been observed for NF membranes [26] as illustrated in Figure 4. 11. The cross-linking chains expand during swelling therefore increasing the size of the pores. This results in a decrease in flux of components through the membrane.

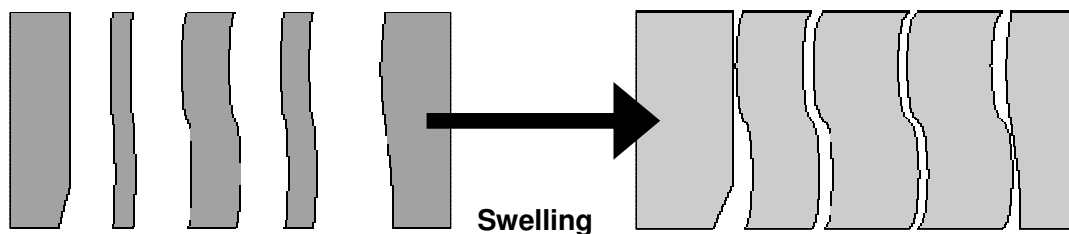


Figure 4. 11: Schematic representation of pore-reduction swelling in NF membranes

The opposite has also been cited as a possible mechanism of swelling in NF membranes [26]. In this process, the polymer chains shrink therefore increasing the size of the pores. This leads to an increase in solvent fluxes, and a reduction in rejection of solutes of interest. Our results agree with the first process, pointing to decreased pore sizes with swelling.

Miller-Chou and Koenig [27] have based the differences in dissolution behaviour to mass and momentum transport in the swelling polymer matrix. They concluded that the nature of the polymer and differences in rigidity are the main parameters that determine polymer swelling behaviour. For the membranes studied here, it is clear that there are similarities in structure and dissolution behaviour. It also clear that the solvents selected in the study have an effect on the membranes. These membrane-solvent interactions however do not alter the membrane structures drastically. For catalyst separation to be effective, the membrane-solvent interactions should not be detrimental. It was therefore concluded that the solvents selected are fit for later use in catalyst retention and separation studies.

4.1.5 Uncharged Solute Rejection Measurements

The molecular weight cut-off (MWCO) of the membranes was determined by retention measurements of uncharged solutes. The properties of the solutes are listed in Table 4. 6. MWCO is defined as the molecular weight at which 90% rejection is obtained by the membrane [28]. The MWCO values were obtained by interpolating to the molecular weight corresponding to 90% rejection in the graph of solute rejection against molecular weight [29]. The graphs are illustrated in Figure 4. 12.

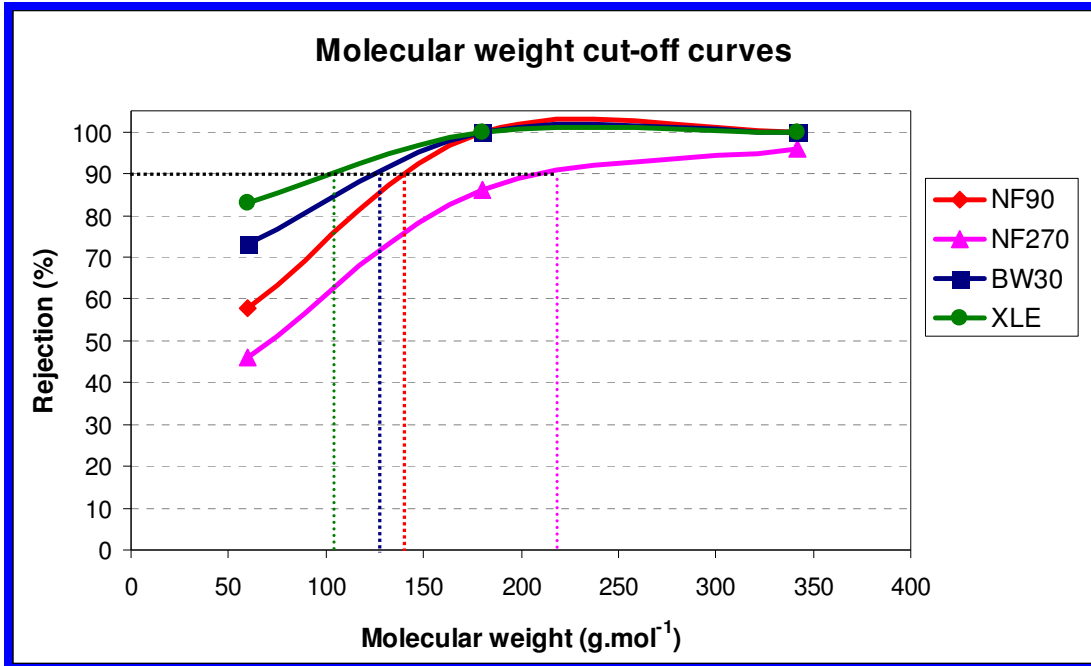


Figure 4. 12: Uncharged solutes retention curves showing interpolated MWCO.

The estimated MWCO values from the curves are 140 Da (NF90), 220 Da (NF270), 125 Da (BW30) and 105 Da (XLE). It can be seen from the results that NF270 has the highest MWCO. The trend in terms of the MWCO is: NF270 > NF90 > BW30 > XLE. The results highlight the influence of membrane-solute interactions. It can be seen from the results that the larger solute is rejected more than the smaller one. According to the steric hindrance pore model, the larger solute will experience more frictional resistance during diffusive and convective transport through the membrane more than the smaller solute.

Table 4. 6: Properties of uncharged solutes used for MWCO determination

Solute	MW (g.mol ⁻¹)	Stokes radius (nm)
2-Propanol	60	0.22
Glucose	180	0.36
Sucrose	342	0.48

4.1.6 Morphological Investigation by Scanning Electron Microscopy (SEM)

The morphology of the membranes was investigated by SEM analysis. SEM allowed for investigation of the surface morphology and microstructure of the polymeric membranes. The images of the surface of the membranes showed the texture and appearance of the membranes. The images point to an inhomogeneous surface covering in the membranes. The images of NF90 illustrate the rough texture of the membrane with some porous and nodular features. NF90, BW30 and XLE have the same type of appearance and texture. NF270 is the exception, with a somewhat smooth surface and texture. NF90 and XLE are the most similar membranes in terms of roughness of the surface.

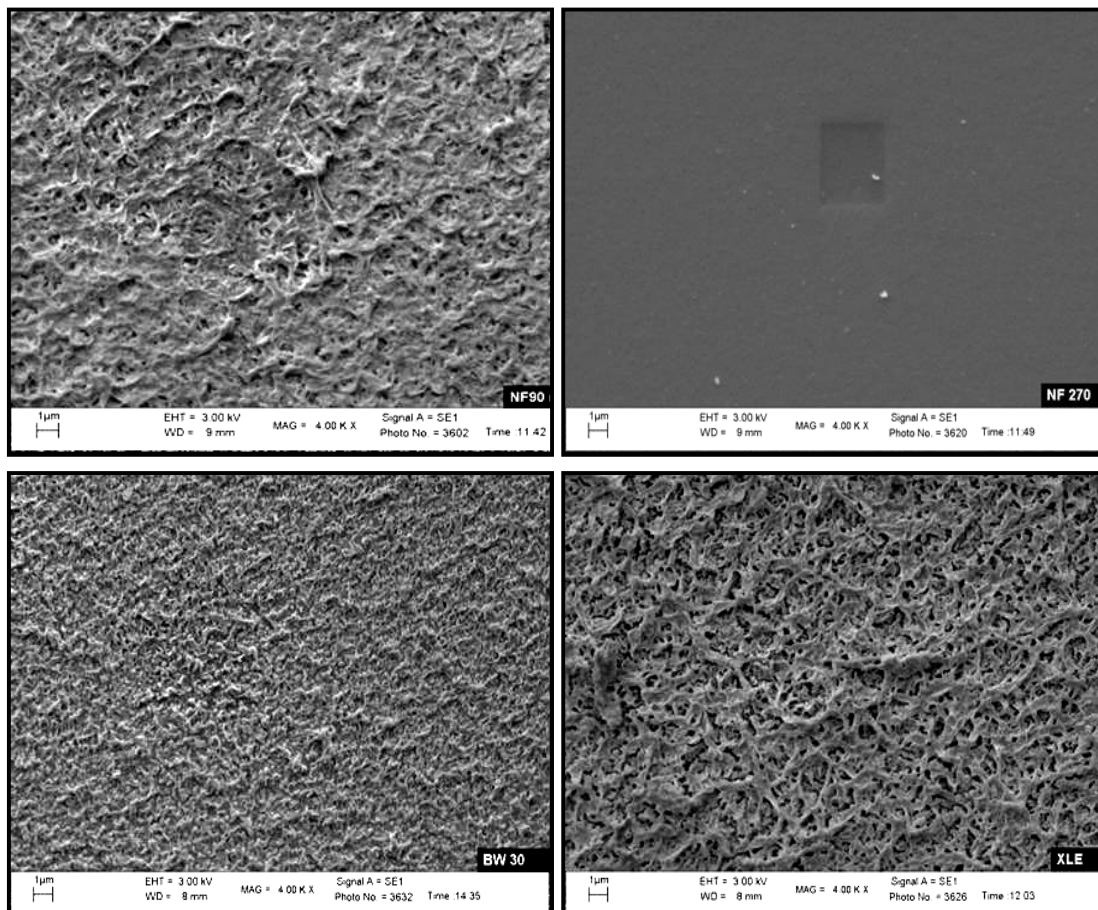


Figure 4. 13: SEM micrographs showing the top view of the membranes (Clockwise from the left: NF90, NF270, XLE and BW30)

The images of the microstructure of the membranes show that they consist of three characteristic layers. These are labelled as (i) top barrier layer, (ii) porous polysulfone layer and (iii) non-woven polyester support layer [30]. A representative image of the cross-sectional view of the membranes is illustrated in Figure 4. 14. Each layer has a definite function. The top layer serves as a separation barrier, separating components based on the MWCO [31]. The polysulfone layer acts as a support layer designed to withstand high pressures during filtration. The non-woven support adds structural support to the whole composite membrane. This layer is tailored to generate a hard, smooth and compact surface [32].

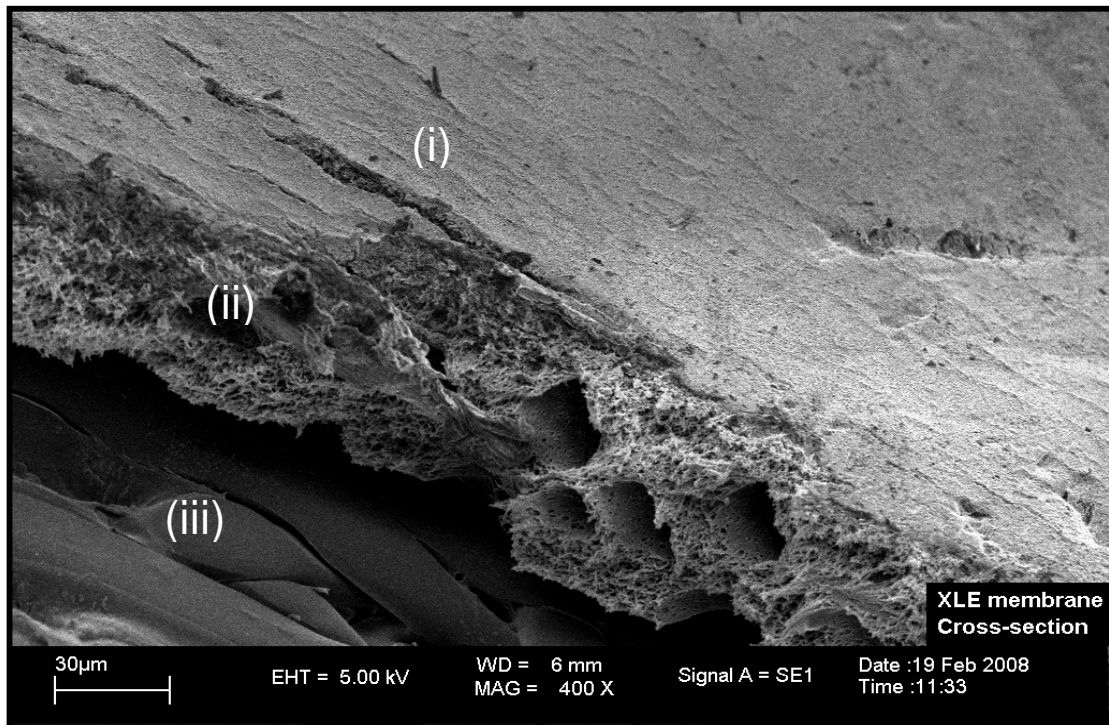


Figure 4. 14: SEM micrograph showing the cross-sectional view of XLE membrane.

The importance of the microstructure of NF membranes has been demonstrated by the development of transport models such as the resistance-in-series model by Machado *et al.* [17]. The research group developed the model based on a resistances encountered in a three-layered composite membrane. An alternative description of Equation 4.8 is illustrated in Equation 4.9.

$$J = \frac{\Delta P}{R_T} = \frac{\Delta P}{R_S^0 + R_\mu^1 + R_\mu^2} \quad \text{Equation 4.9}$$

In the equation, R_S^0 is the surface resistance encountered at the pore entrance, R_μ^1 is the viscous resistance during flow through the NF active layer and R_μ^2 is the viscous resistance through the support layer. It is clear from Equation 4.9 that each layer has a different interaction with solutes and solvents.

4.1.7 Topography and Surface Roughness Investigation by Atomic Force Microscopy (AFM)

The topography of the surface of the membranes was determined by AFM. The AFM images confirmed SEM observations. A representative AFM image of the surface of the membrane is illustrated in Figure 4. 15. All the membranes show a similar appearance which corresponds to SEM observations. The image clearly shows characteristic “hills” and “valleys” associated with the rough texture of the membranes. These “hills” correspond to protrusions on the surface. “Valleys” correspond to surface depressions.

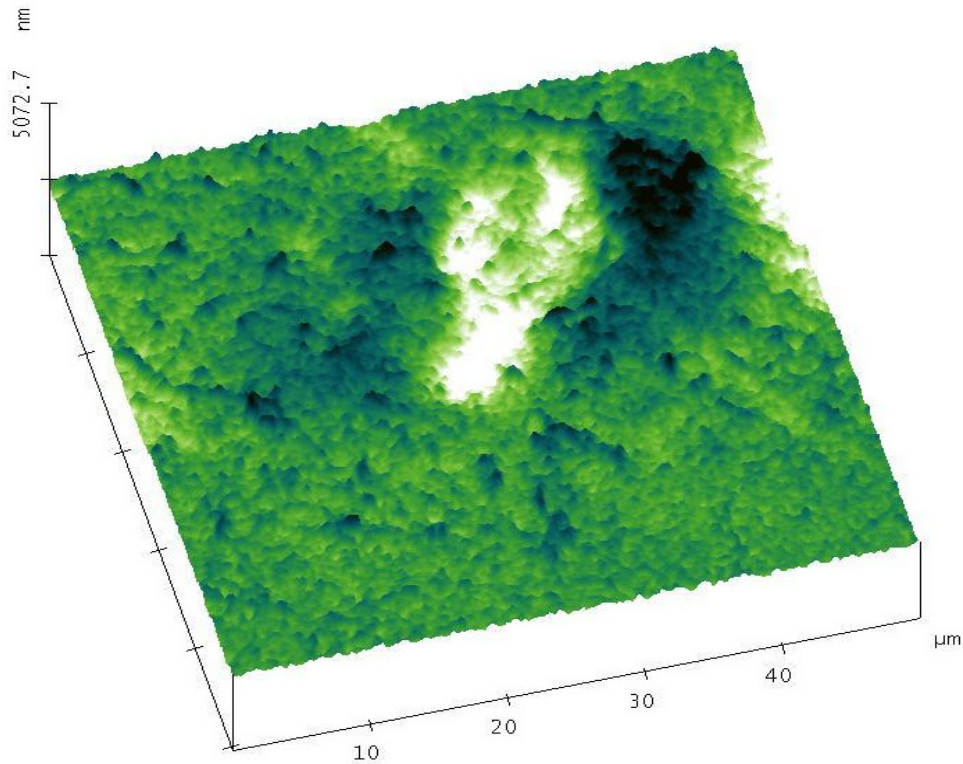


Figure 4. 15: AFM image showing the surface detail of the membrane

The texture of the membranes was further characterized by roughness measurements over an area of $50\ \mu\text{m} \times 50\ \mu\text{m}$. Roughness of a membrane has an effect on permeability and fouling behaviour of the membrane [33]. The results listed in Table 4.6 show that XLE is the roughest membrane.

XLE is followed by NF90, BW30 and NF270. It should be noted however, that RMS roughness measurements depend on the selected scan area and the mode of AFM used for measurement [34]. The values reported in Table 4. 7 may therefore differ from those in literature. Hence the purpose of these roughness results is to show differences in the surface texture of the different membranes.

Table 4. 7: Results of AFM roughness measurements

Membrane	Roughness (nm)
NF90	124.99
NF270	11.40
BW30	95.52
XLE	135.60

In view of the observations by Boussu *et al.* [33] on the effect of roughness on permeability, it was necessary to investigate this relationship for our selected membranes. The roughness results were plotted against pure water permeability results. Pure water permeability (PWP) results were chosen because they are characteristic of each active layer. The results illustrated in Figure 4. 16 show that higher roughness values correspond to lower water permeability. It can be seen from the plots that NF270 with lower RMS roughness has significantly larger pure water permeability. It can also be seen that NF90 and XLE have similar roughness. This is a confirmation of SEM observations. The results clearly show the effect of roughness on porosity.

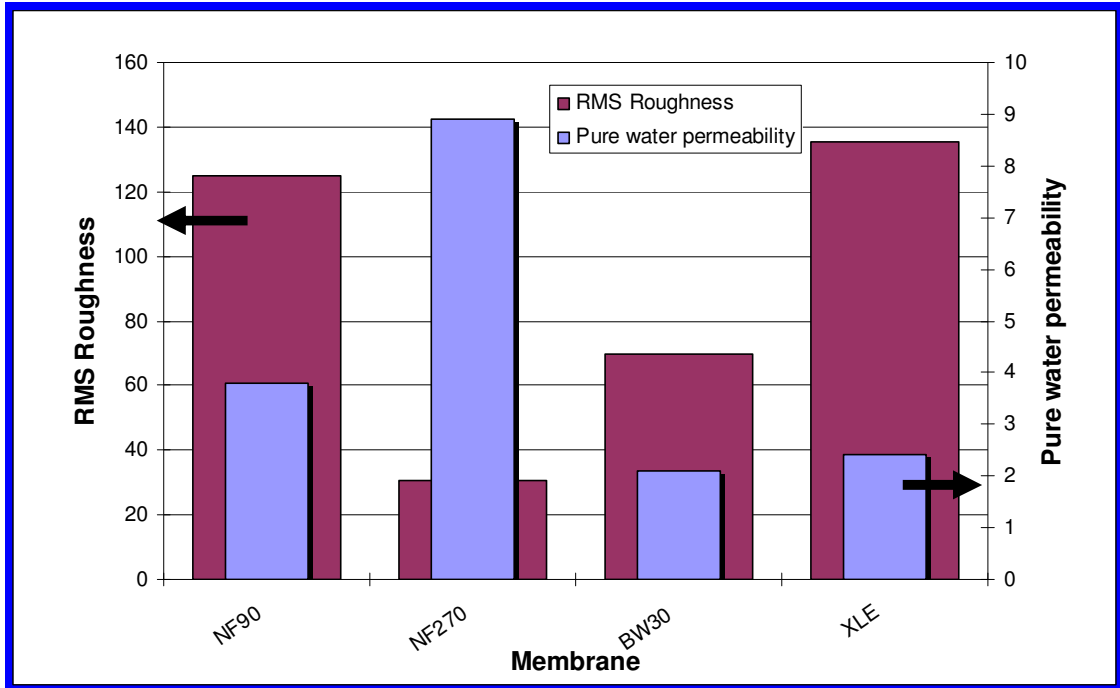


Figure 4. 16: Plots of RMS roughness and pure water permeability

Roughness can also be associated with fouling tendency of a membrane. Tang *et al.* [35] have observed that membranes with lower roughness experience lower flux decline compared to rougher membranes. The observed flux decline in rougher membranes has been attributed to fouling occurring preferentially in the “hills” and “valleys” in the surface of the membrane. Therefore the rougher the membrane, the more significant is the fouling and flux decline.

4.1.8 Membrane Chemical Structure Investigation by Fourier Transform – Infra Red Spectroscopy (FTIR)

The discussion in Section 4.1.6 and 4.1.7 has underlined some important aspects on physical structure and properties of the membranes. In this section, the chemical structure of the membranes is probed. According to the patent by Cadotte, Dow FilmTec membranes are prepared by interfacial polymerization [36].

This polymerization process is based on the combination of 1,3-phenylene diamine and triacid chloride of benzene. The resulting membrane is usually referred to as fully aromatic [7]. In the case where piperazine is used instead of 1,3-phenylene diamine, the resulting membrane is referred to as semi-aromatic [37]. The FTIR spectra of the membranes used in this study are illustrated in Figure 4. 17. The results show that NF90, BW30 and XLE fit the characteristics of fully aromatic polyamides. NF270 has characteristics of semi-aromatic polyamides.

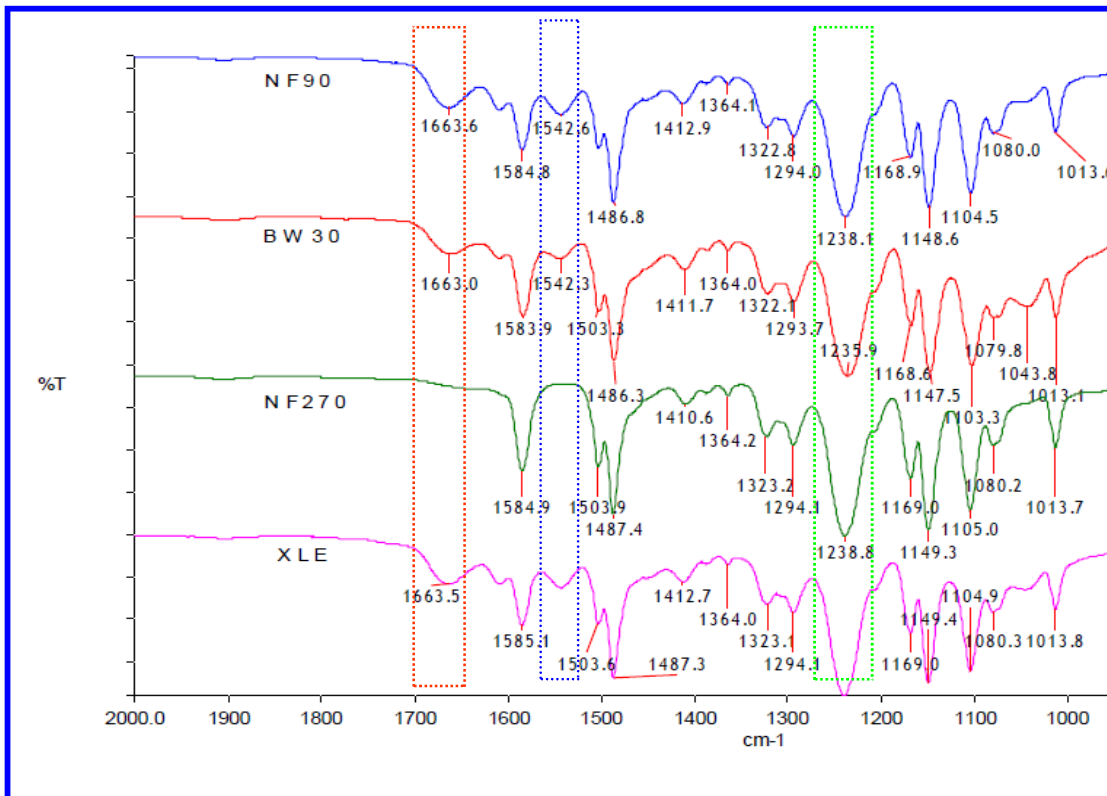


Figure 4. 17: FTIR spectra showing the chemical structure of the membranes

The fully aromatic membranes show a common band at $\sim 1663\text{ cm}^{-1}$. This band can be assigned to C=O stretching. The band is referred to as amide band I for aromatic polyamides. The membranes also share common bands at 1543 cm^{-1} . This band is assigned to in-plane N-H bending and C-N stretching. The band is also known as amide band II and is characteristic of aromatic polyamides [38]. It can be seen from the results that amide band I and II are missing from the spectrum of NF270. This is an indication of a semi-aromatic structure.

All the membranes however do share common bands. These are observed in polyamides in general. The band at 1585 cm^{-1} can be assigned to C=C bond stretching in aromatic rings. The strong band at $\sim 1238\text{ cm}^{-1}$ present in all the membranes spectra can be assigned to C-O stretching. This band points to the presence of carboxylic acid. It has been mentioned that the presence of these carboxylic acids leads to a chemically resistant and robust polymer. The FTIR results show that NF90, BW30 and XLE are similar in terms of chemical structure. NF270 is somewhat different due to the aliphatic influence in its chemical structure.

Overall, the results confirm the presence of different functional groups in the polymeric membranes. The presence of functional groups in the active layer determines the physico-chemical properties of the membrane. Coronell *et al.* [39] have stated that the type and concentration of functional groups present in the membrane active layer affects membrane-solute and membrane-solvent interactions. In turn, membrane performance such as permeability and rejection is influenced. In the membranes studied, it is clear that differences in chemical structure have an impact on the membrane performance.

4.2 CATALYST CHARACTERIZATION

Palladium complexes have been shown to be highly active as catalysts for carbon-carbon coupling reactions [40]. These catalysts are usually based on palladium(II) and palladium(0) compounds. The catalysts can be generated in situ or prepared by simple precursors as already outlined in Section 2.2.2.2. In light of this, it was of importance to characterize the catalysts [Pd(OAc)₂, Pd(OAc)₂(PPh₃)₂, Pd(PPh₃)₂Cl₂ and PdCl₂] used in our study.

4.2.1 Catalyst chemical structure investigation by Fourier Transform – Infra Red Spectroscopy (FTIR)

The chemical structures of the catalysts were determined by FTIR spectroscopy. FTIR allows for a closer investigation of the fine chemical structure of each catalyst. The structure of Pd(OAc)₂ has been the subject of interest. It has been shown that the behaviour and structure of the complex changes in solution [41]. Bakhmutov *et al.* [42] have shown that the compound can exist as a trimer in a solution of glacial acetic acid. The trimer species are said to decompose to form the catalytically active dimer species.

The spectrum of Pd(OAc)₂ is illustrated in Figure 4. 18. The spectrum shows bands at 1596 and 1419 cm⁻¹. The bands correspond to the asymmetric COO stretching characteristic of the bridging acetate in the dimer species. The band at 1350 cm⁻¹ corresponds to the symmetric stretching of the acetate group. The bands at 1045 and 949 cm⁻¹ were assigned to C–CH₃ stretching. The spectrum shows characteristics of trimer species [43].

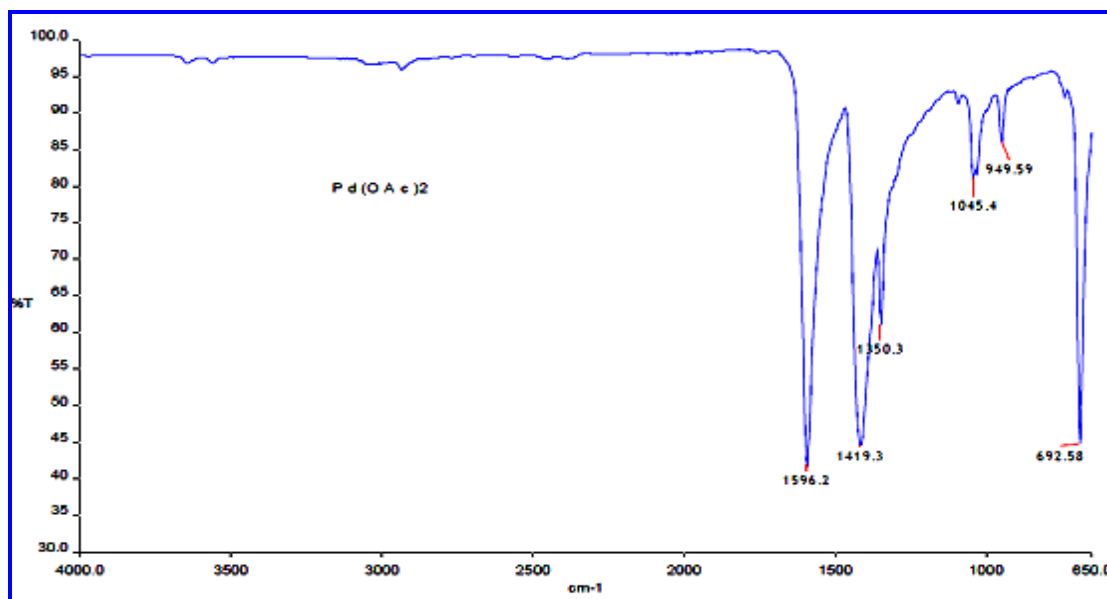


Figure 4. 18: FTIR spectra showing the chemical structure of Pd(OAc)₂

The spectrum of Pd(PPh₃)₂Cl₂ illustrated in Figure 4. 19 shows a band at 3051 cm⁻¹. This band corresponds to C–H stretch for an sp² carbon. The bands at 1598 and 1480 cm⁻¹ correspond to aromatic C=C bond stretch. The band at 743 cm⁻¹ points to an out-of-plane C–H bending, while those at 1098 and 1028 point to in-plane C–H bending.

The spectrum of Pd(OAc)₂(PPh₃)₂ is illustrated in Figure 4. 20. The spectrum shows the characteristic asymmetric stretching band of the COO group at 1598 cm⁻¹ overlapping with the aromatic C=C stretching band. The second C=C stretching band can be seen at 1482 cm⁻¹. The symmetric stretching band can be seen at 1353 cm⁻¹. The bands at 1095 and 952 cm⁻¹, similar to those seen in Pd(OAc)₂ point to C–CH₃ stretching. The spectrum confirms the presence of acetate and phosphine species in the structure.

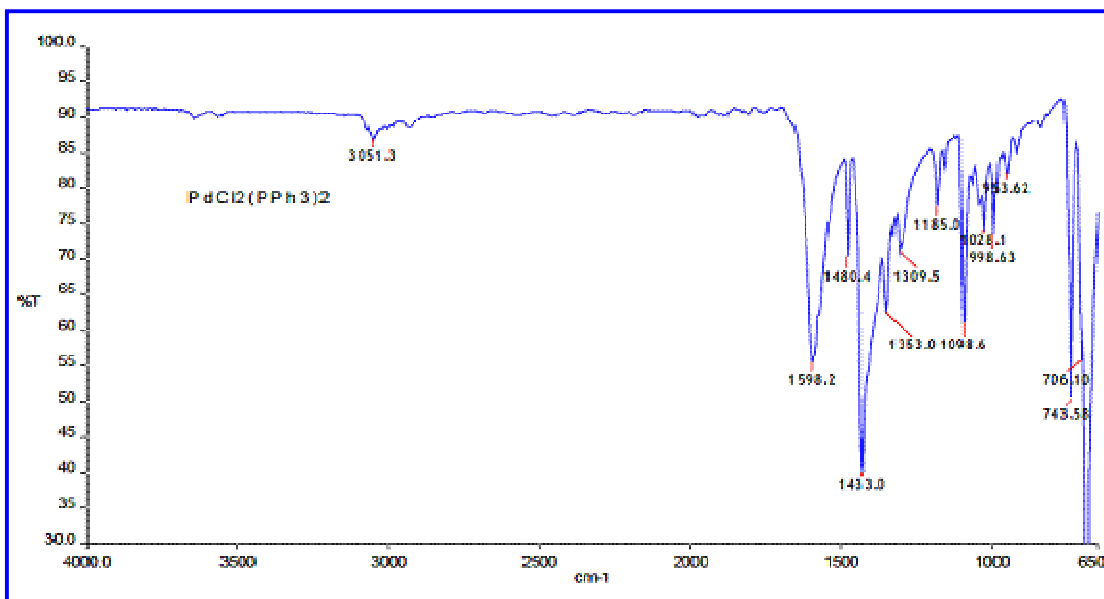


Figure 4. 19: FTIR spectra showing the chemical structure of $\text{Pd}(\text{PPh}_3)_2\text{Cl}_2$

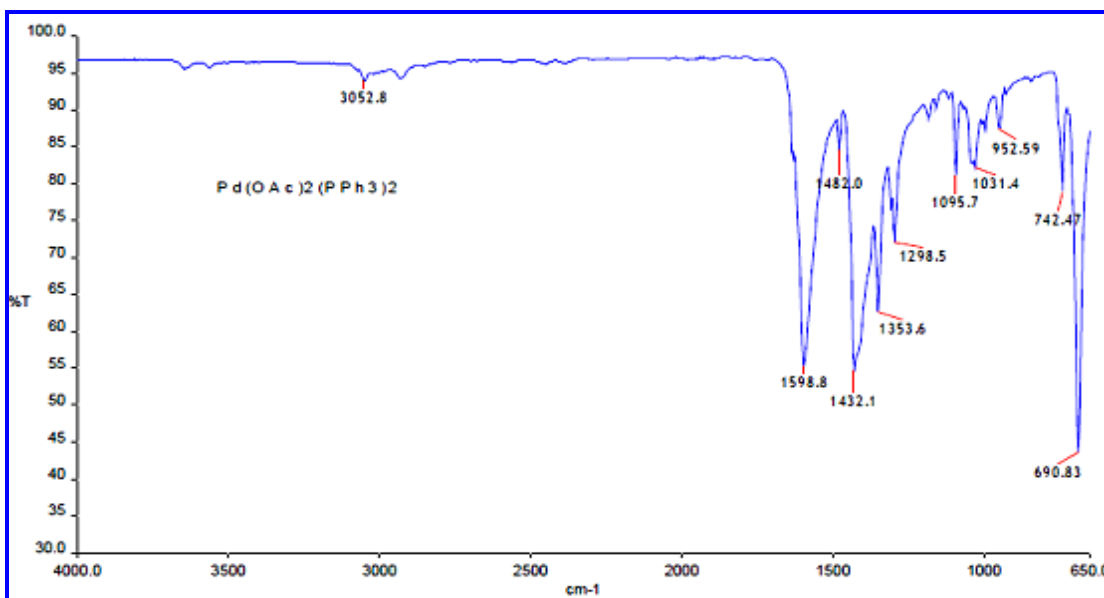


Figure 4. 20: FTIR spectra showing the chemical structure of $\text{Pd}(\text{OAc})_2(\text{PPh}_3)_2$

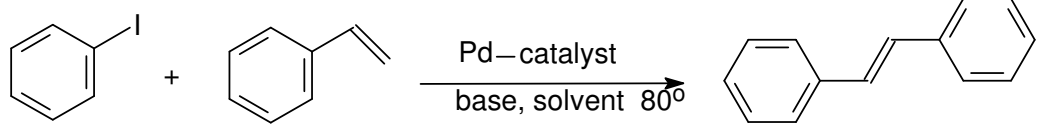
4.2.2 Carbon-carbon Coupling Reactions

Coupling reactions were performed in order to ascertain the performance of the catalysts in the selected solvents. The reaction conditions were initially optimised by screening a number of solvents and bases for the reactions. The Heck, Suzuki and Sonogashira coupling reactions were considered.

4.2.2.1 Heck Coupling Reaction

The coupling reaction of iodobenzene and styrene was studied in a range of solvents. The solvents considered were acetonitrile, 1-propanol, 2-propanol and water. No reaction was observed in the presence of water and 2-propanol irrespective of the catalyst-ligand combination. The solutions remained colourless even after 8 hours. Some reaction took place in the presence of 1-propanol, although rapid precipitation of palladium as Pd(0) black occurred. The best solvent was acetonitrile with satisfactory yields realized.

Ligands were also screened to investigate their effect on conversion. In this case, PPh₃ gave better yields than bipyridyl (bipy). In general Pd(OAc)₂ and PPh₃ were the best catalyst/ligand combination (Entry 1). This system showed the highest yields at catalyst loadings of 0.1 mol%. The second catalyst-ligand combination, Pd(PPh₃)₂Cl₂ and PPh₃ afforded the second highest yields (Entry 3). The combination of Pd(OAc)₂(PPh₃)₂ and PPh₃ gave moderate yields (Entry 2). A summary of the reaction results is given in Table 4. 8. It was therefore decided that Pd(OAc)₂-PPh₃ and Pd(PPh₃)₂Cl₂-PPh₃ would be used in the attempted catalyst separation study.

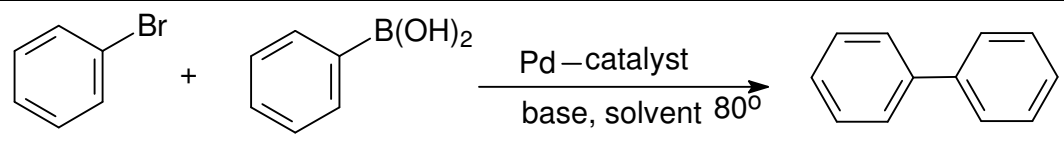
Table 4. 8: Results of Heck coupling reaction

Entry	Catalyst	Base	Ligand	Solvent	Yield
1	Pd(OAc) ₂	Et ₃ N	PPh ₃	Acetonitrile	97%
2	Pd(OAc) ₂ (PPh ₃) ₂	Et ₃ N	PPh ₃	Acetonitrile	50%
3	Pd(PPh ₃) ₂ Cl ₂	Et ₃ N	PPh ₃	Acetonitrile	87%
4	Pd(OAc) ₂ (PPh ₃) ₂	Et ₃ N	Bipy	Acetonitrile	61%
5	Pd(PPh ₃) ₂ Cl ₂	Et ₃ N	Bipy	Acetonitrile	42%

4.2.2.2 Suzuki Coupling Reaction

The coupling reaction of iodobenzene and phenylboronic acid was studied in different solvents, bases and catalysts. Two ligands, bipyridyl and PPh₃ were also compared. Generally, low to moderate yields were obtained with all the catalysts. The solvents screened were 2-propanol, 1-propanol and water. No reaction occurred in the presence of water irrespective of the catalyst used. Some reaction occurred in 1-propanol, although not as satisfactory as in 2-propanol. 2-propanol was therefore selected as the most suitable solvent.

The bases screened were Na₂CO₃, pyrrolidine and triethylamine (Et₃N). Na₂CO₃ afforded acceptable yields. However, a salt precipitate was observed with the use of this base. Triethylamine gave the better yields without forming any precipitate. This base was chosen as the most suitable base. In the ligand comparison study, bipyridyl gave better yields compared to PPh₃. Pd(PPh₃)₂Cl₂ afforded fair yields irrespective of the ligand used (Entry 3 and 5). Pd(OAc)₂ and Pd(OAc)₂(PPh₃)₂ gave poor yields with rapid palladium black formation (Entry 1 and 2). The summarized reaction results are given in Table 4. 9. Due to the low yields, it was deemed pointless to go forward with catalyst separation study in the Suzuki coupling reaction.

Table 4. 9: Results of Suzuki coupling reaction

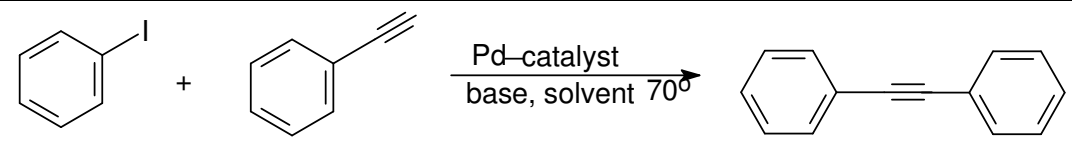
Entry	Catalyst	Base	Ligand	Solvent	Yield
1	Pd(OAc) ₂	Et ₃ N	PPh ₃	2-Propanol	20%
2	Pd(OAc) ₂ (PPh ₃) ₂	Et ₃ N	PPh ₃	2-Propanol	16%
3	Pd(PPh ₃) ₂ Cl ₂	Et ₃ N	PPh ₃	2-Propanol	30%
4	Pd(OAc) ₂ (PPh ₃) ₂	Et ₃ N	Bipy	2-Propanol	31%
5	Pd(PPh ₃) ₂ Cl ₂	Et ₃ N	Bipy	2-Propanol	40%

4.2.2.3 Sonogashira Coupling Reaction (Copper-free)

The coupling of bromobenzene and phenylacetylene was studied in water as solvent and in the absence of copper. This solvent was purposefully chosen to determine the efficiency of coupling reactions in aqueous media. Two bases were screened for the reaction. These were pyrrolidine and triethylamine. Both gave good yields. However pyrrolidine afforded the highest yields of the two bases. Pyrrolidine was selected as the most suitable base. PdCl₂ gave the most decent yields, followed closely by Pd(PPh₃)₂Cl₂. No reaction was observed with the use of Pd(OAc)₂ and Pd(OAc)₂(PPh₃)₂. The reaction solutions of these catalysts remained colourless after 8 hours. Summarized reaction results are given in Table 4. 10.

The results confirmed that Sonogashira coupling can be performed in aqueous media, in spite of the low to moderate yields obtained in this study. The catalyst separation attempt was also aborted for the Sonogashira coupling reaction due to these low yields

Table 4. 10: Results of Sonogashira coupling reaction

					
Entry	Catalyst	Base	Ligand	Solvent	Yield
1	PdCl ₂	Pyrrolidine	PPh ₃	H ₂ O	47%
2	Pd(OAc) ₂	Pyrrolidine	PPh ₃	H ₂ O	No reaction
3	Pd(OAc) ₂ (PPh ₃) ₂	Pyrrolidine	PPh ₃	H ₂ O	No reaction
4	Pd(PPh ₃) ₂ Cl ₂	Pyrrolidine	PPh ₃	H ₂ O	42%

4.3 CATALYST RETENTION MEASUREMENTS

In preceding chapters, the emphasis was on membrane-solvent interactions. In this part of the study membrane-solute and solvent-solute interactions are placed under the spotlight. The effect of these interactions on catalyst retention is discussed. The discussions are centred on the solvent used. Acetonitrile, 2-propanol and water were used in the retention measurements. These solvents were selected based on their performance in Heck, Suzuki and Sonogashira coupling reactions respectively. In the second part of this section, solute-solute interactions come into play. In this part, catalyst retention in the presence of other species was studied in view of catalyst separation.

4.3.1 Retention Measurements in Acetonitrile

The results of catalyst retention in acetonitrile performed at 10 and 20 bar are illustrated in Figure 4. 21 and Figure 4. 22 respectively. The results show very low retention of Pd(OAc)₂ in all the membranes irrespective of the pressure. NF90 showed the highest retention of 40%. XLE showed the second highest retention of 36%. BW30 showed a mere 13% retention while NF270 was the worst with less than 10% of the catalyst retained. The trend with respect to the rejection of Pd(OAc)₂ is: NF90 > XLE > BW30 > NF270.

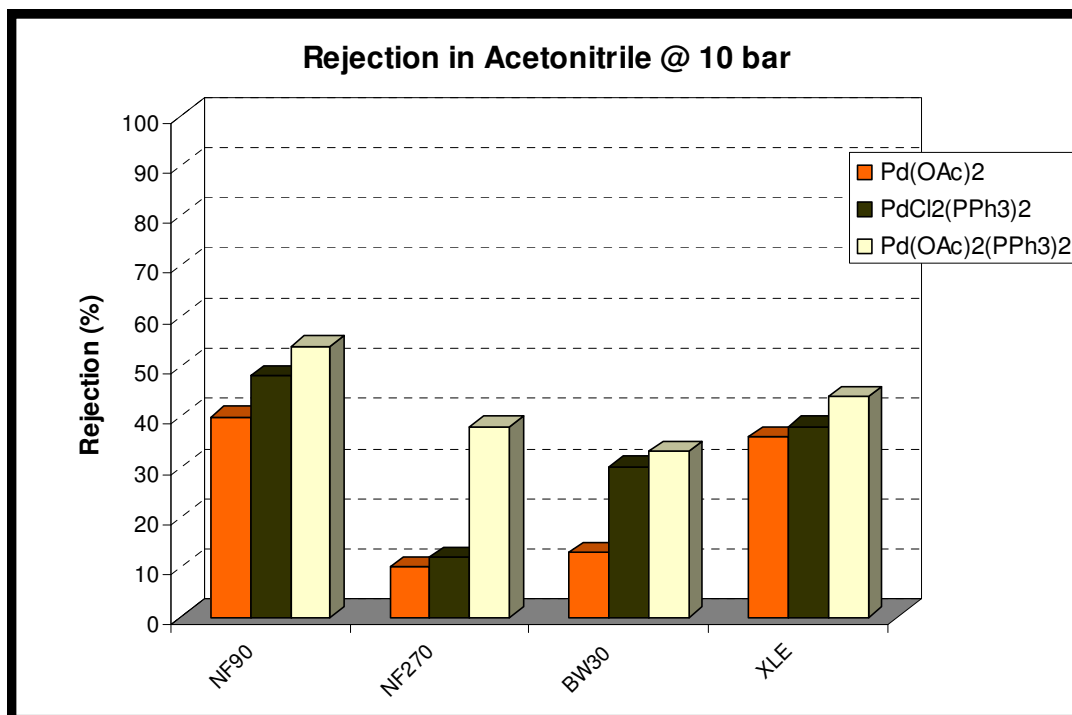


Figure 4. 21: Catalyst retention results in acetonitrile at 10 bar at room temperature

The membranes showed similar retention of Pd(PPh₃)₂Cl₂ in acetonitrile. NF90 once again showed the highest retention of 48%. XLE showed retention of 38%. BW30 showed an improved retention of 30%. NF270 also showed an increased retention of 12%. The increase in retention is however still insignificant with much of the catalyst still permeating through the membranes. The trend with respect to the rejection of Pd(PPh₃)₂Cl₂ is: NF90 > XLE > BW30 > NF270.

The membranes showed an improved retention behaviour of Pd(OAc)₂(PPh₃)₂. NF90 showed retention of more than 50%, while XLE also showed a fair retention of 44%. NF270 showed the most improvement with retention of 38%. BW30 gave the lowest retention of 33%. The rejection trend changed slightly and is as follows: NF90 > XLE > NF270 > BW30. Overall the membranes showed a greater retention of Pd(OAc)₂(PPh₃)₂ than Pd(PPh₃)₂Cl₂ and Pd(OAc)₂. The overall rejection trend at 10 bar with respect to the catalysts is: Pd(OAc)₂(PPh₃)₂ > Pd(PPh₃)₂Cl₂ > Pd(OAc)₂.

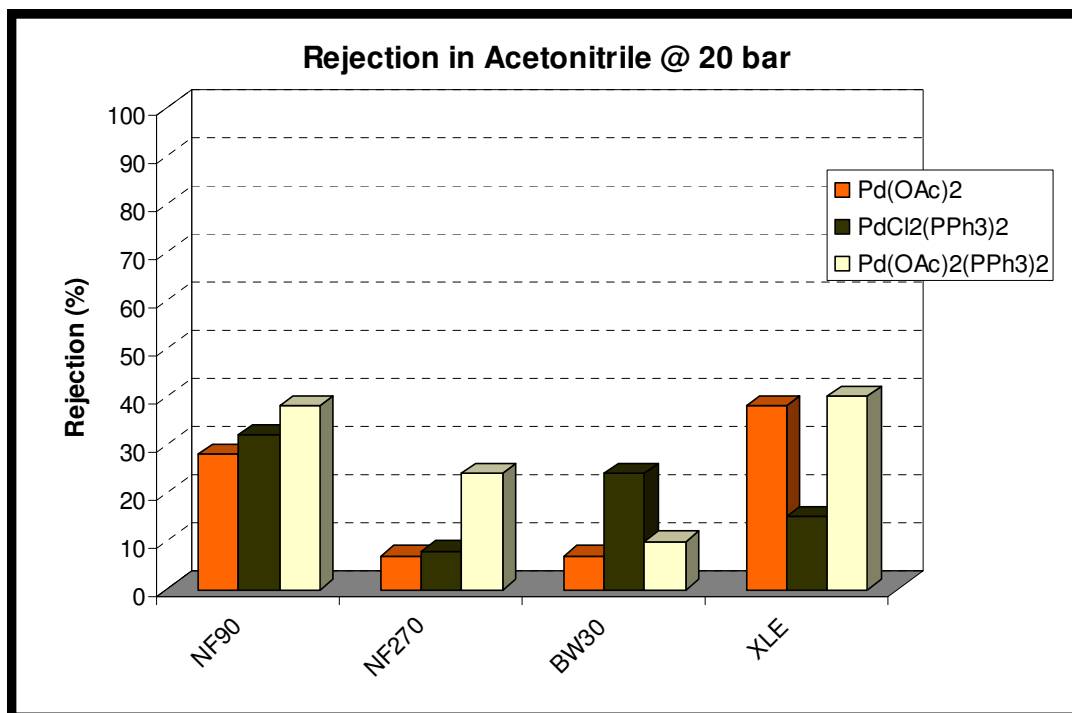


Figure 4. 22: Catalyst retention results in acetonitrile at 20 bar at room temperature

The retention measurements at 20 bar illustrated in Figure 4. 22 show lower retention of the catalysts compared to measurements at 10 bar. In this instance, XLE showed the highest Pd(OAc)₂ retention of 38%. NF90 showed retention of 28%. This observation points towards a 30% decrease in the retention when compared to measurements at 10 bar. BW30 and NF270 showed a similar retention which is less than 10%. The retention in BW30 also showed a 45% decrease when compared to measurements at 10 bar. The trend relating to Pd(OAc)₂ retention at 20 bar is: XLE > NF90 > BW30, NF270.

The retention of Pd(PPh₃)₂Cl₂ in acetonitrile at 20 bar was also lower in all the membranes when compared to 10 bar measurements. NF90 showed the highest retention of 32%. A strange observation was that of BW30. The membrane showed a retention of 24% which is higher than that in XLE. The latter showed retention of 15%. There is almost 33% difference in the retention between the two membranes.

This may relate back to characterization results in which the two membranes showed interchanging characteristics. NF270 showed the lowest retention of 8%. The retention of $\text{Pd}(\text{OAc})_2(\text{PPh}_3)_2$ in all the membranes at 20 bar showed a significant reduction when compared to measurements at 10 bar. XLE showed retention of 40%. NF90 showed retention of 38%. NF270 and BW30 showed retentions of 24% and 10% respectively. BW30 showed the most drastic reduction in retention when compared to measurements at 10 bar. This may indicate a significant change in polymer properties due to solvent and pressure effects. The trend relating to $\text{Pd}(\text{OAc})_2(\text{PPh}_3)_2$ retention at 20 bar is : XLE > NF90 > NF270 > BW30.

4.3.2 Retention Measurements in 2-Propanol

The results of catalyst retention in 2-propanol at 10 bar are illustrated in Figure 4. 23. The membranes showed slightly higher retentions compared to those in acetonitrile. NF90 showed the highest $\text{Pd}(\text{OAc})_2$ retention of 74%. XLE showed retention of 44%. NF270 and BW30 showed poor retentions of 9% and 4% respectively. $\text{Pd}(\text{OAc})_2$ rejection trend at this point is: NF90 > XLE > NF270 > BW30.

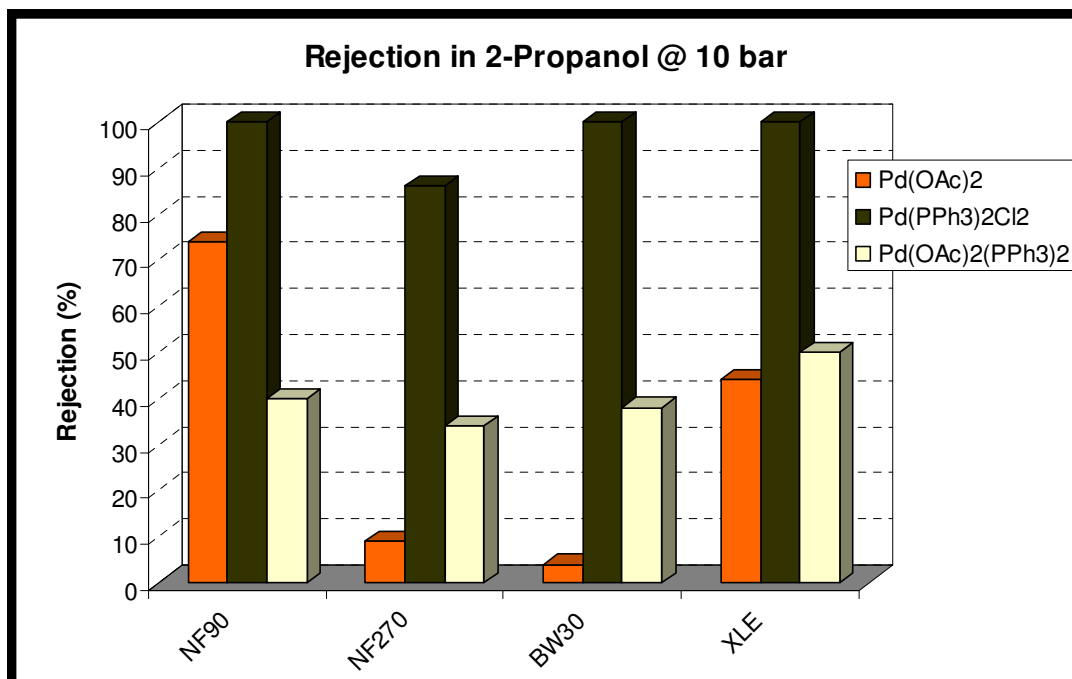


Figure 4. 23: Catalyst retention results in 2-propanol at 10 bar at room temperature

The most obvious observation from the results is the retention of Pd(PPh₃)₂Cl₂. It can be seen that the catalysts was well retained by all membranes. NF90, BW30 and XLE showed retentions of >99%. NF270 showed retention of 86% which is still fairly high when compared to retention measurements in acetonitrile.

The retention of Pd(OAc)₂(PPh₃)₂ in 2-propanol at 10 bar did not differ significantly from that in acetonitrile. XLE showed the highest retention with 50% of the catalyst retained. NF90 showed retention of 40%. BW30 and NF270 showed retentions of 38% and 34% respectively. The trend associated with Pd(OAc)₂(PPh₃)₂ is: XLE > NF90 > BW30 > NF270. Overall, the results at 10 bar show a different trend with respect to catalyst retention when compared to those in acetonitrile. The trend observed is: Pd(PPh₃)₂Cl₂ > Pd(OAc)₂(PPh₃)₂ > Pd(OAc)₂. Results of retention results performed at 20 bar are illustrated in Figure 4. 24.

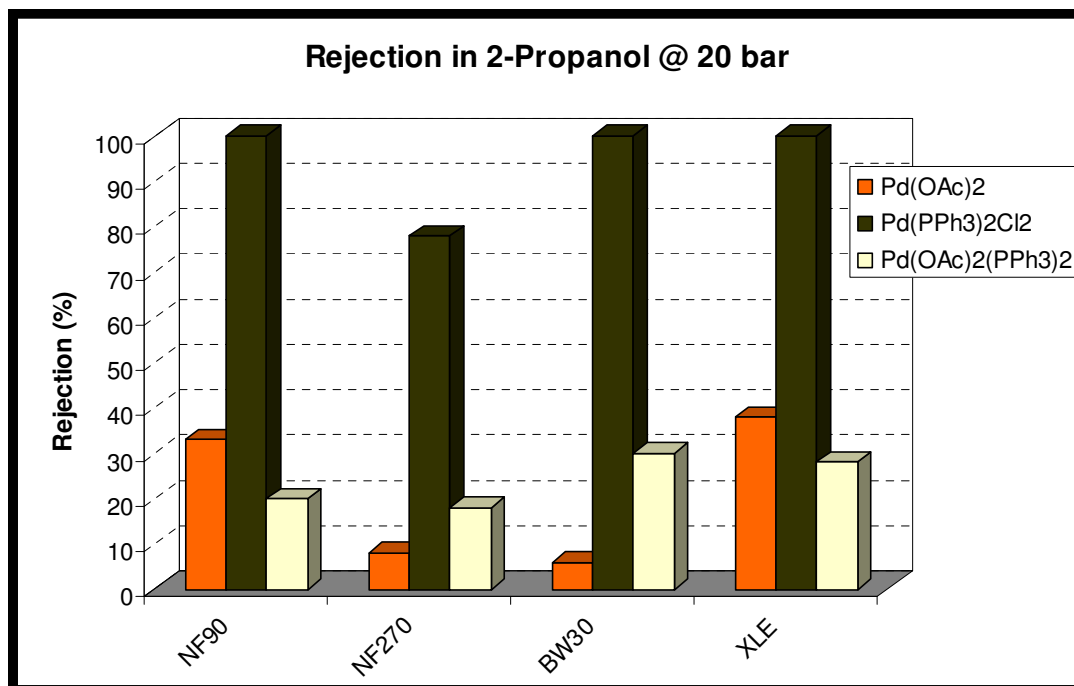


Figure 4. 24: Catalyst retention results in 2-propanol at 20 bar at room temperature

The results show a decrease in catalyst retention. XLE showed the highest retention with 38% of Pd(OAc)₂ retained. NF90 showed retention of 33%. This is an indication of a 55% reduction in retention, compared to 10 bar measurements. NF270 and BW30 showed very poor retentions of 8% and 6% respectively. The rejection trend at this point is: XLE > NF90 > NF270 > BW30.

The retention of Pd(PPh₃)₂Cl₂ at 20 bar did not change much. Most of the membranes showed very good retention of the catalyst. NF90, BW30 and XLE showed retentions up to >99%. NF270 showed a retention of 78%. The results therefore indicate that pressure does not significantly influence retention in 2-propanol.

$\text{Pd}(\text{OAc})_2(\text{PPh}_3)_2$ retention in all the membranes at 20 bar showed a significant decrease. NF90 showed a 50% decrease in retention. XLE showed a 44% decrease. BW30 did not change much with 38% of the catalyst retained. NF270 also showed a 47% decrease in retention. This clearly shows the effect of pressure on catalyst retention.

All our results show a decrease in retention with increasing pressure. This is in contrary to observations by Scarpello *et al.* [44]. The group observed increased retentions with increasing pressure. It should be kept in mind however, that they used solvent-resistant polyimide and polysiloxane membranes. Therefore their chemical properties will differ from the polyamide membranes used in our study. Consequently, membrane performances such as flux and rejection will also differ.

4.3.3 Retention Measurements in Water

Retention measurements of $\text{Pd}(\text{OAc})_2$ and PdCl_2 were performed in water. This was done in order to determine the separation of the catalysts from aqueous media. Therefore the low solubility of $\text{Pd}(\text{OAc})_2$ in water should be kept in mind. PdCl_2 was dissolved in a small amount of HCl before dilution with distilled water. Total dissolution of the complex was achieved. Retention results are illustrated in Figure 4. 25 and Figure 4. 26. The retention measurements performed at 10 bar are illustrated in Figure 4. 25.

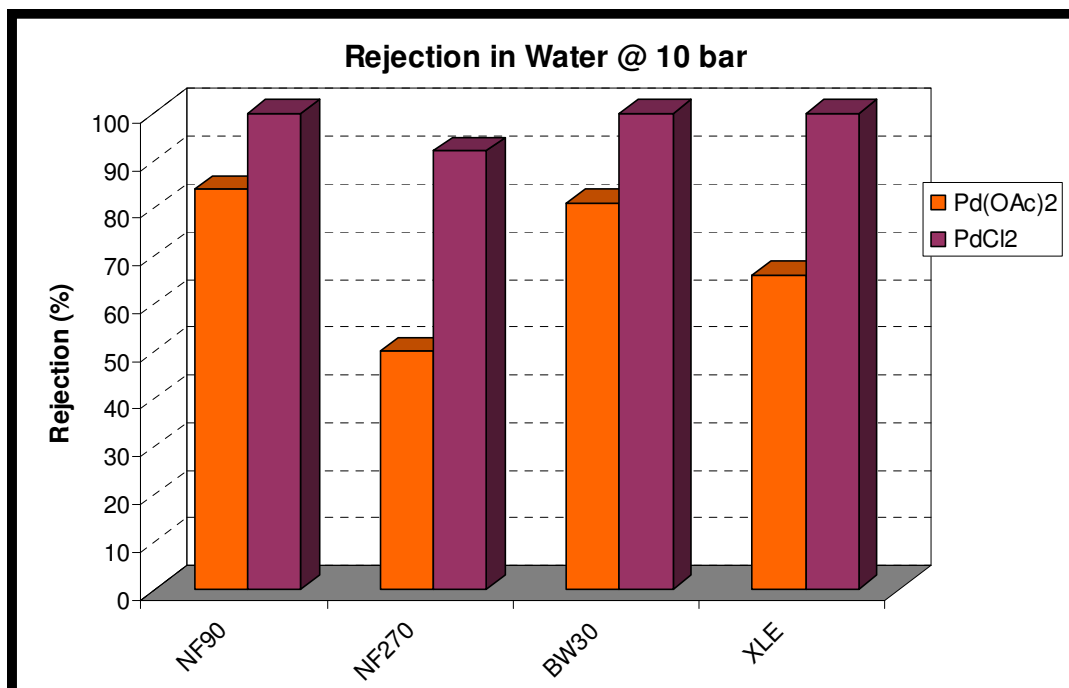


Figure 4. 25: Catalyst retention results in water at 10 bar at room temperature

The results show good retention of Pd(OAc)₂ in all membranes. NF90 showed the highest retention of 84%. BW30 showed a comparable retention of 81%. XLE and NF270 showed a reasonable retention of 66% and 50% respectively. The trend observed with respect to Pd(OAc)₂ retention in water, is different from that observed in retention measurements where organic solvents were used. In the former, the trend is NF90 > BW30 > XLE > NF270.

All the membranes showed very good retention of PdCl₂. NF90, BW30 and XLE showed retentions of up to >99%. NF270 also showed a notable retention of 92%. These retention results are similar to those of Pd(PPh₃)₂Cl₂ in 2-propanol. The results may be strange if one looks at the sizes of the solutes alone. PdCl₂ has a smaller MW than Pd(OAc)₂. It was expected that PdCl₂ would be poorly retained than Pd(OAc)₂. But this was not the case. The results therefore highlight that other transport mechanisms have to be taken into consideration when addressing retention data.

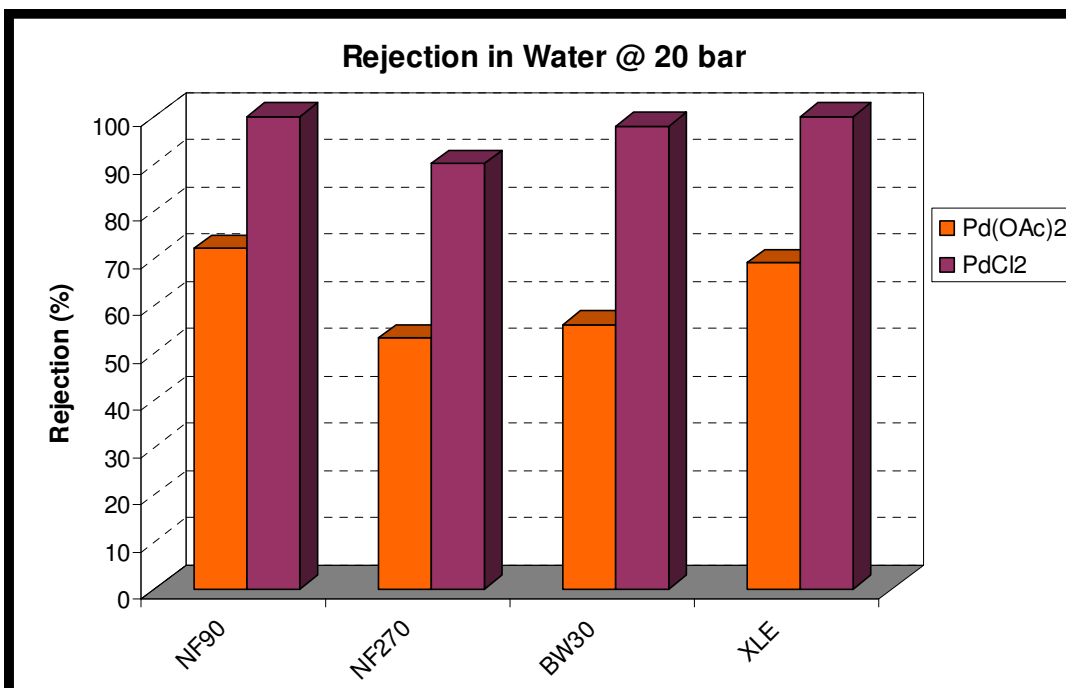


Figure 4.26: Catalyst retention results in water at 20 bar at room temperature

The results of retention measurements at 20 bar are illustrated in Figure 4. 26. The results show that 70% of Pd(OAc)₂ was retained in NF90. XLE showed an increase in retention compared to measurements at 10 bar, with 69% retention achieved. BW30 showed a 31% reduction in the retention compared to 10 bar measurements. The membrane showed retention of 56%. NF270 realized a slight increase in retention with 53% retention. The rejection trend at this point is: NF90 > XLE > BW30 > NF270. Overall, the membranes showed the highest catalyst retention in water compared to retention in organic solvents.

The catalyst retention results in acetonitrile, 2-propanol and water show the influence of solvent-solute interactions. Solvents differ in the way they interact with solutes. The concept of solvation has been shown to be of importance in addressing solvent-solute interactions. Solvation has been defined as the phenomenon in which each dissolved molecule or ion is surrounded by a shell of solvent molecules [45].

Reichardt [46] has explained that solvation increases with increasing polarity of the solvent. Our results show that catalyst retention generally increases with increasing polarity of solvent as listed in Table 4.4. It can be assumed then, that better solvation of the solute leads to increased retention. This is line with observations by Geens *et al.* [47]. They observed higher retentions in methanol than in ethanol. They based their results on solvation properties of the two solvents.

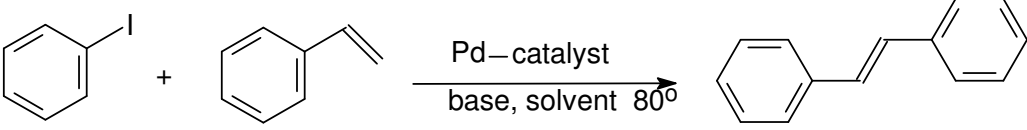
Membrane-solute interactions are also of importance. Looking at the overall retention results, it can be seen that solute size and steric hindrance effects come into play. The larger catalyst was rejected better on average irrespective of the solvent. This observation points towards membrane-solute interactions in which parameters such as surface resistance and mass transfer resistance have influence. The larger catalyst will experience more of these effects than the smaller catalysts.

4.4 CATALYST SEPARATION AND REUSE

The concept of catalyst separation was investigated for a real post-reaction mixture. The Heck coupling reaction was selected for this part of the study. In an earlier study, it was observed that the product was not retained significantly. Retention of 3% in NF90 at 10 bar was realized. This observation was good enough to proceed. The separation of two catalysts [$\text{Pd}(\text{OAc})_2$ and $\text{Pd}(\text{PPh}_3)_2\text{Cl}_2$] by NF90 at 10 bar was studied.

The reaction results of $\text{Pd}(\text{OAc})_2$ from reaction mixture Run 18, and $\text{Pd}(\text{PPh}_3)_2\text{Cl}_2$ from Run 26 are listed in Table 4. 11. The coupling reaction – recycle procedure was run for two cycles for each catalyst. The retention results of $\text{Pd}(\text{OAc})_2$ are illustrated in Figure 4. 27.

Table 4. 11: Results of Heck catalyst reaction – recycle procedure

					
Run	Catalyst	Base	Ligand	Solvent	Yield
18	Pd(OAc) ₂	Et ₃ N	PPh ₃	Acetonitrile	97%
18b	Pd(OAc) ₂	Et ₃ N	Bipy	Acetonitrile	49%
18c	Pd(OAc) ₂	Et ₃ N	Bipy	Acetonitrile	No reaction
26	Pd(PPh ₃) ₂ Cl ₂	Et ₃ N	PPh ₃	Acetonitrile	87%
26b	Pd(PPh ₃) ₂ Cl ₂	Et ₃ N	PPh ₃	Acetonitrile	6%
26c	Pd(PPh ₃) ₂ Cl ₂	Et ₃ N	PPh ₃	Acetonitrile	No reaction

The reaction, Run 18 reached near complete conversion in 4 hours. The first filtration cycle yielded 52% retention of the catalyst. This was a reasonable retention of the catalyst. The second reaction, Run 18b which was initiated using the retentate from Run 18, fresh reactants and solvent reached moderate conversions in 8 hours, with 49% yields realized. The system was clearly showing some decline in catalytic activity. The second filtration cycle resulted in a mere 10% catalyst retention. The retentate from this cycle was used to initiate reaction Run 18c. No reaction was noticeable even after 8 hours. The lack of reaction could be linked to the low catalyst concentration, and the subsequent loss of catalyst activity resulting from catalyst decomposition.

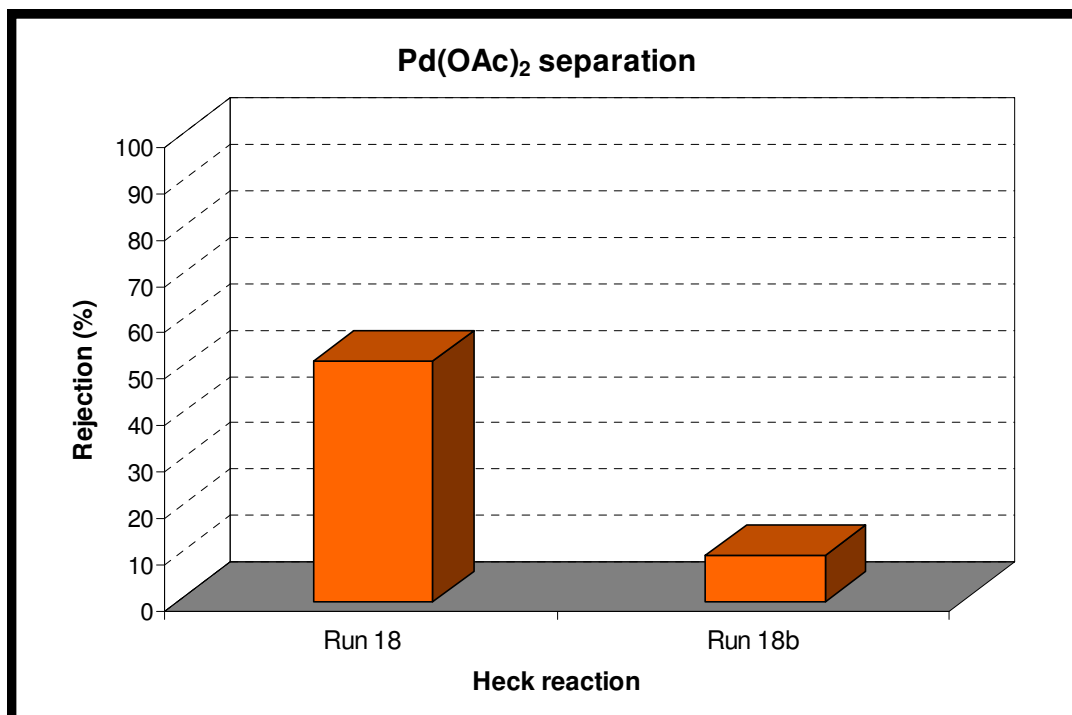


Figure 4. 27: Pd(OAc)₂ retention and recycle results in acetonitrile at 10 bar at room temperature

The reaction, Run 26 performed with Pd(PPh₃)₂Cl₂ reached reasonable conversions after 4 hours, with 87% yields obtained. The first filtration cycle resulted in 58% retention of the catalyst as illustrated in Figure 4. 28 . The retentate from this cycle was used to initiate reaction Run 26b with fresh reactants and solvent. This reaction was plagued by palladium black formation. An insignificant reaction yield of 6% was realized after 8 hours. For totality, the second filtration cycle was performed. This cycle yielded 36% catalyst retention. It is not clear whether the precipitated palladium black had influenced catalyst retention. The retentate from this cycle clearly contained deactivated catalyst. This was evident in reaction Run 26c which did not show any conversion after 8 hours. It was decided that the catalyst had totally lost activity.

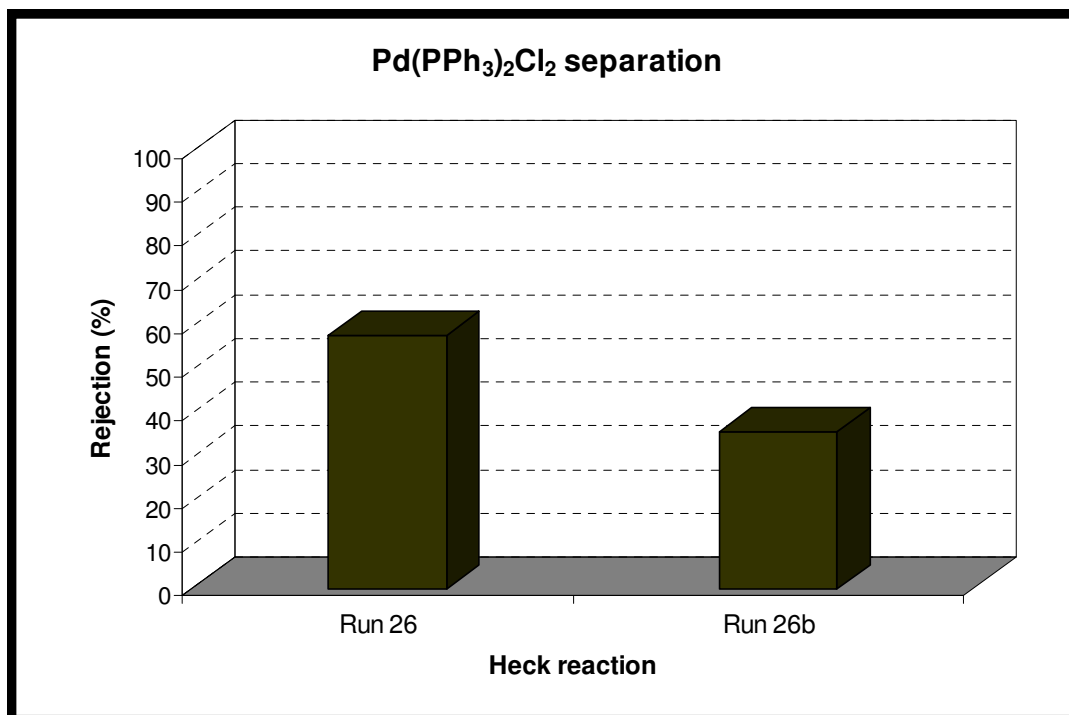


Figure 4. 28: Pd(PPh₃)₂Cl₂ retention and recycle results in acetonitrile at 10 bar at room temperature

These results highlight that catalyst decomposition has to be taken into account to address losses during nanofiltration of transition-metal catalysts. It has been shown that catalysts are reduced from Pd(II) to Pd(0) during Heck reaction [41]. This palladium(0) complex is prone to deactivation into palladium black entities [48]. The exact mechanism of deactivation is beyond the scope of this study.

It should be kept in mind that our system was not isolated, and therefore deactivation due to oxidation was imminent. The results however show that catalyst recycling is possible. This procedure appears to be a trade off between reduced reaction rates and catalyst loss. Our system did not show robustness. Only two nanofiltration cycles were possible. This is somewhat unreasonable when compared to other author's reports of up to ten filtration cycles [49,50]. Our observations show that many factors have to be taken into account when considering such a catalyst-recycle process.

REFERENCES

1. KATCHALKY, A. & KEDEM, O. 1958 Thermodynamics of flow processes in biological systems. *Membrane Biophysics*. **1** 53 – 78.
2. KOŠUTIĆ, K., DOLAR, D. & KUNST, B. 2006. On the experimental parameters characterizing the reverse osmosis and nanofiltration membranes' active layer. *Journal of Membrane Science*. **282** (1-2) 109 – 114.
3. HU, K. & DICKSON, J.M. 2006. Nanofiltration membrane performance on fluoride removal from water. *Journal of Membrane Science*. **279** (1-2) 529 – 538.
4. KOŠUTIĆ, K., KAŠTELAN, L. & KUNST, B. 2000. Porosity of some commercial reverse osmosis and nanofiltration polyamide thin-film composite membranes. *Journal of Membrane Science*. **168** (1-2) 101 – 108.
5. MOHAMMAD, A.W., HILAL, N., AL-ZOUBI, H. & DARWISH, N.A. 2007. Prediction of permeate fluxes and rejections of highly concentrated salts in nanofiltration membranes. *Journal of Membrane Science*. **289** (1-2) 40 – 50.
6. MÄNTTÄRI, M., PEKURI, T. & NYSTRÖM, M. 2004. NF270, a new membrane having promising characteristics and being suitable for treatment of dilute effluents from the paper industry. *Journal of Membrane Science*. **242** (1-2) 107 – 116.
7. NGHIEM, L.D. & COLEMAN, P.J. 2008. NF/RO filtration of the hydrophobic ionogenic compound triclosan: transport mechanisms and the influence of membrane fouling. *Separation and Purification Technology*. **62** (1) 709 – 716.

-
8. Dow FilmTec Technical Manual. 2005 <http://www.dow.com/liquidseps/> accessed 25/05/2009.
 9. ZHAO, Y. & YUAN, Q. 2006. A comparison of nanofiltration with aqueous and organic solvents. *Journal of Membrane Science*. **279** (1-2) 453 – 458.
 10. OUANO, A.C., & CAROTHERS, F.A. 1980. Dissolution dynamics of some polymers: solvent-polymer boundaries. *Polymer Engineering Science*. **20** (2) 160 – 166.
 11. SEE TOH, Y.H., LIM, F.W. & LIVINGSTON, A.G. 2007. Polymeric membranes for nanofiltration in polar aprotic solvents. *Journal of Membrane Science*. **301** (1-2) 3 – 10.
 12. YANG, X.J., LIVINGSTON, A.G. & FREITAS DOS SANTOS, L. 2001. Experimental observations of nanofiltration with organic solvents. *Journal of Membrane Science*. **190** (1-2) 45 – 55.
 13. HANSEN, C.M. 2007. Hansen solubility parameters: a user's handbook. 2nd ed. CRC Press. Florida: Boca Raton.
 14. KOSOWER, E.M. 1968. An introduction to physical organic chemistry. New York: Wiley.
 15. ROBINSON, J.P., TARLETON, E.S., MILLINGTON, C.R. & NIJMEIJER, A. 2004. Solvent flux through dense polymeric nanofiltration membranes. *Journal of Membrane Science*. **230** (1) 29 – 37.

-
16. JOHANSSON, G. & BOESEN, C.S. 1975. Water and solute transport through cellulose acetate reverse osmosis membranes. *Desalination*. **17** (1) 145 – 165.
 17. MACHADO, D.R., HASSON, D. & SEMIAT, R. 2000. Effect of solvent flow through nanofiltration membranes. Part II. Transport model. *Journal of Membrane Science*. **166** (1-2) 63 – 69.
 18. NOORDMAN, T.R. & WESSELINGH, J.A. 2002. Transport of large molecules through membranes with narrow pores The Maxwell-Stefan description combined with hydrodynamic theory. *Journal of Membrane Science*. **210** (1-2) 227 – 243.
 19. EBERT, K., KOLL, J., DIJKSTRA, M.F.J. & EGGERS, M. 2006. Fundamental studies on the performance of a hydrophobic solvent stable membrane in non-aqueous solutions. *Journal of Membrane Science*. **285** (1-2) 75 – 80.
 20. PEREIRA, A.M.M. 2007. Characterization of polymeric membranes for non-aqueous separations. PhD Thesis. Eindhoven University of Technology.
 21. TARLETON, E.S., ROBINSON, J.P., MILLINGTON, C.R., NIJMEIJER, A. & TAYLOR, M.L. 2006. The influence of polarity on flux and rejection behaviour in solvent resistant nanofiltration – experimental observations. *Journal of Membrane Science*. **278** (1-2) 318 – 327.
 22. SILVA, P., HAN, S. & LIVINGSTON, A.G. 2005. Solvent transport in organic solvent nanofiltration membranes. *Journal of Membrane Science*. **262** (1-2) 49 – 59.

-
23. ZHAO, Y. & YUAN, Q. 2006. Effect of membrane pre-treatment on performance of solvent resistant nanofiltration membranes in methanol solutions. *Journal of Membrane Science*. **280** (1-2) 195 – 201.
 24. GEENS, J., VAN DER BRUGGEN, B. & VANDECASTEELE, C. 2004. Characterization of the solvent stability of polymeric nanofiltration membranes by measurement of contact angles and swelling. *Chemical Engineering Science*. **59** (1-2) 1161 – 1164.
 25. FREGER, V., BOTTINO, A., CAPANNELLI, G., PERRY, M., GITIS, V. & BELFER, S. 2005. Characterization of novel acid-stable NF membranes before and after exposure to acid using ATR-FTIR, TEM and AFM. *Journal of Membranes Science*. **256** (1-2) 134 – 142.
 26. DARVISHMANESH, S., DEGRÈVE, J. & VAN DER BRUGGEN, B. 2009. Comparison of pressure driven transport of ethanol/n-hexane mixtures through dense and microporous membranes. *Chemical Engineering Science*. **64** 3914 – 3927.
 27. MILLER-CHOU, B.A. & KOENIG, J.L. 2003. A review of polymer dissolution. *Progress in Polymer Science*. **28** 1223 – 1270.
 28. PATTERSON, D.A., LAU, L.Y., ROENGPITHYA, C., GIBBINS, E.J. & LIVINGSTON, A.G. 2008. Membrane selectivity in the organic solvent nanofiltration of trialkylamine bases. *Desalination*. **218** (1) 248 – 256.
 29. SEE TOH, Y.H., LOH, X.X., LI, K., BISMARCK, A. & LIVINGSTON, A.G. 2007. In search of a method for the characterization of organic solvent nanofiltration membranes. *Journal of Membrane Science*. **291** (1-2) 120 – 125.

-
30. CORONELL, O., MARIÑAS, B.J., ZHANG, X. & CAHILL, D.J. 2008. Quantification of functional groups and modelling of their ionization behaviour in the active layer of FT30 reverse osmosis membrane. *Environmental Science & Technology*. **42** (14) 5260 – 5266.
 31. MULDER, M. 1998. Basic Principles of Membrane Technology. 2nd ed. Netherlands: Alinea.
 32. PATTERSON, D.A., HAVILL, A., COSTELLO, S., SEE-TOH, Y.H., LIVINGSTON, A.G. & TURNER, A. 2009. Membrane characterisation by SEM, TEM and ESEM: The implications of dry and wetted microstructure on mass transfer through integrally skinned polyimide nanofiltration membranes. *Separation and Purification Technology*. **66** (1-2) 90 – 97.
 33. BOUSSU, K., VAN DER BRUGGEN, B., VOLODIN, A., SNAUWAERT, J., VAN HAESDONCK, C. & VANDECASSTEELE, C. 2005. Roughness and hydrophobicity studies of nanofiltration membranes using different modes of AFM. *Journal of Colloidal and Interface Science*. **286** (1-2) 632 – 638.
 34. BOUSSU, K., VAN DER BRUGGEN, B., VOLODIN, A., VAN HAESDONCK, C., DELCOUR, J.A., VAN DER MEEREN, P. & VANDECASSTEELE, C. 2006. Characterization of commercial nanofiltration membranes and comparison with self-made polyethersulfone membranes. *Desalination*. **191** (1-2) 245 – 253.
 35. TANG, C.Y., FU, Q.S., CRIDDLE, C.S. & LECKIE, J.O. 2007. Effect of flux (transmembrane pressure) and membrane properties on fouling and rejection of reverse osmosis and nanofiltration membranes treating

perfluorooctane sulfonate containing wastewater. *Environmental Science & Technology*. **41** (6) 2008 – 2014.

36. CADOTTE, J.E. 1981. Interfacially synthesized reverse osmosis membrane. Patentee FilmTec Corporation. (US Patent 4,277,344).
37. MANSOURPANAH, Y., MADAENI, S.S. & RAHIMPOUR, A. 2009. Preparation and investigation of separation properties of polyethersulfone supported poly(piperazineamide) nanofiltration membrane using microwave-assisted polymerization. *Separation and Purification Technology*. **69** (3) 234 – 242.
38. XU, X. & KIRKPATRICK, R.J. 2006. NaCl interaction with interfacially polymerized polyamide films of reverse osmosis membranes: a solid-state ²³Na NMR study. *Journal of Membrane Science*. **280** (1) 226 – 233.
39. CORONELL, O., MARIÑAS, B.J., ZHANG, X. & CAHILL, D.G. 2008. Quantification of functional groups and modelling of their ionization behaviour in the active layer of FT30 reverse osmosis membrane. *Environmental Science & Technology*. **42** (14) 5260 – 5266.
40. BARNARD, C. 2008. Palladium-catalysed C-C coupling: Then and now. *Platinum Metals Revision*. **52** (1) 38 – 45.
41. AMATORE, C., CARRÉ, E., JUTAND, A., M'BARKI, M.A. & MEYER, G. 1995. Evidence for the ligation of palladium(0) complexes by acetate ions: consequences on the mechanism of their oxidative addition with phenyl iodide and PhPd(OAc)(PPh₃)₂ as intermediate in the Heck reaction. *Organometallics*. **14** (12) 5605 – 5614.

-
42. BAKHMUTOV, V.I., BERRY, J.F., COTTON, A.F., IBRAGIMOV, S. & MURILLO, C.A. 2005. Non-trivial behaviour of palladium(II) acetate. *Dalton Transactions*. 1989 – 1992.
43. STOYANOV, E.S. 2000. IR study of the structure of palladium(II) acetate in chloroform, acetic acid and their mixtures in solution and in liquid-solid subsurface layers. *Journal of Structural Chemistry*. **41** (3) 440 – 445.
44. SCARPELLO, J.T., NAIR, D., FREITAS DOS SANTOS, L.M., WHITE, L.S. & LIVINGSTON, A.G. 2002. The separation of homogeneous organometallic catalyst using solvent resistant nanofiltration. *Journal of Membrane Science*. **203** (1-2) 71 – 85.
45. PERSON, I. 1986. Solvation and complex formation in strongly solvating solvents. *Pure & Applied Chemistry*. **58** (8) 1153 – 1161.
46. REICHARDT, C. 2003. Solvents and solvent effects in organic chemistry. 3rd ed. Weinheim: Wiley-VCH verlag.
47. GEENS, J., HILLEN, A., BETTENS, B., VAN DER BRUGGEN, B. & VANDECASTEELE, C. 2005. Solute transport in non-aqueous nanofiltration: effect of membrane material. *Journal of Chemical Technology and Biotechnology*. **80** 1371 – 1377.
48. TSUJI, Y. & FUJIHARA, T. 2007. New design in homogeneous palladium catalysis: study of transformation of Group 14 element compounds and development of nanosize palladium catalysts. *Bulletin of Korean Chemical Society*. **28** (11) 1902 – 1909.

-
49. NAIR, D., SCARPELLO, J.T., WHITE, L.S., FREITAS DOS SANTOS, L.M., VANKELECOM, I.F.J. & LIVINGSTON, A.G. 2001. Semi-continuous nanofiltration-coupled Heck reactions as a new approach to improve productivity of homogeneous catalysts. *Tetrahedron Letters*. **42** (46) 8219 – 8222.
50. NAIR, D., LUTHRA, S.S., SCARPELLO, J.T., VANKELECOM, I.F.J., FREITAS DOS SANTOS, L.M., WHITE, L.S., KLOETZING, R.J., WELTON, T & LIVINGSTON, A.G. 2002. Increased catalytic productivity for nanofiltration-coupled reactions using highly stable catalyst systems. *Green Chemistry*. **4** (1) 319 – 324.

CHAPTER 5 – CONCLUSIONS AND RECOMMENDATIONS

This chapter summarizes findings from the study. Important points from membrane and catalyst characterization studies are highlighted. A summary of catalyst retention studies is also given. Conclusions reached as a result of the findings are also discussed.

TABLE OF CONTENTS

5.1	SUMMARY	145
5.2	CONCLUDING REMARKS	146
5.3	RECOMMENDATIONS	147
5.4	REFERENCES	148

5.1 SUMMARY

Membrane separation processes offer a promising alternative to energy-intensive separation processes such as distillation and solvent extraction. NF and RO are among the most investigated membrane processes with a potential use in the chemical industry [1].

In this study, the aim was to determine the potential application of these membrane processes in the separation and recovery of transition-metal catalyst systems from reaction mixtures. The main goal was achieved through a series of structured activities which include a literature study, membrane and catalyst characterization, catalyst retention and recovery. These activities make up this dissertation and are summarized below.

- In the first chapter, an introduction into the concept of catalysis was given. Different catalyst systems were identified. Their strengths and weaknesses concerning industrial application were discussed. An introduction into membrane technology was also given. In this case, a brief description of membrane processes was given.
- Chapter 2 elaborated on the foundation laid out in the first chapter. Theory of transition-metals was discussed in view of highlighting their application in homogeneous catalysis. Catalyst design and development was discussed. A background on carbon-carbon coupling reactions was also given. In the second part, fundamental studies on transport mechanisms governing nanofiltration processes were identified.
- The experimental approach was outlined in Chapter 3. All analytical instrumentation used was given. The methodology involved in membrane and catalyst characterization was also discussed.

- The polymeric membranes were thoroughly characterized for physical and chemical properties. The behaviour of the membranes in the selected organic solvents was highlighted. The morphology of the membranes was studied. Overall, NF90 was considered as the preferred membrane. This membrane showed characteristics that were of interest for achieving the objectives set out for the study. This membrane showed stability in the selected organic solvents.
- Catalyst retention studies showed the influence of membrane-solute interactions such as steric hindrance and size exclusion. The larger catalyst, Pd(OAc)₂(PPh₃)₂ was rejected better by all the membranes irrespective of the solvent used. The smaller catalyst, Pd(OAc)₂ was the most poorly rejected catalyst.
- Catalyst separation using NF90 membrane was attempted for the Heck coupling reaction system. The reaction-separation procedure was repeated for two filtration cycles with rapid activity decline evident. This is very poor when compared to reports in literature [2,3,4] of up to seven reaction-filtration cycles.

5.2 CONCLUDING REMARKS

This study has revealed that polymeric membranes show low efficiency in separating transition-metal catalysts from solution and reaction mixtures. It has been shown that membranes designed for aqueous applications perform poorly in organic solvents. The study has given insight that catalyst-separation is influenced by the following factors:

- Membrane-solvent interactions, such as swelling, solvent polarity and membrane hydrophobicity or hydrophilicity.
- Solute-solvent interactions, such as solvation and solubility. These interactions influence the stability of the catalysts in the solvents.

- Membrane-solute interactions which include size exclusion, surface resistance and mass transfer resistance.

It can be concluded that for such a catalyst separation system to be effective, the issues discussed above should be addressed in detail. These issues are currently not fully understood and provide exciting challenges for further research. In the meantime, these issues are major limitations for industrial application of the membrane-catalyst separation protocol.

5.3 RECOMMENDATIONS

- Research into solvent resistant membranes such as polyimides could be advantageous for catalyst separation in organic solvents. Other types of NF membranes such as chitosan, cellulose and inorganic membranes may be applicable.
- The application of ionic liquids in carbon-carbon coupling reactions may also offer green alternatives to harsh organic solvents. Investigation into catalyst separation in these liquids by membrane technology may be worthwhile.
- A suitable isolation system is required for the experimental setup used for coupling reactions. Isolation is necessary to prevent oxidation of the catalysts used and subsequent palladium black formation. Systems such as nitrogen, argon or Schlenck isolation techniques may be sufficient

REFERENCES

1. NOBLE, R. & AGRAWAL, R. 2005. Separation research needs for the 21st century. *Industrial & Engineering Chemistry Research*. **44** (9) 2887 – 2892.
2. NAIR, D., SCARPELLO, J.T., WHITE, L.S., FREITAS DOS SANTOS, L.M., VANKELECOM, I.F.J. & LIVINGSTON, A.G. 2001. Semi-continuous nanofiltration-coupled Heck reactions as a new approach to improve productivity of homogeneous catalysts. *Tetrahedron Letters*. **42** (46) 8219 – 8222.
3. NAIR, D., LUTHRA, S.S., SCARPELLO, J.T., VANKELECOM, I.F.J., FREITAS DOS SANTOS, L.M., WHITE, L.S., KLOETZING, R.J., WELTON, T & LIVINGSTON, A.G. 2002. Increased catalytic productivity for nanofiltration-coupled reactions using highly stable catalyst systems. *Green Chemistry*. **4** (1) 319 – 324.
4. AERTS, S., BUEKENHOUDT, A., WEYTEN, H., GEVERS, L.E.M., VANKELECOM, I.F.J. & JACOBS, P.A. 2006. The use of solvent resistant nanofiltration in the recycling of the Co-Jacobsen catalyst in the hydrolytic kinetic resolution (HKR) of epoxides. *Journal of Membrane Science*. **280** (1-2) 245 – 252.